Characterisation of novel potential phosphorylation sites in the tumour suppressor Merlin in Drosophila

by

Sophia Yip

A thesis submitted in partial fulfillment of the requirements for the degree of

Master of Science

in

Medical Sciences – Medical Genetics

University of Alberta

Abstract

Neurofibromatosis Type II is an inherited cancer that manifests as various tumours in the nervous system. Mutations and deletions in the tumour suppressor Merlin (moesin, ezrin, radixin-like protein) are linked to the development of the disease. The mechanism by which Merlin suppresses cell growth is not yet clearly understood, however studies have shown that phosphorylation plays an important role in regulating the sub-cellular localisation, conformation, and activity of Merlin. Using *in vivo* genetic methods in *Drosophila melanogaster*, I undertook a characterisation of two novel potential phosphorylation sites that appear to be regulating Merlin function.

In this thesis, I show that two phosphorylatable residues, serine 371 and threonine 18, in Drosophila Merlin affect the sub-cellular localisation and function of the Merlin protein.

Preface

This thesis is an original work by Sophia Yip. No part of this thesis has been previously published.

Preliminary work in identifying the amino acid residues of interest, preparation of the reagents for my work, and preliminary *in vitro* and *in vivo* analyses of potential Merlin phosphorylation sites, as described in Chapter 2 and Chapter 3, were performed by Albert Leung and Angela Effa. Ubiquitination experiments presented in Chapter 3 were performed by David Primrose.

For my beloved grandfather and grandmother, whose love for me was only ever unconditional.

Acknowledgments

I would like to extend a heartfelt thank you to my supervisor, Dr Sarah Hughes, for her guidance and patience during my time in her lab, starting from my undergrad all through my MSc. Thank you, Sarah, for being a mentor in every way, and for caring about each and every one of us as individuals. Thank you for being more than 'just a boss'. I have learned so much from you, and I have been so fortunate to have found my way to your lab.

I would like to thank the members of my supervisory committee, Dr Rachel Wevrick and Dr David Eisenstat, for their guidance and feedback during my project. I would also like to thank Dr Shelagh Campbell for being on my examining committee.

To Dr Andrew Simmonds, thank you for being a second advisor, whether it was regarding science or just general discussions about life. Talking to you has definitely turned my world view on its side, and I appreciate your patience with me every time I came running to you for technical support. That nickname is still my favourite, by the way.

The work in this thesis would not have been possible without the rest of the Hughes lab. I would like to thank David Primrose for the banter and for answering my many questions and requests, even after I've long exhausted my quota. Thank you to Rika Maruyama for being the 'rock' of the lab and someone who we can always go to for advice or feedback. To Namal Abeysundara, it was a blast having you as company and growing along with you from our Biology 499 days through grad school. Thanks for all of the great conversations. To Kirsten Arnold, you survived sharing a bay with clumsy me! I've had incredibly funny and interesting conversations with you – you have a wicked humorous

streak. To Xiao Li, thanks for being the big brother. I'd also like to thank Angela Effa and Albert Leung, whose work built the foundation for a very interesting Masters project. I also want to thank all of the other past members of the Hughes lab: Annie Smylie, Tyler Pertman, Matt McDermand, Yang Yang, Fareena Contractor, Ryan Au, Yibo Yu…and the past and present members of the Simmonds lab for making the labs such a fun place to be. You guys are the reason I love coming to work…I love you guys.

To all of my colleagues in Medical Genetics, I love you guys. I can't believe how lucky I am to be in a department full of dynamic, fun, caring people. I've gone on more adventures with you guys over the past few years than I ever would have imagined. Thanks for everything!

Finally, I would like to thank my family and friends for all of their support throughout this journey. I would especially like to thank all of my family who have shown unconditional support for my work, despite not having a clue about what I study, or why I do my work in fruit flies.

I love you all.

Soaps

Table of Contents

List of Tables

List of Figures

Chapter 1

Introduction

1 Chapter 1: Introduction

1.1 Neurofibromatosis Type II

Neurofibromatosis Type 2, or NF2, is an autosomal dominant, inherited cancer of the nervous system characterised by tumours such as schwannomas, meningiomas, and ependymomas (Evans et al. 1992, Baser et al. 2003). The hallmark of the disease is the formation of bilateral vestibular schwannomas in the superior vestibular branch of the eight cranial nerve (Evans et al. 1992), and the majority of NF2 patients present with hearing loss (Evans et al. 2000). Studies suggest that the incidence of NF2 may be as high as 1 in 25 000 (Evans et al. 2005).

The *NF2* gene was identified on chromosome 22q12 in 1993 (Rouleau et al. 1993, Trofatter et al. 1993). Mutations and deletions in the *NF2* gene are linked to the development of NF2 tumours; almost all sporadic vestibular schwannomas and 50-70% of sporadic meningiomas have a biallelic inactivation of the *NF2* gene, and 33-60% of patients with NF2 carry inactivating germline mutations in the *NF2* gene (Ruttledge et al. 1994, MacCollin et al. 1996). The inactivation of the *NF2* gene was observed in tumour samples but not in the blood of the affected individuals, suggesting that one mutated allele is inherited, and a somatic mutation in the second allele leads to a loss of heterozygosity and the development of tumours (Ruttledge et al. 1994).

The inheritance of NF2 is consistent with Knudson's 'two-hit' hypothesis, where one mutant allele is inherited and the high chance of a somatic mutation of the remaining wild-type allele leads to a dominant inheritance of the disease. Tumour initiation, however, requires both 'hits', or mutations, and thus tumorigenesis is recessive (Knudson 1971). The first naturally-occurring model of a 'two-hit' cancer was the Eker rat for tuberous sclerosis (Eker and Mossige 1961), where a germline insertion mutation in the *Tsc2* gene lead to aberrant RNA expression, and the majority of the tumours had lost the wild-type allele (Yeung et al. 1994). However, manifestation of tumours in the Eker rat model do not fully mirror that of the human disease (Hino et al. 1994, Kobayashi et al. 1995).

1.2 *NF2* gene and Merlin

The *NF2* gene contains 17 exons and encodes for the protein product merlin (moesin, ezrin, radixin-like protein) (Trofatter et al. 1993), a 595-amino acid protein in mammalian cells related to the ezrin, radixin, and moesin (ERM) family of proteins. Loss of merlin protein function has been found in sporadic meningiomas, ependymomas, and almost all sporadic schwannomas (Gutmann et al. 1997, Stemmer-Rachamimov et al. 1997). Merlin localizes to cell-cell boundaries and membrane ruffles to mediate contact-dependent inhibition of proliferation, and can suppress growth of both normal and oncogenic cells (Tikoo et al. 1994, Lutchman and Rouleau 1995, Gonzalez-Agosti et al. 1996,

Maeda et al. 1999, Lallemand et al. 2003). In addition, merlin has been found to impair processes involved in tumorigenesis such as cell adhesion, motility and spreading (Gutmann et al. 1999, Lallemand et al. 2003, Gladden et al. 2010), suggesting that it functions as a tumour suppressor. Merlin has been linked to several pathways, including the suppression of Rac-PAK signaling to mediate contact inhibition (Shaw et al. 2001, Kissil et al. 2003, Okada et al. 2005) and the suppression of the mTORC1 pathway(James et al. 2009, Lopez-Lago et al. 2009). Merlin has also been identified as an upstream regulator in the Hippo tumour suppressor pathway (Zhang et al. 2010). The mechanism of merlin's action, however, is still unclear.

1.2.1 Ezrin, Radixin, and Moesin

Ezrin, radixin, and moesin, collectively known as the ERMs, assemble membrane complexes and link them to the actin cytoskeleton. Ezrin was first discovered in the chicken intestinal cell brush border, and was enriched in surface structures such as microvilli (Bretscher 1983). It was also found to be recruited to microvillar structures in the human placenta (Bretscher 1989). Radixin was first isolated from adherens junctions in the rat liver (Tsukita et al. 1989, Tsukita and Tsukita 1989), and also localises to the cleavage furrow during cytokinesis to connect actin filaments to the plasma membrane (Sato et al. 1991). Moesin was initially discovered as a receptor for heparin sulfate and was later determined to

be related to ezrin (Lankes et al. 1988, Lankes and Furthmayr 1991). The ERMs can directly associate with plasma membrane proteins, such as the hylauronate receptor CD44 (Tsukita et al. 1994). Ezrin interacts with intercellular adhesion molecule-2 (ICAM-2) (Heiska et al. 1998, Yonemura et al. 1998). The ERMs can also bind membrane proteins indirectly through the PDZ domain-containing adaptor proteins ezrin-radixin-moesin (ERM)–binding phosphoprotein 50 (EBP50), also known as Na+/H+ exchanger 3 regulating factor (NHERF1), and can also bind the exchanger 3 kinase A regulatory protein (E3KARP) (Reczek et al. 1997). Drosophila Moesin antagonizes the Rho1 pathway to affect actin localisation and to maintain epithelial integrity (Speck et al. 2003).

1.2.1.1 *Structure of the Merlin Protein and the ERMs*

Like the ERM proteins, merlin contains a conserved N-terminal FERM (4.1 Ezrin Radixin Moesin) domain and a coiled-coil domain (Huang et al. 1998). Actin-binding in ERMs is mediated through the C-terminal actin-binding domain (C-ERMAD) (Turunen et al. 1994), which is not present in merlin, suggesting that it has functions distinct from the ERMs (Turunen et al. 1994). Merlin binds actin through regions within the N-terminal domain (James et al. 2001) or through βII spectrin, paxillin, and EBP50, or by interaction with the ERMs (Scoles et al. 1998, Gronholm et al. 1999, Meng et al. 2000, Nguyen et al. 2001, Fernandez-Valle et al. 2002, Manetti et al. 2012).

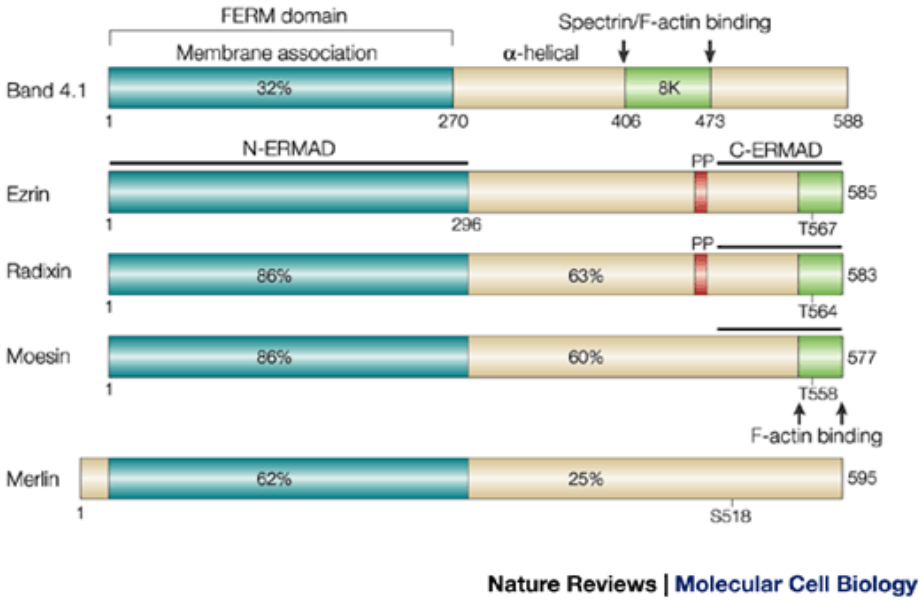

Figure 1-1. Mammalian merlin and the ERMs.

All four proteins share a conserved FERM domain (blue) and a α-helical domain. Sequence identity is compared with ezrin. Ezrin, radixin, and moesin have an F-actin binding domain in the C-terminal, actin-binding domain (C-ERMAD), which merlin does not share. Serine 518 (S518) is a phosphorylation site in mammalian merlin that regulates merlin function. Figure from (Bretscher et al. 2002). Image used with permission (Nature Publishing Group Licence number 3420880615721).

1.2.2 Merlin function as a tumour suppressor

In humans, merlin is classified as a tumour suppressor, and can inhibit cell growth (Lutchman and Rouleau 1995). In mice, *NF2* knock-outs fail to implant and are embryonic lethal (McClatchey et al. 1997), whereas heterozygous *NF2*$^{+/-}$ mice develop various metastatic tumours instead of schwannomas and other tumours characteristic of NF2 (McClatchey et al. 1998), which suggests that merlin also plays a role in cancers other than NF2. Conditional removal of the *NF2* allele in Schwann cells in mice leads to the development of schwannomas (Giovannini et al. 1999), and the inactivation of the *NF2* allele in mouse arachnoidal cells leads to the development of meningiomas (Kalamarides et al. 2002), recapitulating the human disease. In *Drosophila melanogaster*, Merlin loss-of-function clones in the eye leads to overproliferation phenotypes (LaJeunesse et al. 1998), and studies with Expanded, another member of the FERM protein family, show that Merlin and Expanded work together to regulate cell proliferation (McCartney et al. 2000).

1.2.3 Dual role of Merlin in controlling cell polarity and cell proliferation

Merlin is considered a 'novel' type of tumour suppressor, as it does not directly control the cell cycle machinery in the nucleus like the 'classic' tumour suppressors p53 and Rb (Kastan et al. 1991, Weinberg 1995), but instead associates with the cytoskeleton (Rouleau et al. 1993). The loss of merlin changes

actin cytoskeleton morphology in human Schwannoma cells (Pelton et al. 1998), and merlin is involved in the stabilisation and maturation of the adherens junctions (Lallemand et al. 2003, Gladden et al. 2010). In addition, merlin can inhibit the function of N-WASP, an actin nucleator Arp2/3 inhibitor (Manchanda et al. 2005). Thus, merlin may function as more than a simple tumour suppressor to play an additional role in maintaining cell adhesion and polarity.

1.2.4 Regulation of ERMs and Merlin by Phosphorylation

Phosphorylation regulates the N- and C-terminal intracellular interactions of the ERM proteins, which in turn regulates their active and inactive state. The ERMs are activated when the N- and C-terminal domains are not associated with each other (Gary and Bretscher 1995), which involves phosphorylation of residues in the C-terminal domain by kinases such as PKC (Pietromonaco et al. 1998, Simons et al. 1998). A conformational activation model has been proposed for the ERMs where activation leads to the exposure of the N- and C-terminal domains, as well as the C-terminal F-actin binding site (Gary and Bretscher 1995).

Merlin activity is also regulated in part by phosphorylation, and previous studies have linked merlin conformation and the intramolecular interactions between its N- and C-terminal domains with phosphorylation (Sherman et al. 1997). Merlin is thought to be active when closed and non-phosphorylated, but inactive when

open and phosphorylated (Sherman et al. 1997, Shaw et al. 1998, Gutmann et al. 1999), which is opposite to the effect of phosphorylation on the ERM proteins (Simons et al. 1998). Recent work, however, presents new insight. Sher et al. (Sher et al. 2012) have provided contrary findings on the relationship of phosphorylation with merlin conformation: consistent with previous findings, merlin phosphorylation is inactivating, but they determined that phosphorylation leads to a more closed conformation compared to wild-type. The authors also present a hierarchical model of merlin conformation where, instead of a binary open/closed conformation, Merlin can exist in a range of conformations, from relatively more tightly-closed to relatively more open. Another recent study also suggests that the F2 subdomain of the merlin FERM domain is in an open configuration, allowing dimerization or interaction with other proteins (Yogesha et al. 2011). In another study using Fluorescence Resonance Energy Transfer analysis, Hennigan et al. (Hennigan et al. 2010) examined the interaction of the merlin FERM domain with the C-terminal domain and proposed a model where the merlin FERM domain and C-terminal domain are maintained in close proximity and the changes in merlin conformation are subtle instead of fully 'open' and 'closed', with the native conformation favouring the slightly 'closed' conformation.

A phosphomimetic of the serine residue at position 518 (Merlin^{S518D}) in human merlin, previously found to be phosphorylated by Rac1 (Shaw et al. 2001, Xiao et al. 2002) impairs merlin's wild-type phenotype such as growth suppression and the impairment of cell motility (Surace et al. 2004). This mutation also affects merlin subcellular distribution from the plasma membrane to increased perinuclear staining (Kissil et al. 2002). It was also noted that the expression of Merlin^{S518D} changed the cell morphology of rat RT4 Schwannoma cells (Surace et al. 2004), indicating that the phosphorylation state of key residues affect merlin function in addition to conformation.

Merlin has also been shown to undergo phosphorylation at different residues by different kinases. In mammalian merlin, p21-activated kinase (PAK) has been shown to phosphorylate merlin at serine 518 to control merlin's growth suppression functions and localisation (Kissil et al. 2002, Rong et al. 2004), and studies have shown that merlin is both a target and a regulator of the Rac/Cdc42 pathway (Shaw et al. 2001, Xiao et al. 2002). Akt phosphorylation of merlin has been shown to enhance merlin interaction with CD44 and phosphatidylinositol lipids (Okada et al. 2009), and Akt phosphorylation specifically at threonine 230 and serine 315 leads to the disruption of merlin intracellular interactions *in vitro*, as well as merlin degradation (Tang et al. 2007). Further work also suggested that the phosphorylation of serine 10 is involved in merlin degradation (Laulajainen

et al. 2011). Protein kinase A (PKA) can phosphorylate serine 10 and serine 518, which affects merlin interactions with ezrin and with F-actin (Alfthan et al. 2004, Laulajainen et al. 2008). Thus, both phosphorylation and conformation appear to be important in regulating merlin activity.

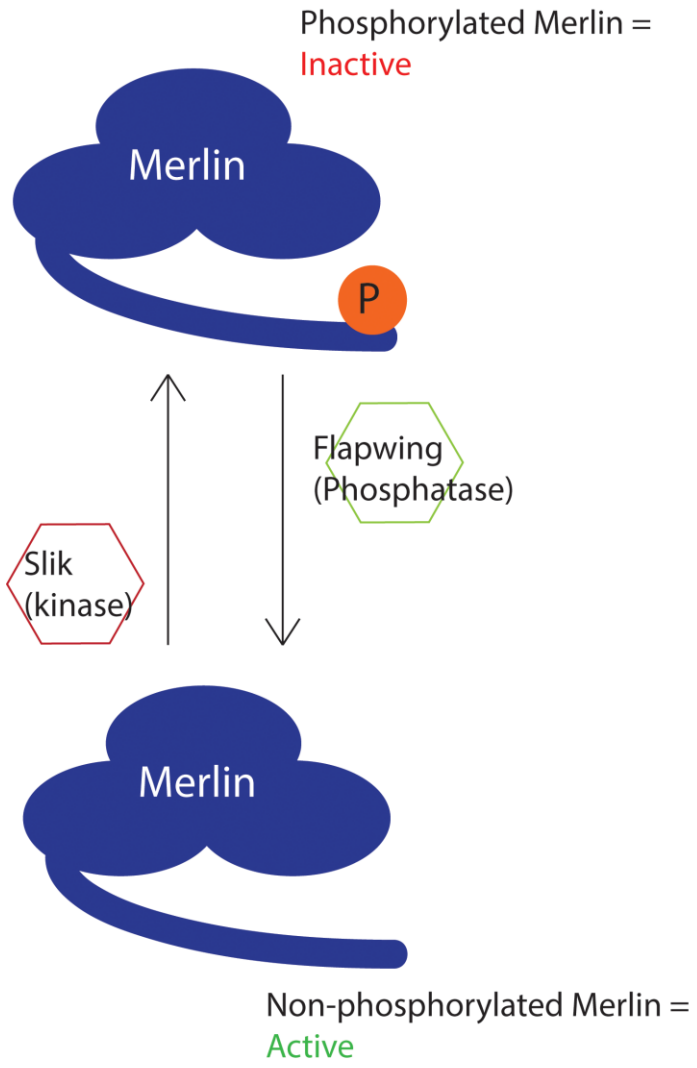

Figure 1-2. Phosphorylation control of Merlin.

In Drosophila, phosphorylation of Merlin by the Ste20 kinase Slik leads to the inactivation of Merlin. Dephosphorylation by the PP1 phosphatase Flapwing leads to the activation of Merlin.

1.2.5 Drosophila as a Model System for Studying the ERMs and Merlin

A well-conserved Merlin homologue is present in *Drosophila melanogaster* (McCartney and Fehon 1996). The Drosophila Merlin protein is longer than the mammalian merlin protein and does not have alternatively-spliced isoforms. A single ERM homologue Moesin is also present in flies (McCartney and Fehon 1996). This allows for the study of the relationship between these two proteins without the problem of redundancy in function. Expression of a dominant-negative form of Drosophila Merlin in the adult wing and Merlin loss-of-function clones in the adult eye leads to overproliferation phenotypes (LaJeunesse et al. 1998). The expression of human merlin is sufficient to rescue lethal Drosophila Merlin alleles (LaJeunesse et al. 1998, Gavilan et al. 2014), indicating a functional conservation of the protein in humans and flies.

Advantages of using Drosophila include genetic tools such as the UAS-GAL4 system for tissue-specific expression of Merlin mutants (Brand and Perrimon 1993), and Mosaic Analysis with a Repressible Cell Marker (MARCM) that allows the simultaneous removal of a specific gene and the over-expression of other specific alleles or genes in a wild-type background (Lee and Luo 1999).

1.3 Sip1 and ezrin-radixin-moesin (ERM)–binding phosphoprotein 50 (EBP50)

SRY-interacting protein, or Sip1, is the Drosophila homologue of EBP50 (Hughes et al. 2010). EBP50 is a phosphoprotein containing two PDZ domains to mediate protein-protein interactions (Yun et al. 1997). PDZ domain-containing proteins are often involved in cell signaling and promoting complex formation at the plasma membrane (Doyle et al. 1996). EBP50 inhibits the internalisation of the thromboxane A_2 β receptor (TPβ) receptor in Gα protein-mediated internalisation of G-protein coupled receptors, (Rochdi and Parent 2003), and regulates cell growth through interactions with merlin to sequester EGFR into insoluble membrane compartments to prevent EGFR internalisation and signaling (Curto et al. 2007). EBP50 interacts directly with merlin and the ERMs (Murthy et al. 1998) through a non-PDZ site in the EBP50 C-terminal domain (Reczek and Bretscher 1998), and is often apically expressed in different types of epithelia (Stemmer-Rachamimov et al. 2001).

In flies, Sip1 is involved in the phosphorylation of Moesin by Ste20 kinase Slik, as the loss of Sip1 results in Slik mislocalisation (Hughes et al. 2010). Slik regulates the activity of Moesin and Merlin in opposite manners (Hughes and Fehon 2006), providing evidence for a Sip1/Merlin/Moesin/Slik complex, illustrated in Figure 1-3.

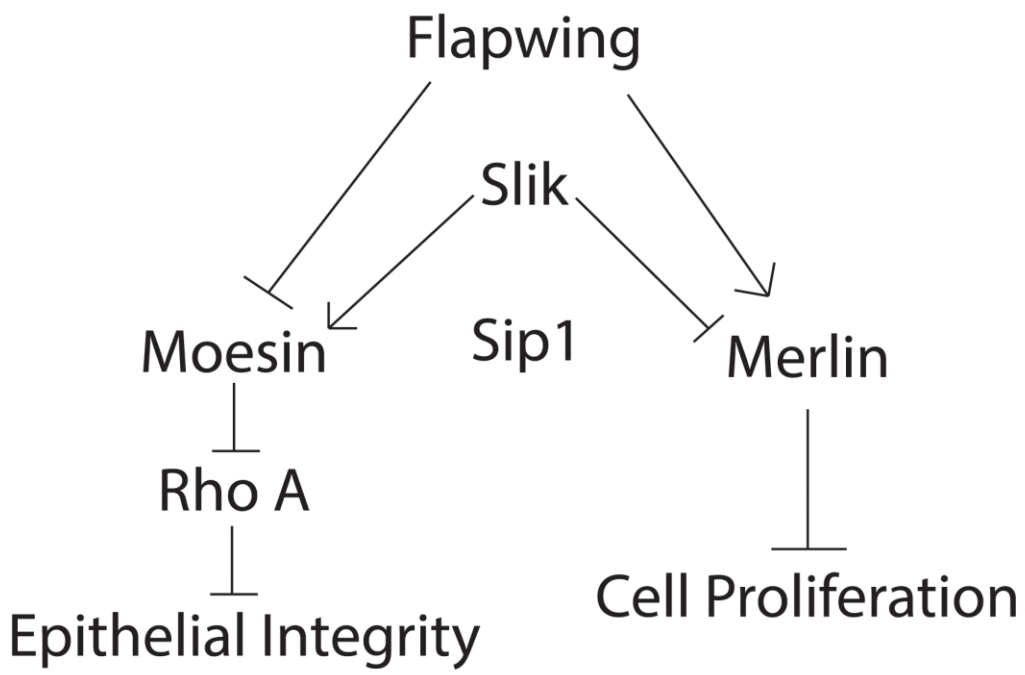

Figure 1-3. The Merlin/Moesin/Sip1/Slik/Flapwing Switch Hypothesis.

We hypothesise that the control of Merlin and Moesin is through a 'switch' mechanism mediated by Sip1. During cell growth, Slik will phosphorylate both Merlin and Moesin, simultaneously deactivating and activating the proteins, respectively, and leading to cell proliferation and the establishment of cell membrane integrity. During changes in cell morphology and low proliferation, the opposite will be true, and the proteins are dephosphorylated by Flapwing. Sip1 may act as a scaffolding protein on which Slik, Flapwing, Merlin, and Moesin can bind and interact. Adapted from (Hughes and Fehon 2006).

1.4 Rationale for Project

Previous studies have suggested that the phosphorylation status of Merlin is related to its function and localisation (Kissil et al. 2002, Surace et al. 2004). Slik was found to coordinately regulate Merlin and Moesin through the phosphorylation of both proteins in Drosophila (Hughes and Fehon 2006). Flapwing has also been shown to regulate the two proteins in Drosophila (Yang et al. 2012). This suggests the possibility of a 'switch' mechanism to regulate the activity of Merlin and the ERM proteins, where the phosphorylation status of the proteins will oppositely control cell proliferation and epithelial membrane integrity. This hypothesis is illustrated in Figure 1-3. The loss of the regulation controlling this switch between proliferation and the maintenance of epithelial integrity may then lead to an imbalance, in turn leading to over-proliferation and the formation of tumours.

Previous studies addressing the role of Merlin phosphorylation suggest that the control of Merlin function is complicated, and may involve finely-tuned regulation through the phosphorylation of many different residues (Laulajainen et al. 2011). The characterisation of novel potential phosphorylation sites could help us better understand the mechanisms regulating Merlin's activity, and ultimately lead to potential treatments for NF2.

1.5 Project Hypothesis

Two novel phosphorylatable residues in Drosophila Merlin, serine 371 and threonine 18, are hypothesised to regulate Merlin function in controlling cell proliferation and maintaining epithelial integrity through phosphorylation. Phosphorylation of these two residues is hypothesised to inactivate Merlin's tumour suppressor function, whereas dephosphorylation of these two residues is hypothesised to activate Merlin's tumour suppressor function.

Chapter 2

Materials and Methods

2 Chapter 2: Materials and Methods

2.1 Identification and Characterisation of Potential Novel Merlin Phosphorylation Sites

2.1.1 Identification of Potential Phosphorylation Sites

The computer-based phosphorylation prediction programs NetPhos 2.0 (http://www.cbs.dtu.dk/services/NetPhos/) and GPS 2.1 (http://gps.biocuckoo.org/) were used to predict Drosophila Merlin residues with an 80% or greater chance of phosphorylation *in vivo*, with sequences recognisable by known kinases. NetPhos 2.0 uses an artificial neural network-based method to predict potential serine, threonine, or tyrosine phosphorylation sites in protein sequences (Blom et al. 1999). GPS 2.1 uses sequence similarity-based clustering methods (Xue et al. 2008, Miller and Blom 2009). Fourteen potential phosphorylation sites were found using the two programs by Albert Leung (see Figure 2-1). Preliminary functional analyses performed by Albert Leung and Angela Effa identified serine 371 and threonine 18 as potential phosphorylation sites. Serine 371 has a 99.5% predicted chance of phosphorylation, and is conserved across Merlin proteins in human, Drosophila, mouse, rat, *Xenopus*, and zebrafish. Threonine 18 was predicted to have a 85.6% chance of phosphorylation.

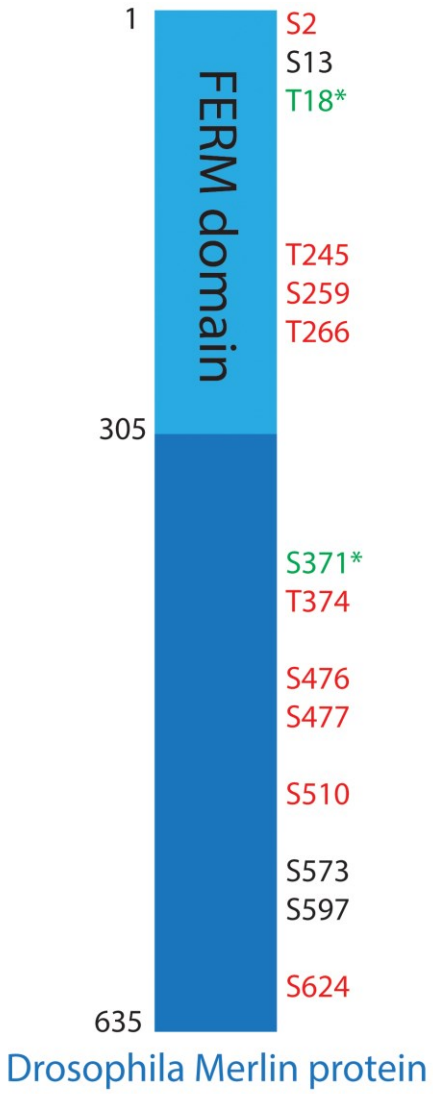

Figure 2-1. Predicted novel phosphorylation sites of Drosophila Merlin.

Fourteen potential phosphorylation sites were predicted by NetPhos 2.0 and GPS 2.1 to have a greater than 80% chance of being phosphorylated by serine/threonine kinases. Residues coloured in red have been tested by Angela Effa and do not affect Merlin localisation in a modified pulse-chase assay (see Section 2.1.3). Results for residues coloured in black are presented in Chapter 3. Residues coloured in green and highlighted with an asterisk (*) had an effect on Merlin localisation in a modified pulse-chase assay. The results and further *in vivo* analyses are presented in Chapter 3.

2.1.2 Site-Directed Mutagenesis of Potential Phosphorylation Sites

An approach of substituting potentially phosphorylatable amino acids in the merlin protein to non-phosphorylatable alanine or phosphomimetic aspartic acid to examine the effects of merlin phosphorylation has been previously used in mammalian cells (Surace et al. 2004). Based on this approach, forward and reverse PCR primers were designed to contain single amino acid mutations at serine 371 or at threonine 18 to alanine or aspartic acid. The Stratagene QuikChange Site-Directed Mutagenesis Kit was used to create Merlin mutants containing either a non-phosphorylatable alanine or a phosphomimetic aspartic acid at serine 371 or threonine 18. The resulting DNA was sequence-confirmed and cloned into the pHGW vector, which contains a heat-shock promoter and a GFP tag, and the pTMW vector, which contains a UAS promoter, a red eye marker to allow identification of transgenic animals, and a MYC tag. Both vectors are from The Drosophila Gateway™ Vector Collection (https://emb.carnegiescience.edu/labs/murphy/Gateway%20vectors.html). Experiments were performed by Angela Effa.

2.1.3 In-Vitro Assay: Modified Pulse-Chase Assay

2.1.3.1 *Drosophila Schneider 2 (S2) Cell Culture*

Drosophila Schneider 2 (S2) cells, a semi-adherent cell line derived from late Drosophila embryonic stages (Schneider 1972), were cultured in Serum-Free

Media (SFX; Thermo Scientific) and 1% w/v penicillin/streptomycin in T25 flasks at 25°C. The cells were split approximately once per week at a dilution of 1:5. To prepare for transfection, cells were split at 1:1 dilution, 1 day before transfection.

2.1.3.2 *Transfection of S2 cells*

120 μL of Didecyldimethylammonium bromide (DDAB) and 60 μL of SFX was incubated in a 1.5 mL microcentrifuge tube for every construct to be transfected, 15 minutes at 25°C. 2 μg of each GFP-tagged Merlin DNA construct was then added to the mixture and incubated for 15-20 minutes at 25°C. pHGW vector alone was used as a negative control. Modified from (Hughes and Fehon 2006).

Confluent S2 cells were counted and resuspended in SFX to a final concentration of 10^6 cells/mL. 3 mL of cells were transferred to each well in a 6-well plate. DNA/DDAB/SFX mixture was added drop-wise to each well while swirling gently. S2 cells were then incubated at 25°C for 48 hours.

2.1.3.3 *Heat-shock (pulse) and chase assay*

6-well plates containing transfected S2 cells were heat-shocked by incubation at 37°C for 30 minutes, then returned to 25°C for recovery. At 1 hour, 3 hours, and 6 hours after heat-shock, 750 μL of cells from each well were transferred to a 1.5 mL tube. The cells were spun 3 times at 900xg, rotating the tube 180° each time, and fixed in 800 μL 2% formaldehyde for 15 minutes at 25°C on a rocker. The

tubes were then spun down as above and washed in 1 mL sterile PBS, then resuspended in 25 μL of Prolong Gold Mountant (Invitrogen). 10-12 μL of cells were mounted onto a microscope slide and allowed to dry overnight. Slides were stored at 4°C.

2.1.3.4 *Cell Counting*

Cells were counted on a Nikon Eclipse TE2000-U microscope using a 100X oil immersion lens (N.A. 1.30 oil). The phenotypes were scored based on the criteria described in Table 1 and illustrated in Figure 2-2. Bias was eliminated by asking another person to cover up the slide labels with lab tape and by choosing slides at random to count. Lab tape was not removed from the slide labels until all of the slides had been scored for phenotypes. All fluorescent cells in any given field-of-view were scored, and care was taken to prevent repeat scoring. At least 100 cells were scored for each genotype at each time-point.

Table 1. Criteria used to score the GFP-tagged Merlin phosphorylation mutant localisation phenotypes in S2 cells in the modified pulse-chase assays.

Phenotype A	Completely membranous. GFP-Merlin is localised almost entirely at the cell membrane. The membrane can be clearly distinguished by the GFP signal when cycling through the cell.
Phenotype B	Mostly membranous. GFP-Merlin can still be seen on the membrane while cycling through the cell, but there is a notable amount of GFP-Merlin within the cell.
Phenotype C	Intracellular punctae. Most of the GFP-Merlin is present as small intracellular punctae inside the cell, but there is still a small amount of GFP-Merlin present on the cell membrane.
Phenotype D	Large intracellular vesicles. Most of the GFP-Merlin is in large intracellular punctae, and there is almost no GFP-Merlin on the cell membrane.

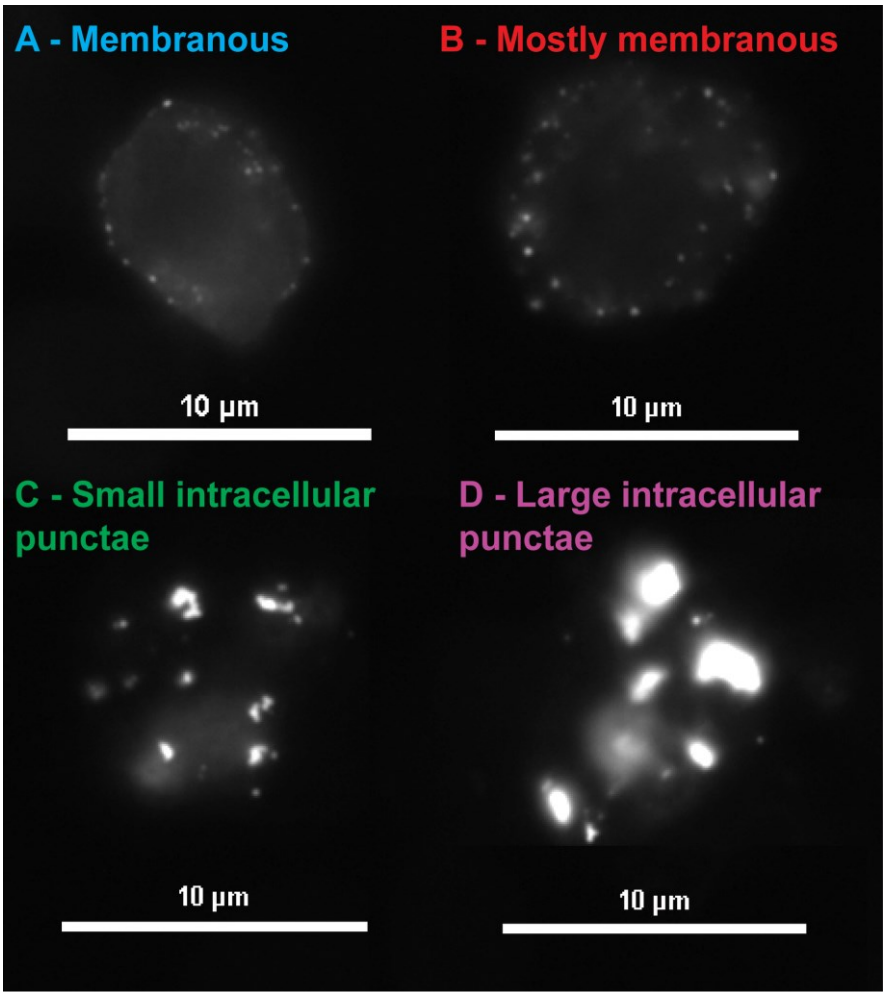

Figure 2-2. Representative images of pulse-chase assay phenotypes.

Visual criteria used to score the GFP-tagged Merlin phosphorylation mutant localisation phenotypes in S2 cells. Images were taken on the Nikon Eclipse TE2000-U with a 100X oil immersion lens (N.A. 1.30 oil).

2.1.4 In-Vivo Assay: Measurements of Adult Drosophila Wings

2.1.4.1 *UAS-GAL4 system*

The UAS-GAL4 system was used to specifically express the serine 371 and threonine 18 mutants in Drosophila tissues. Adapted from yeast, the *GAL4* gene is located near a cell-type specific promoter. The GAL4 binding site, or upstream activation sequence (UAS), is fused to the target gene (Brand and Perrimon 1993). The GAL4 protein then drives the transcription of the UAS-fusion gene in a cell- or tissue-specific pattern (Phelps and Brand 1998).

Transgenic Drosophila were made by the company Best Gene to carry a gene encoding a MYC-tagged serine 371 or threonine 18 mutant Merlin under the control of a UAS promoter. The transgenic flies were crossed to various tissue-specific GAL4 driver lines.

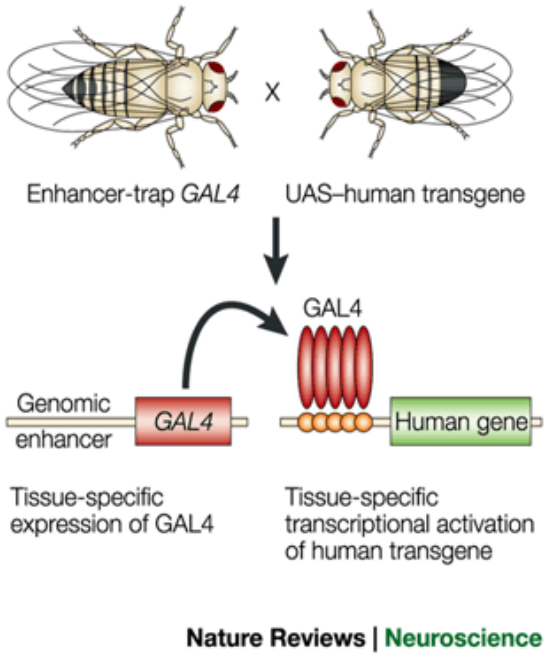

Figure 2-3. Schematic of the UAS-GAL4 system.

A fly carrying a UAS (upstream activation sequence)-tagged transgene (the human transgene in this example) is crossed to a fly with an enhancer-trap *GAL4*. The GAL4 protein will be expressed in a tissue-specific manner and bind to the UAS to drive the transcription of the human transgene in the specific tissue of choice. Image from (Muqit and Feany 2002). Image used with permission (Nature Publishing Group Licence Number 3420951019445).

2.1.4.2 *Drosophila melanogaster culture*

Drosophila stocks were cultured in standard media currently used by the Bloomington Stock Centre. Stocks were transferred approximately once per week, and the food was supplemented with *Saccharomyces cerevisiae*.

Table 2. Drosophila stock lines

Hughes Lab stock number	**Transgene Line**
SCH 0717	7280-2-2M chr3 UAS Merlin 371A 1107
SCH 0741	S371D 8310-1-6M Chr 3
SCH 0802	MycMer T18A/TM3(Sb) Line 1-3M
-	9100-2-5M UASmycMerlin T18D
SCH 0627	6232-1-4 M chr 3 TM3 UAS Myc Merlin
A248	*patched*-GAL4
-	*fkh*^{III}-GAL4
0405 (C. Berg)	MARCM line

2.1.4.3 *Crosses for wing measurements and larval wing discs*

Patched-GAL4 virgins were collected in separate tubes and kept at 18°C for up to one week before crossing with males from the appropriate lines at a ratio of ~2 virgin females:1 male. Crosses were incubated at 25°C and transferred once per day.

2.1.4.4 *Collection and dissection of third instar larval wing discs*

Third instar larvae of the proper genotype, identified as very mobile larvae crawling along the lower half of the vial away from the food, were collected and dissected in PBS, fixed for 25 minutes in 4% formaldehyde, and blocked for at

least 90 minutes in PTN (0.1% Triton X-100, 1% Normal Goat Serum/Normal Donkey Serum in PBS) at room temperature. Tissue was stained in the appropriate primary antibodies in PTN overnight (16 hours) at 4°C on a rocker, washed 3x in PBS, then washed 30 minutes in PTN at room temperature. Secondary antibodies at 1:2000 dilution were incubated with the tissue at room temperature for 45-60 minutes in PTN, washed 3x in PBS, then washed 30 minutes in PTN. DAPI (1:10000 in PTN) was added for 10 minutes at room temperature and washed out twice in PBS. Wing discs were dissected out of the tissue and mounted with Prolong Gold Mountant onto a microscope slide and allowed to dry overnight. Slides were stored at 4°C. At least 6-8 wing discs were mounted per slide, and each wing disc was examined for the localisation patterns of the various markers.

Z-stacks of wing discs were taken on a Zeiss LSM 700 confocal microscope with a 63X oil immersion lens (N.A. 1.4 oil). Single-plane images depicting the apical surfaces of the wing discs were chosen by starting at the peripodial membrane and moving downward through the z-sections until the nuclei of the peripodial membrane disappear. The first z-section depicting apical actin or apical DE-cadherin was chosen as the most apical section of the wing disc. Images were compiled using Adobe Illustrator.

2.1.4.5 *Collection and analysis of adult Drosophila wings*

Adult flies of the proper genotype were anesthetised and placed in 70% ethanol for at least 16 hours. Wings were dissected and mounted onto microscope slides using Aqua Mount. Slides were kept for at least 24 hours on a baking dish with a magnet on the coverslip to completely flatten the wings (LaJeunesse et al. 1998). Wings were collected from three independent experimental replicates. Approximately 70 to 90 wings were collected for each genotype in total. Images of the wings were taken on a Coolsnap HQ (Photometrics) camera mounted on a Zeiss Axioskop microscope using a 5X lens. Area measurements were obtained by outlining the perimeter of the *patched* region (Figure 3-6 A) using the free hand draw tool in Image J (NIH).

2.1.4.6 *Statistical Analysis of adult Drosophila wing measurements*

Statistical analyses were done with Microsoft Excel. Measurements from three independent experimental replicates were analysed with the Levene's test for homogeneity of variance (Levene 1960), to verify the assumption that the variances are equal across the three independent experiments. Scatter plots were then used to remove any outliers. The measurements were then tested for normality. All three independent experiments passed for both tests and the values were pooled together and a *p*-value was determined using a t-test. Average wing sizes were compared between the Merlin mutants and wild-type

Merlin, or Merlin mutants and a w^{1118} outcross. *P*-values were considered significant if the value was smaller than 0.01 between individual paired comparisons. Analysis performed by David Primrose.

2.1.5 In-Vivo Assay: Mosaic Analysis of Repressible Cell Marker (MARCM)

2.1.5.1 *Recombination crosses to build up Mer^4 fly lines*

Parental Cross: Mer^4 19A FRT/FM7-GFP;+;Sb/Ser-GFP, TM3 virgins were collected and crossed to males from UASmycMerlin S371A 2M and UASmycMerlin S371D 6M lines.

Progeny Cross 1: Y/FM7-GFP;+; UASmycMerlin S371A/Sb males OR Y/FM7-GFP;+; UASmycMerlin S371D/Sb males were collected and crossed to Mer^4 19A FRT/FM7-GFP;+;Sb/Ser-GFP, TM3 virgins. Non-Sb, FM7, Ser progeny were chosen to establish stocks (Mer^4 lines).

Other Mer^4 lines: Mer^4/FM7-GFP;+;UASmycMerlin^{T18A} , Mer^4;+;UASmycMerlin^{T18D} , and Mer^4;+;UASmycMerlin^{WT} lines were obtained from Matt McDermand (undergraduate student, Hughes Lab).

2.1.5.2 *MARCM crosses*

Mer^4 lines were crossed to a MARCM line with a hs-FLP recombinase and a CD8::GFP to positively mark the clones (0405 MARCM line, from C. Berg,

University of Washington). Crosses were tipped after 12 hours and larvae were heat-shocked at least 40 hours after egg-laying.

Heat shock program: 1 hour heat-shock at 37°C, 1 hour recovery at 25°C, 1 hour heat-shock at 37°C. Some crosses were heat-shocked during the larval stage on 2 consecutive days on a 24-hour cycle.

2.1.5.3 *Collection of ovaries*

Progeny from the MARCM crosses (Section 2.1.5.2) were collected into separate vials and allowed to mature for 4-7 days. Flies were then anesthetised and ovaries were dissected out of non-balancer, non-GFP female flies in PBS, fixed in 4% formaldehyde for 20 minutes, then blocked in PTN for at least 90 minutes. Appropriate antibodies were incubated as per the procedure described in Section 2.1.4.4. Images of wing discs were taken on a Zeiss LSM 700 confocal microscope with a 40X oil immersion lens (N.A. 1.3 oil) or 63X oil immersion lens (N.A. 1.4 oil) and compiled using Adobe Illustrator. 3D visualisation of images was done using the image analysis software BitPlane Imaris. 3D screen captures were obtained using the Snapshot function in Imaris.

Table 3. List of antibodies used for immunofluorescence.

Antibody Name	Epitope	Company	Dilution
SC-216	aPKC	Santa Cruz	1:500
C566.9C	Coracle	DHSB	1:500
G15.16	Coracle	DHSB	1:500
D3571	DAPI	Invitrogen	1:10000
DCAD2	DE-cadherin	DHSB	1:400 to 1:500
4370	Moesin	Cell Signaling	1:100
C3956	MYC	Sigma	1:500
Apa1	*patched*	DHSB	1:250
A12379	Phalloidin AlexaFluor 488	Invitrogen	1:1000 to 1:1500
A22283	Phalloidin AlexaFluor 546	Invitrogen	1:2000
1475	Sip1	Fehon Lab	1:1000
ab7254	Ubiquitin	ABCAM	1:3000

2.1.6 Ubiquitination of Threonine 18

Co-transfection of S2 cells were performed as described in Section 2.1.3.2 with 2 μg of actin-GAL4 and UAS-MYC-Merlin^{WT}, UAS-MYC-Merlin^{T18A}, or UAS-MYC-Merlin^{T18D}. After incubating overnight at 25°C, DMSO alone, 5 μM MG132 in DMSO, or 50 μM MG132 in DMSO was added to the wells. Cells were incubated at 16 hours at 25°C. An immunoprecipitation with an anti-MYC antibody was carried out using a 0.1% SDS RIPA buffer (50 mM HEPES pH 7.4, 150 mM NaCl, 1% Ipegal CA-630, 0.5% Na-deoxycholate, 2 mM $MgCl_2$, 0.1% SDS, 1.25% Octyl β-glucoside, 1% N-laurylsarcosine, 1 Roche EDTA-free protease inhibitor tablet). Proteins were run on 10% SDS-PAGE gels and probed with anti-ubiquitin primary antibody and anti-mouse AlexaFluor 680 secondary antibody. Blots were visualized with the Licor System (Odyssey). Experiment was performed by David Primrose.

Chapter 3

Results

3 Chapter 3: Results

3.1 Identification and characterisation of potential novel Merlin phosphorylation sites

Of the 14 predicted potential phosphorylation sites that were initially identified (Leung 2011), serine 371 and threonine 18 appeared to affect Merlin localisation and function in preliminary experiments (Leung 2011, Effa and Hughes, unpublished). Serine 13, serine 573, and serine 597 were also tested for their effects on Merlin localisation.

3.1.1 Serine 13, Serine 573, and Serine 597 are potential phosphorylation sites and do not regulate Merlin localisation and function

To examine the effect of the potential phosphorylation sites on Merlin sub-cellular localisation, GFP-tagged Merlin constructs containing single amino acid substitutions of serine 13, serine 573, and serine 597 to non-phosphorylatable alanine (A) or a phosphomimetic aspartic acid (D), under a heat-shock promoter, were transfected into Drosophila S2 cells. A modified pulse-chase assay was performed to examine the localisation patterns of the mutants over time. This method had been previously used to examine the effects of a threonine 616 mutation in Merlin, and the mutations to alanine and aspartic acid were chosen to be consistent with previous approaches (LaJeunesse et al. 1998, Hughes and Fehon 2006).

At 1 hour after heat-shock, GFP-tagged wild-type Merlin (HS-Merlin^{WT}) changes from a more membranous localisation pattern (~50-60% of the cells counted show Merlin localised partly or completely to the membrane; Phenotypes A and B; Figure 3-1 B) to a more intracellular localisation pattern (over 90% of cells counted show Merlin localised into small or large intracellular punctae; Phenotypes C and D) by 6 hours after heat-shock. Representative images of the phenotypes are shown in Figure 2-2.

Mutating serine 13, serine 573, and serine 597 to either alanine or aspartic acid did not affect Merlin localisation patterns in S2 cells after heat-shock when compared to wild-type Merlin (Figure 3-1, Figure 3-2, Figure 3-3).

Figure 3-1. Mutating serine 13 to alanine or aspartic acid does not affect Merlin localisation patterns in S2 cells over time.

Cells were collected at 1, 3, and 6 hours after 30 minute heat-shock at 37°C. At least 100 cells were counted at each time point.

(A) Visual criteria used to score the GFP-tagged Merlin phosphorylation mutant localisation phenotypes in S2 cells.

(B) GFP-tagged wild-type Merlin changes from a more membranous localisation pattern at 1 hour after heat-shock to a more intracellular localisation pattern by 6 hours after heat-shock.

GFP-tagged Merlin^{S13A} and Merlin^{S13D} localisation after heat-shock is comparable to wild-type.

A

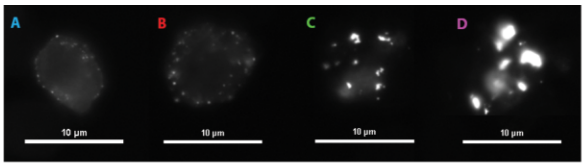
A
B
C
D
10 µm
10 µm
10 µm
10 µm

B

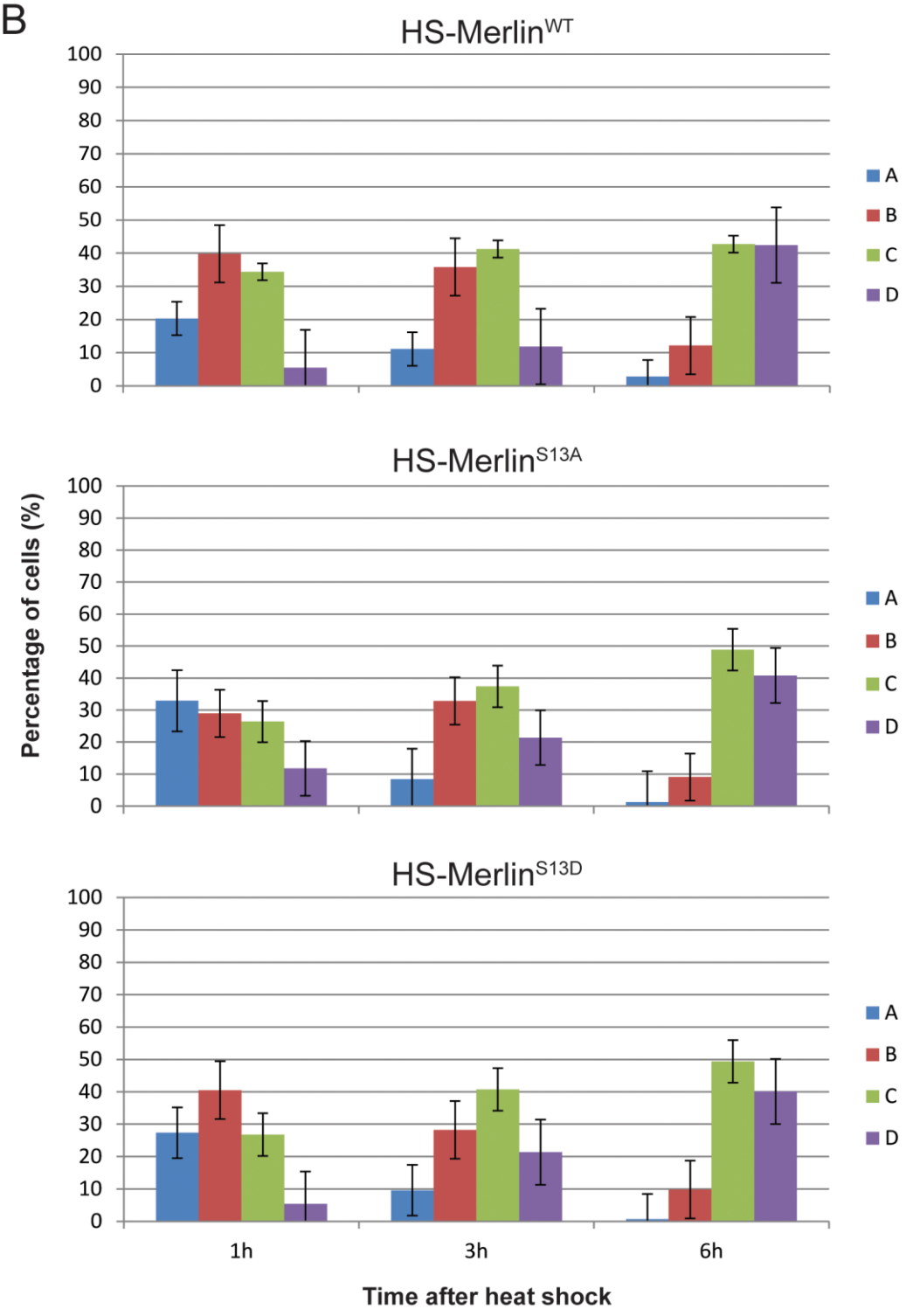
HS-Merlin^WT
HS-Merlin^S13A
HS-Merlin^S13D
Percentage of cells (%)
100
90
80
70
60
50
40
30
20
10
0
A
B
C
D
1h
3h
6h
Time after heat shock

Figure 3-2. Mutating serine 573 to alanine or aspartic acid does not affect Merlin localisation patterns in S2 cells over time.

Cells were collected at 1, 3, and 6 hours after 30 minute heat-shock at 37°C. At least 100 cells were counted at each time point.

(A) Visual criteria used to score the GFP-tagged Merlin phosphorylation mutant localisation phenotypes in S2 cells.

(B) GFP-tagged wild-type Merlin changes from a more membranous localisation pattern at 1 hour after heat-shock to a more intracellular localisation pattern by 6 hours after heat-shock.

GFP-tagged Merlin^{S573A} and Merlin^{S573D} localisation after heat shock is comparable to wild-type.

A

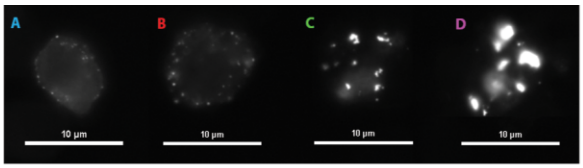
A
B
C
D
10 µm
10 µm
10 µm
10 µm

B

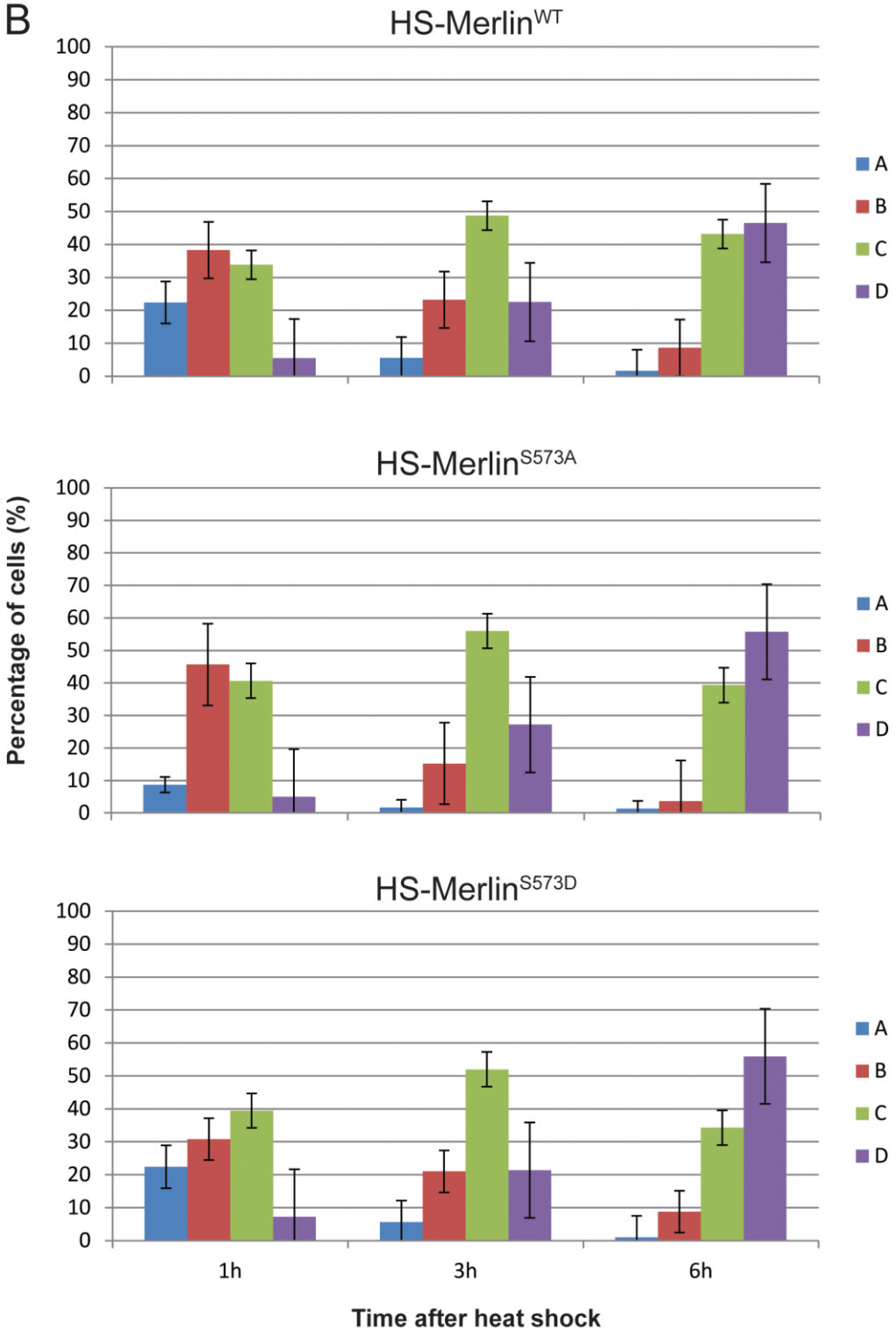
HS-MerlinWT
HS-MerlinS573A
HS-MerlinS573D
Percentage of cells (%)
100
90
80
70
60
50
40
30
20
10
0
A
B
C
D
1h
3h
6h
Time after heat shock

Figure 3-3. Mutating serine 597 to alanine or aspartic acid does not affect Merlin localisation patterns in S2 cells over time.

Cells were collected at 1, 3, and 6 hours after 30 minute heat-shock at 37°C. At least 100 cells were counted at each time point.

(A) Visual criteria used to score the GFP-tagged Merlin phosphorylation mutant localisation phenotypes in S2 cells.

(B) GFP-tagged wild-type Merlin changes from a more membranous localisation pattern at 1 hour after heat-shock to a more intracellular localisation pattern by 6 hours after heat-shock.

GFP-tagged Merlin^{S597A} and Merlin^{S597D} localisation after heat-shock is comparable to wild-type.

A

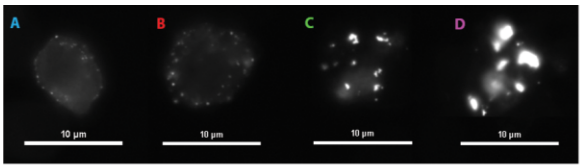
A
B
C
D
10 µm
10 µm
10 µm
10 µm

B

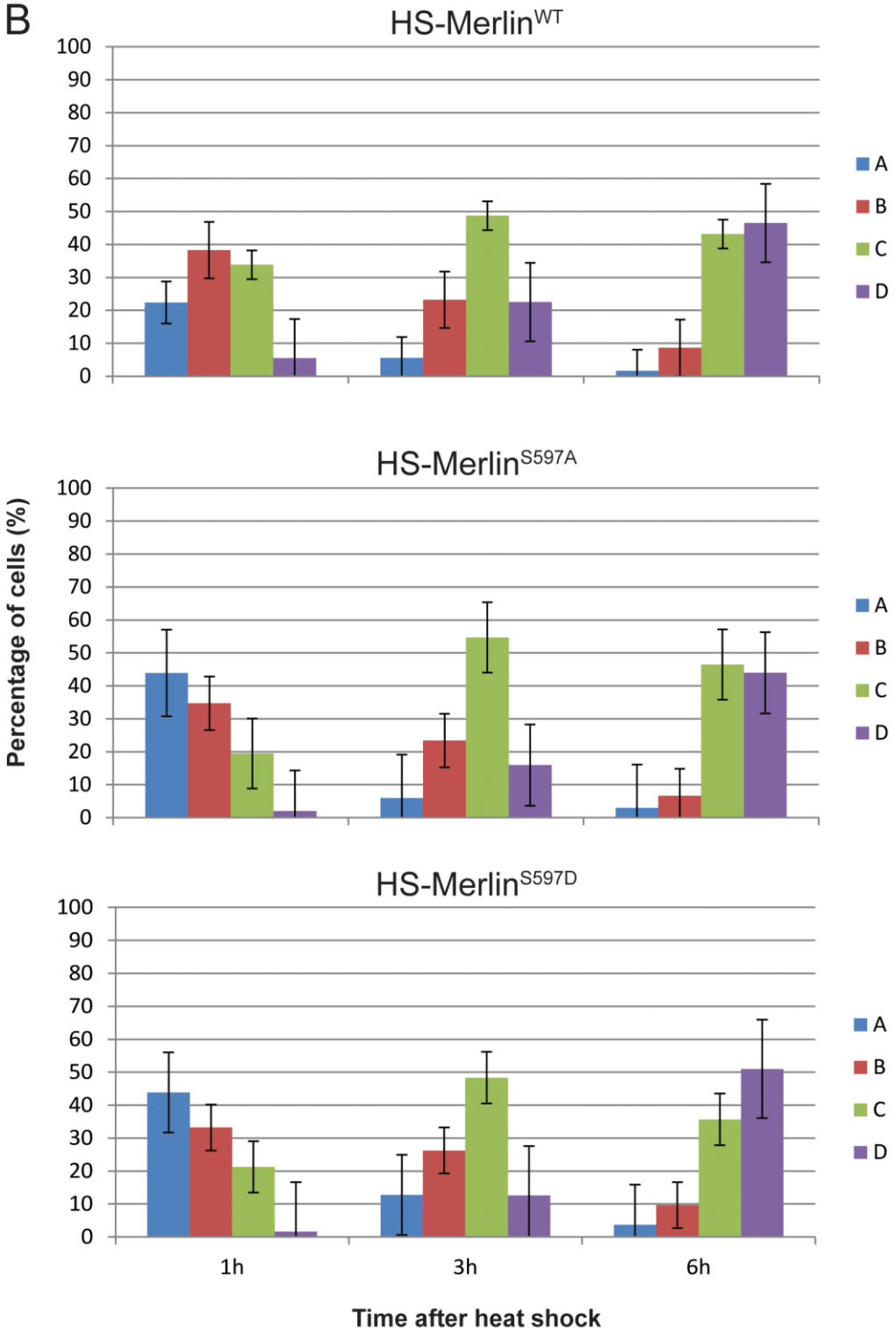
HS-MerlinWT
HS-MerlinS597A
HS-MerlinS597D
Percentage of cells (%)
100
90
80
70
60
50
40
30
20
10
0
A
B
C
D
1h
3h
6h
Time after heat shock

3.1.2 Serine 371 and Threonine 18 are novel Merlin phosphorylation sites that regulate Merlin function

3.1.2.1 *Serine 371 and Threonine 18 mutants affect Merlin localisation in Schneider 2 cells over time in modified pulse-chase assay*

When serine 371 is mutated to alanine (HS-Merlin^{S371A}), the localisation pattern over time is similar to wild-type Merlin in the modified pulse-chase assay (Figure 3-4 B), but serine 371 mutated to aspartic acid (HS-Merlin^{S371D}) causes the Merlin protein to associate more strongly with the cell membrane. Over 70% of cells show Merlin^{S371D} localised to the membrane at 1 hour after heat-shock, and Merlin^{S371D} was observed in the membranous A and B phenotypes in a larger proportion (~40% of cells) even at 6 hours after heat-shock, compared to wild-type Merlin and Merlin^{S371A}.

When threonine 18 is mutated to alanine (HS-Merlin^{T18A}), the localisation pattern is similar to wild-type Merlin (Figure 3-5 B). When threonine is mutated to aspartic acid (HS-Merlin^{T18D}), over 80% of the cells show Merlin^{T18D} localised to the plasma membrane at 1 hour after heat-shock, and this pattern is maintained even 6 hours after heat-shock.

This data suggests that serine 371 and threonine 18 are novel Merlin phosphorylation sites that regulate Merlin localisation and may also play a role in regulating Merlin function.

Figure 3-4. Mutating serine 371 to aspartic acid affects Merlin localisation patterns in S2 cells over time.

Cells were collected at 1, 3, and 6 hours after 30 minute heat-shock at 37°C. At least 100 cells were counted at each time point. Experiments were performed by Angela Effa.

(A) Visual criteria used to score the GFP-tagged Merlin phosphorylation mutant localisation phenotypes in S2 cells.

(B) GFP-tagged wild-type Merlin changes from a more membranous localisation pattern at 1 hour after heat-shock to a more intracellular localisation pattern by 6 hours after heat-shock.

GFP-tagged Merlin^{S371A} localisation after heat-shock is comparable to wild-type.

GFP-tagged Merlin^{S371D} localisation is more membranous than wild-type at 1 hour after heat-shock, and larger proportions of membranous Merlin^{S371D} can still be observed at 6 hours after heat-shock.

A

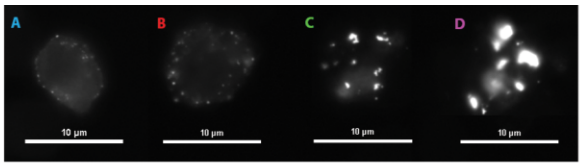
A
B
C
D
10 µm
10 µm
10 µm
10 µm

B

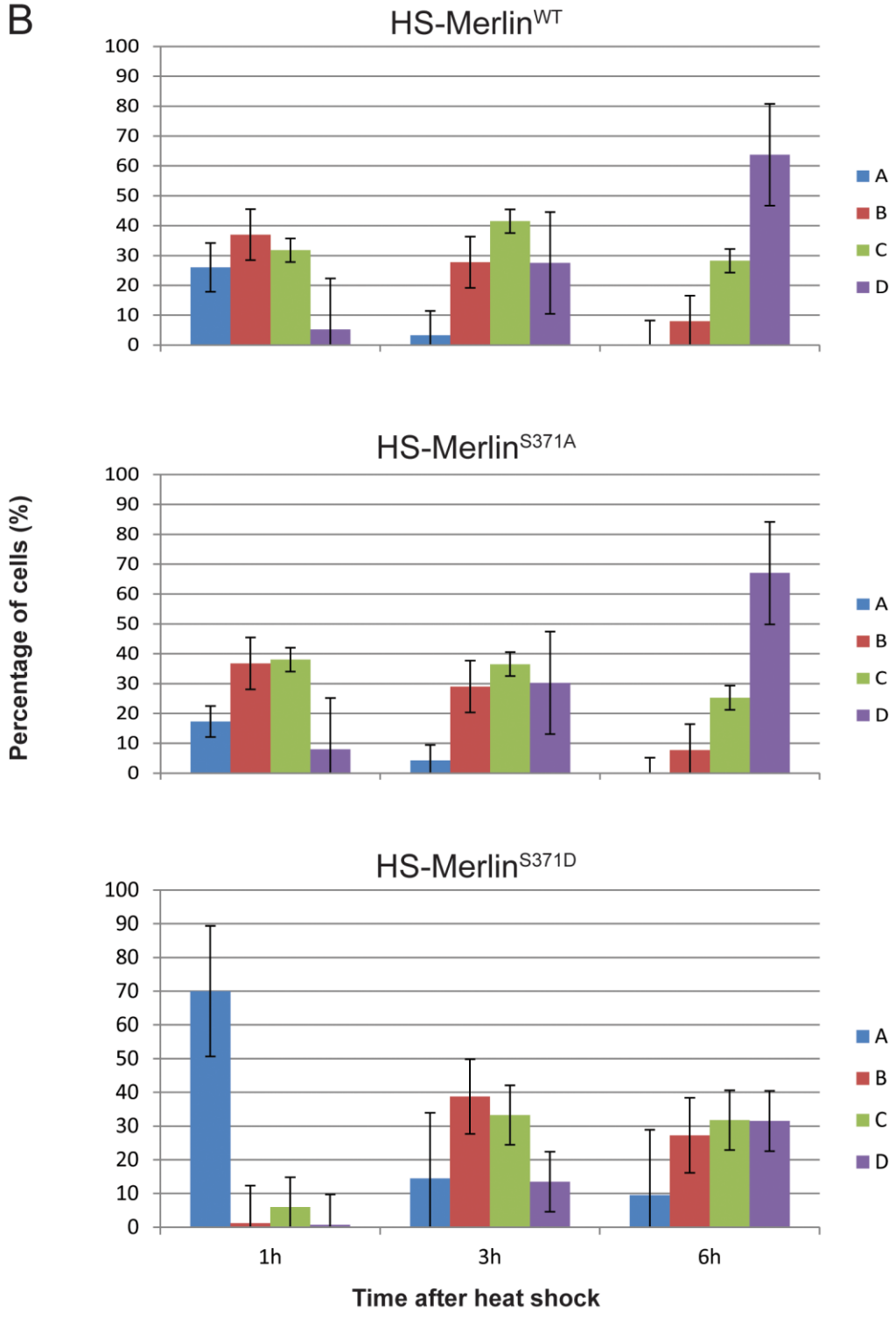
HS-Merlin^WT
HS-Merlin^S371A
HS-Merlin^S371D
Percentage of cells (%)
100
90
80
70
60
50
40
30
20
10
0
A
B
C
D
1h
3h
6h
Time after heat shock

Figure 3-5. Mutating threonine 18 to aspartic acid affects Merlin localisation patterns in S2 cells over time.

Cells were collected at 1, 3, and 6 hours after 30 minute heat-shock at 37°C. At least 100 cells were counted at each time point.

(A) Visual criteria used to score the GFP-tagged Merlin phosphorylation mutant localisation phenotypes in S2 cells.

(B) GFP-tagged wild-type Merlin changes from a more membranous localisation pattern at 1 hour after heat-shock to a more intracellular localisation pattern by 6 hours after heat-shock.

GFP-tagged Merlin^{T18A} localisation after heat-shock is comparable to wild-type.

GFP-tagged Merlin^{T18D} localisation results in large proportions of Merlin^{T18D} being retained at the membrane even at 6 hours after heat-shock.

A

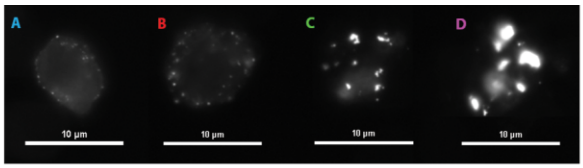
A
B
C
D
10 µm
10 µm
10 µm
10 µm

B

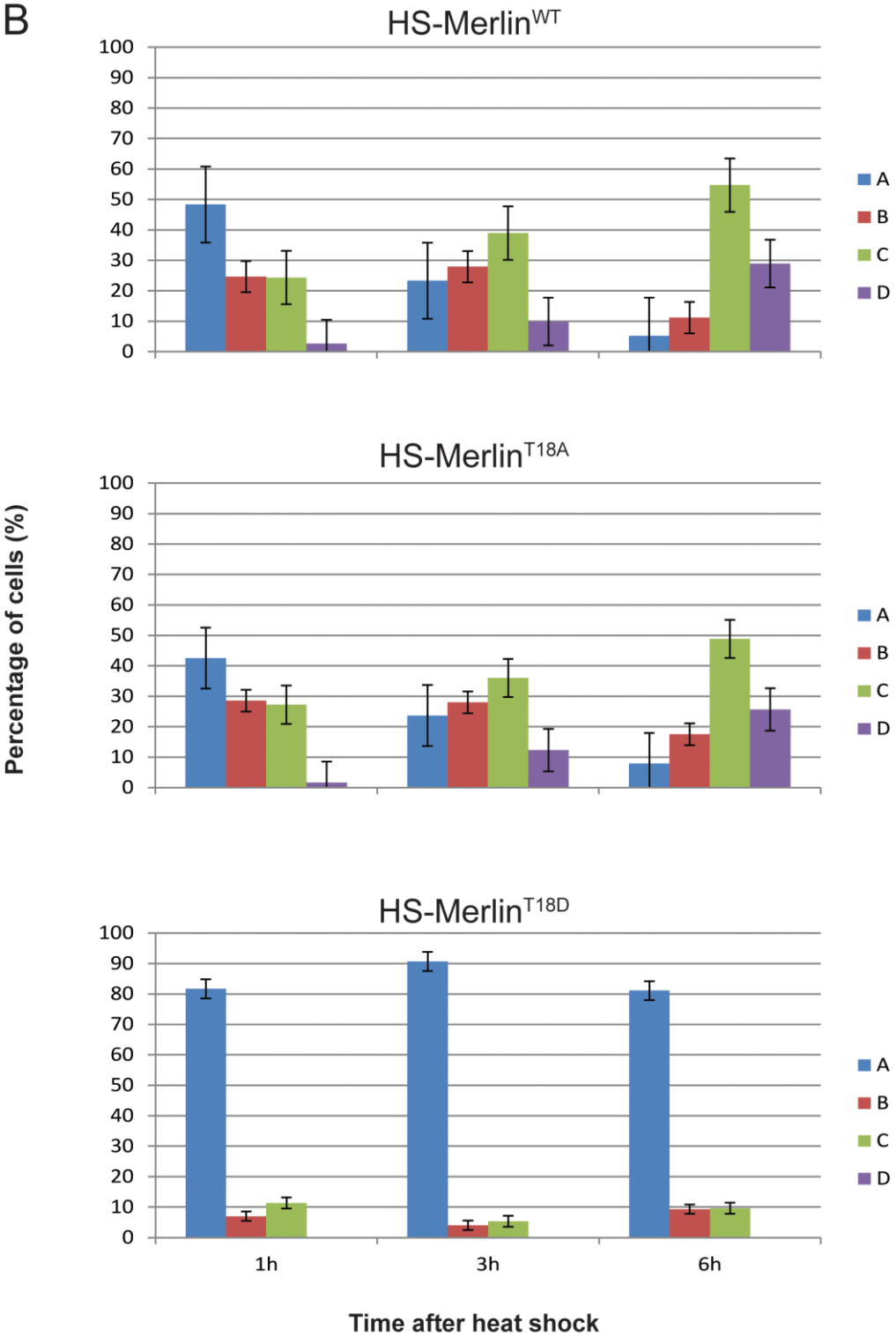
HS-MerlinWT
HS-MerlinT18A
HS-MerlinT18D
Percentage of cells (%)
100
90
80
70
60
50
40
30
20
10
0
A
B
C
D
1h
3h
6h
Time after heat shock

3.1.2.2 *Serine 371 and Threonine 18 mutations affect* patched *region size in adult Drosophila wings*

To further examine the role of serine 371 and threonine 18 in Merlin regulation of cell proliferation *in vivo*, transgenic fly lines carrying UAS-MYC-tagged Merlin serine 371 (UAS-Merlin^{S371}) or threonine 18 (UAS-Merlin^{T18}) mutants were crossed to a *patched*-GAL4 driver fly line, to over-express the Merlin phosphorylation mutants specifically in the *patched* region between the L3 and L4 veins of the of the adult wing (outlined in yellow in Figure 3-6 A).

Adult wings were collected from three independent experimental replicates and the area of the *patched* region was measured. The average areas are shown in Figure 3-6 B. Over-expression of UAS-Merlin^{S371A} and UAS-Merlin^{S371D} both resulted in a significantly larger *patched* region compared to over-expression of wild-type Merlin (UAS-Merlin^{WT}). Over-expression of UAS-Merlin^{T18D} resulted in a significantly smaller area compared to over-expression of wild-type Merlin, and is comparable to a control cross to the standard w^{1118} control. Over-expression of UAS-Merlin^{T18A} did not result in significant differences compared to over-expression of UAS-Merlin^{WT}. This suggests that serine 371 and threonine 18 are crucial phosphorylation sites that affect Merlin function in regulation of cell proliferation.

Figure 3-6. Serine 371 and Threonine 18 mutations affect *patched* region size.

(A) Adult Drosophila wing. The *patched* region (between the L3 and L4 veins) is outlined in yellow.

(B) Area of adult Drosophila wings over-expressing Merlin phosphorylation mutants under the *patched*-GAL4 driver. 70 to 90 adult wings were measured for each genotype.

The asterisks (*) denote significance, with a *p*-value smaller than 0.01. All of the genotypes were significantly different from the w^{1118} out-cross except for UAS-Merlin^{T18D}.

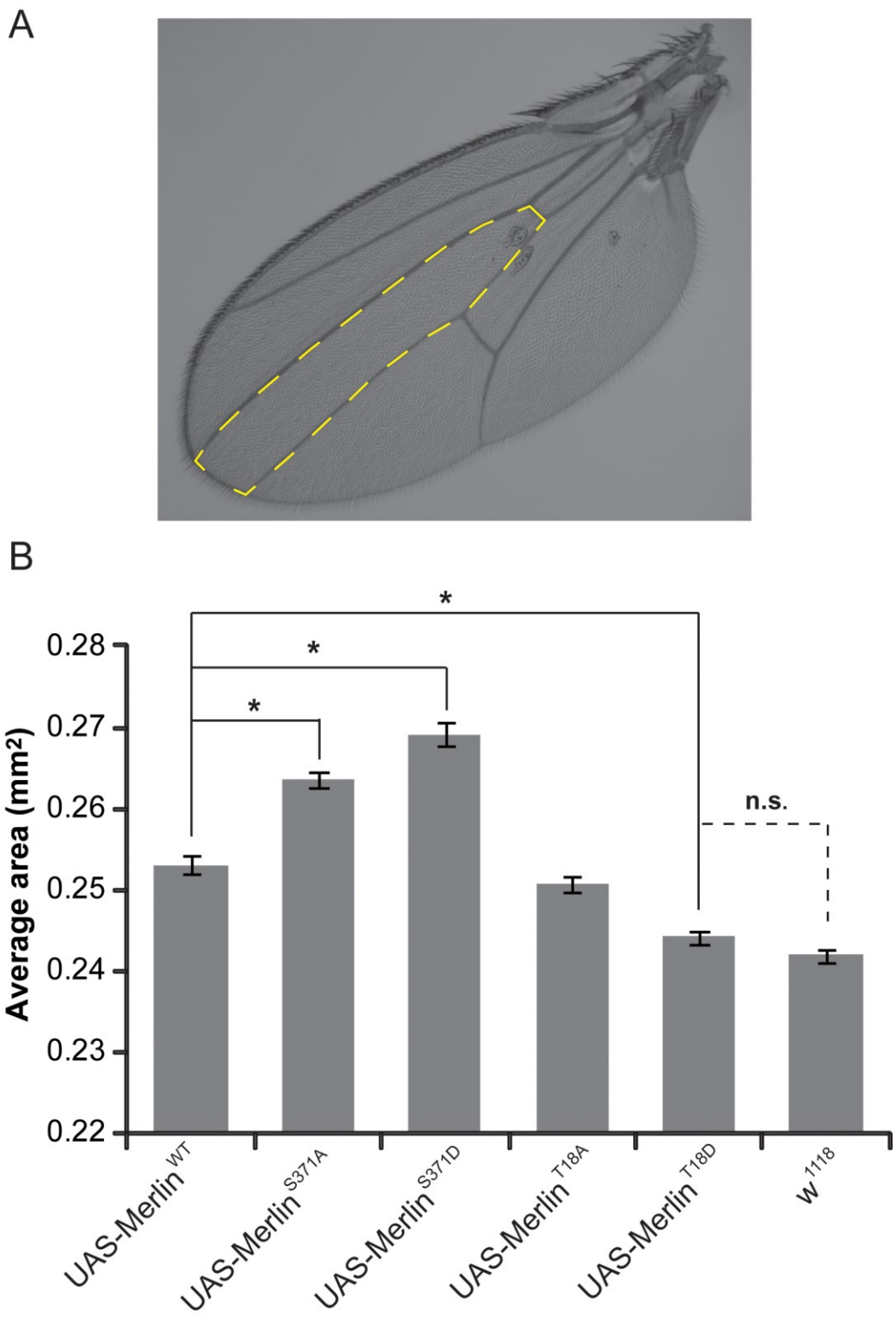
A
B
Average area (mm²)
0.28
0.27
0.26
0.25
0.24
0.23
0.22
*
*
*
n.s.
UAS-Merlin WT
UAS-Merlin S371A
UAS-Merlin S371D
UAS-Merlin T18A
UAS-Merlin T18D
w 1118

3.1.2.3 *Serine 371 and Threonine 18 mutations affect Merlin localisation in third instar larval wing discs*

Third instar larval wing discs were collected from the *patched*-GAL4 crosses to examine the effects of the over-expression of serine 371 or threonine 18 mutations on the cellular localisation of Merlin and on membrane morphology. Using the adherens junction protein DE-cadherin as a plasma membrane marker, MYC-tagged wild-type Merlin (MYC-Merlin^{WT}) was observed to have a membranous localisation (Figure 3-7 A-C). Merlin^{S371A} and Merlin^{S371D} both appear to be more cytoplasmic compared to Merlin^{WT} (Figure 3-7 D-F, G-I), and Merlin^{S371D} appears to be more cytoplasmic than Merlin^{S371A}, whereas Merlin^{S371A} localises to both the plasma membrane and the cytoplasm. Merlin^{T18A} also localises to both the plasma membrane and the cytoplasm (Figure 3-7 J-L), whereas Merlin^{T18D} is more cytoplasmic when compared to both wild-type Merlin and Merlin^{T18A} (Figure 3-7 M-O). This suggests that the mutations at serine 371 and threonine 18 have an effect on Merlin sub-cellular localisation *in vivo.*

Figure 3-7. Localisation of serine 371 and threonine 18 phosphorylation mutants in third instar larval wing imaginal discs.

MYC-tagged Merlin^{S371} and Merlin^{T18} alanine and aspartic acid mutants were over-expressed in the *patched* region of third instar larval wing imaginal discs using the *patched*-GAL4 driver. Dorsal is at the top of the image. The *patched* region is indicated by the blue dotted line in the wing disc schematic in (P). Single plane confocal images at the apical side of the wing discs are shown. DE-Cadherin (DCAD) is used as a membrane marker. Scale bars represent 5 μm.

MYC-tagged wild-type Merlin is membranous (A-C).

MYC-tagged Merlin^{S371A} and Merlin^{S371D} are more cytoplasmic compared to wild-type. Merlin^{S371A} (D-F) localises to both the membrane and the cytoplasm. Merlin^{S371D} (G-I) is more cytoplasmic than Merlin^{S371A}.

MYC-tagged Merlin^{T18A} localises to both the membrane and the cytoplasm (J-L). Merlin^{T18D} has a very cytoplasmic localisation (M-O).

(P) Wing disc schematic. D – dorsal; V – ventral; A – anterior; P – posterior.

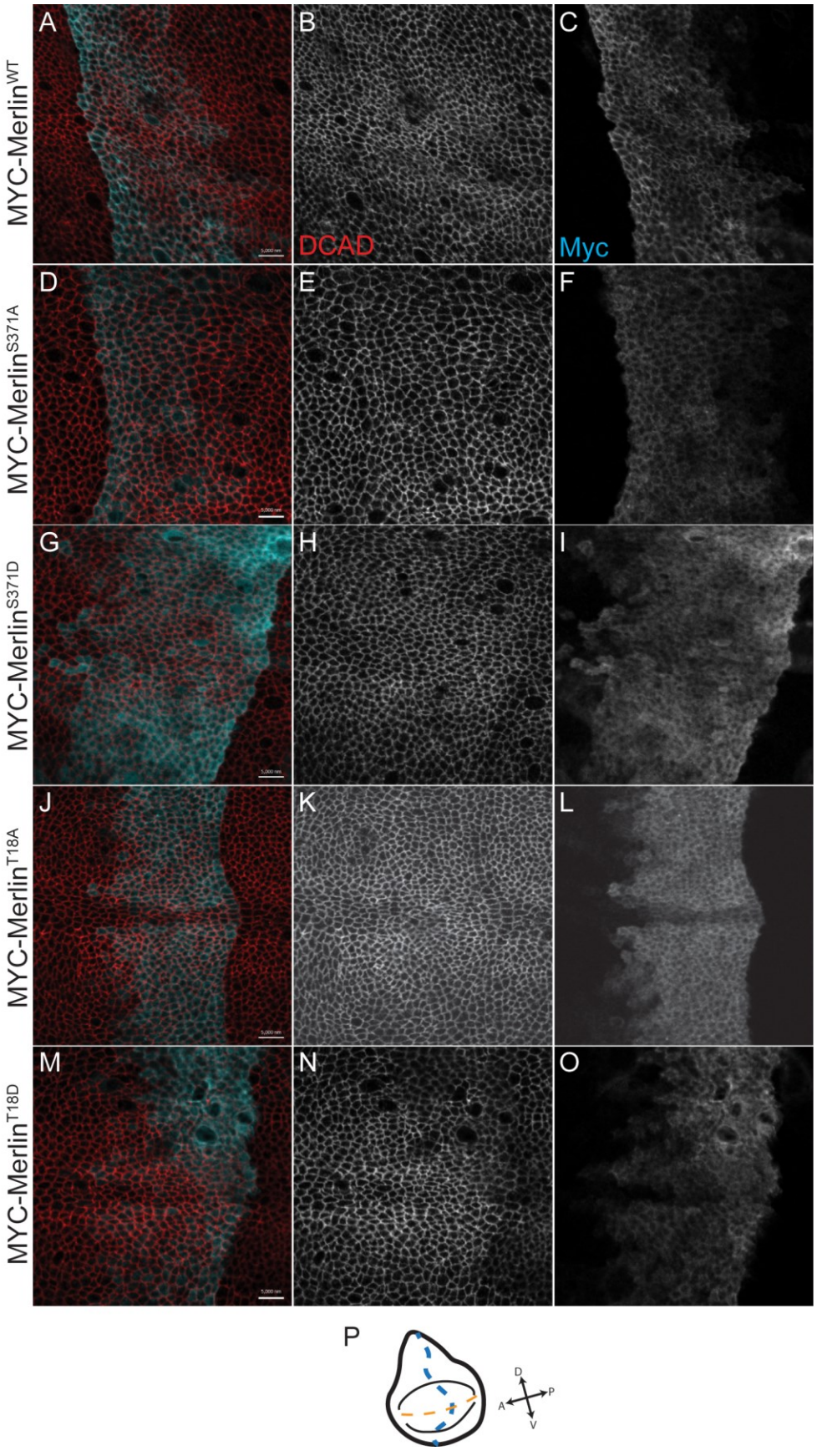
A
B
C
DCAD
Myc
MYC-Merlin^WT
D
E
F
MYC-Merlin^S371A
G
H
I
MYC-Merlin^S371D
J
K
L
MYC-Merlin^T18A
M
N
O
MYC-Merlin^T18D
P
D
A
P
V

3.1.2.4 *Serine 371 and Threonine 18 mutations affect DE-cadherin, but not Sip1 localisation, in third instar larval wing discs*

As Merlin localisation is related to function (Kissil et al. 2002), the change in localisation of the serine 371 and threonine 18 mutants in the wing discs suggests that these two potential phosphorylation sites may be having an effect on Merlin function. The effect of mutating serine 371 and threonine 18 on the expression of the adherens junction marker DE-cadherin and the scaffolding protein Sip1 was examined. DE-cadherin localisation was examined because Merlin has been shown to co-localise and interact with components of the adherens junctions, and Merlin has been suggested to stabilise the adherens junctions and link it with the actin cytoskeleton (Lallemand et al. 2003). Sip1 interacts with Merlin and is thought to facilitate the phosphorylation of Merlin by Slik (Abeysundara, in review, (Hughes and Fehon 2006, Abeysundara et al. in review).

Third instar larval wing discs over-expressing the phosphorylation mutants in the *patched* expression region were examined for changes in the localisation of DE-cadherin and Sip1. Brighter DE-cadherin staining was observed below the apical surface of the disc when the serine 371 and threonine 18 mutants are over-expressed (Figure 3-8 G, J, Q, U) when compared to over-expression of wild-type (Figure 3-8 C). The brighter DE-cadherin staining is visible along the region of transgene expression, indicated by MYC staining. This effect is most noticeable

around the region where the dorsal-ventral boundary and the anterior-posterior boundary intersect (indicated by the asterisk in Figure 3-8; wing disc schematic Figure 3-7 P). Sip1 expression, however, seems unaffected by either the serine 371 or the threonine 18 mutations (Figure 3-8 F, P, T). Sip1 staining appears to be brighter in the wing disc expressing Merlin^{S371D} (Figure 3-8 M), but that is due to bleed-through from the bright MYC signal.

Figure 3-8. Sip1 and DE-cadherin localisation in third instar larval wing discs.

Single-focal plane images below the apical surface of the Drosophila wing disc are shown. Dorsal is indicated by the yellow 'D'. Scale bars represent 20 μm. Schematic of the wing disc in Figure 3-7 (P).

DE-cadherin appears to be brighter below the apical surface of the disc when the serine 371 and threonine 18 mutants are over-expressed (G, J, Q, U). The brighter DE-cadherin staining is visible along the region of transgene expression, as indicated by MYC staining. The intersection of the dorsal-ventral and anterior-posterior boundary is indicated by the asterisk (*). Sip1 localisation appears unchanged. The bright Sip1 staining in panel (M) appears to be bleedthrough from (N).

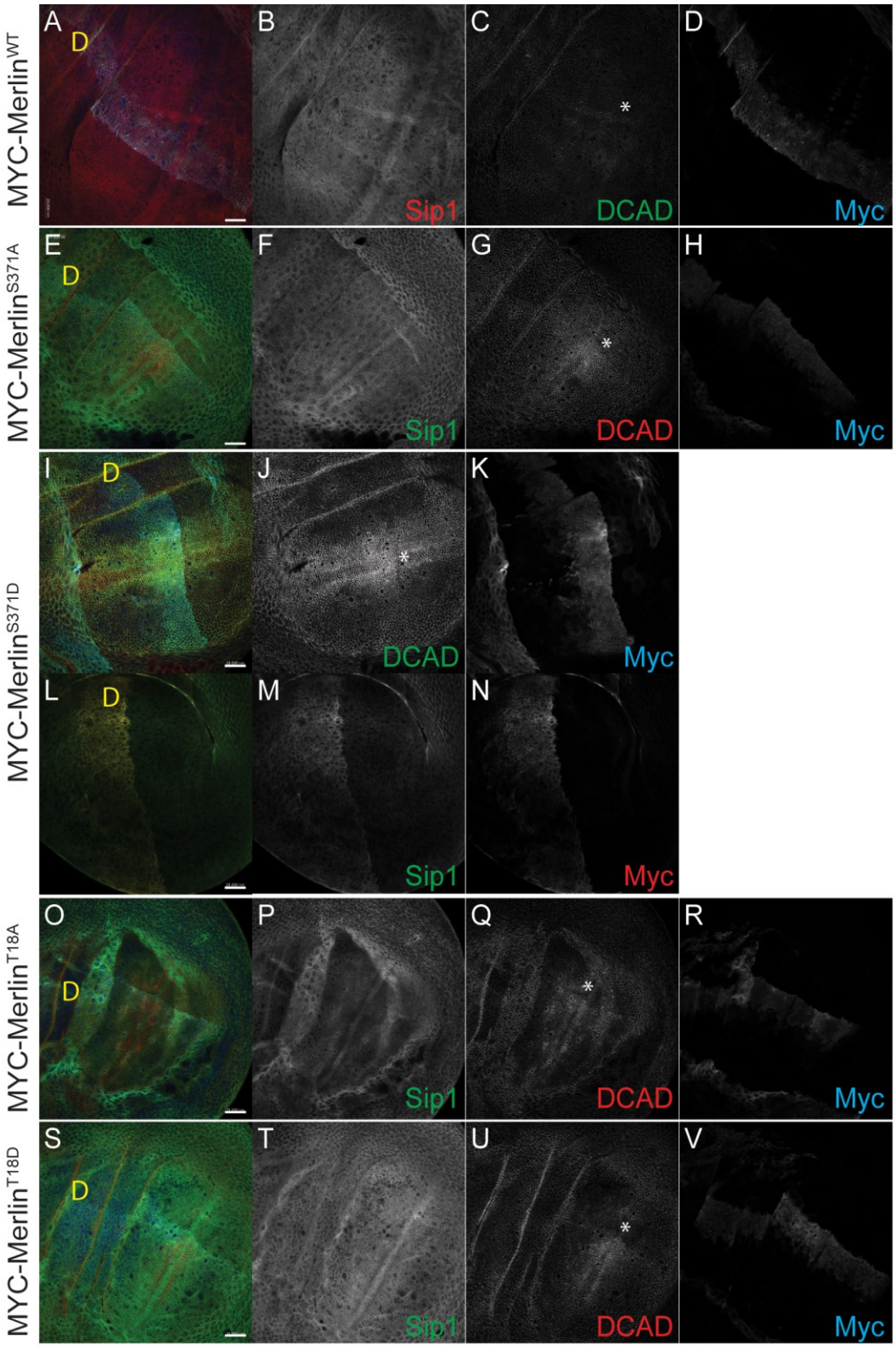
MYC-Merlin^WT
MYC-Merlin^S371A
MYC-Merlin^S371D
MYC-Merlin^T18A
MYC-Merlin^T18D
A
B
C
D
E
F
G
H
I
J
K
L
M
N
O
P
Q
R
S
T
U
V
D
Sip1
DCAD
Myc

3.1.2.5 *Serine 371 mutation to alanine affects F-actin localisation in third instar larval wing discs*

The effect of the serine 371 and threonine 18 mutations on the localisation of F-actin was examined in the third instar larval wing discs. Merlin interacts with F-actin (James et al. 2001), and studies in mammalian systems has shown that merlin-actin association is required for the formation of membrane protrusions and merlin has a role in the organisation of the actin cytoskeleton (Lallemand et al. 2009, Lallemand et al. 2009).

The over-expression of Merlin^{S371A} in third instar larval wing discs shows a subtle increase in F-actin staining along the edge of the over-expression region as indicated by the *patched* stripe in Figure 3-9 (F), especially in the dorsal compartment. The over-expression of wild-type Merlin, Merlin^{S371D}, Merlin^{T18A}, and Merlin^{T18D} do not appear to affect F-actin localisation in the expression region (indicated by MYC or *patched* staining; Figure 3-9 C, I, L, O).

Figure 3-9. Actin localisation in third instar larval wing discs.

Single-focal plane images below the apical surface of the Drosophila wing disc are shown. Dorsal is indicated by the yellow 'D'. Scale bars represent 20 μm. Schematic of wing disc in Figure 3-7 (P).

Expression region of the Merlin mutants is indicated by MYC or *patched* staining.

Over-expression of Merlin^{S371A} in the *patched* region of the wing disc results in a subtle increase in F-actin along the edge of the expression region (F, yellow arrowhead) in the dorsal compartment. Over-expression of Merlin^{S371D}, Merlin^{T18A}, and Merlin^{T18D} do not appear to affect F-actin localisation.

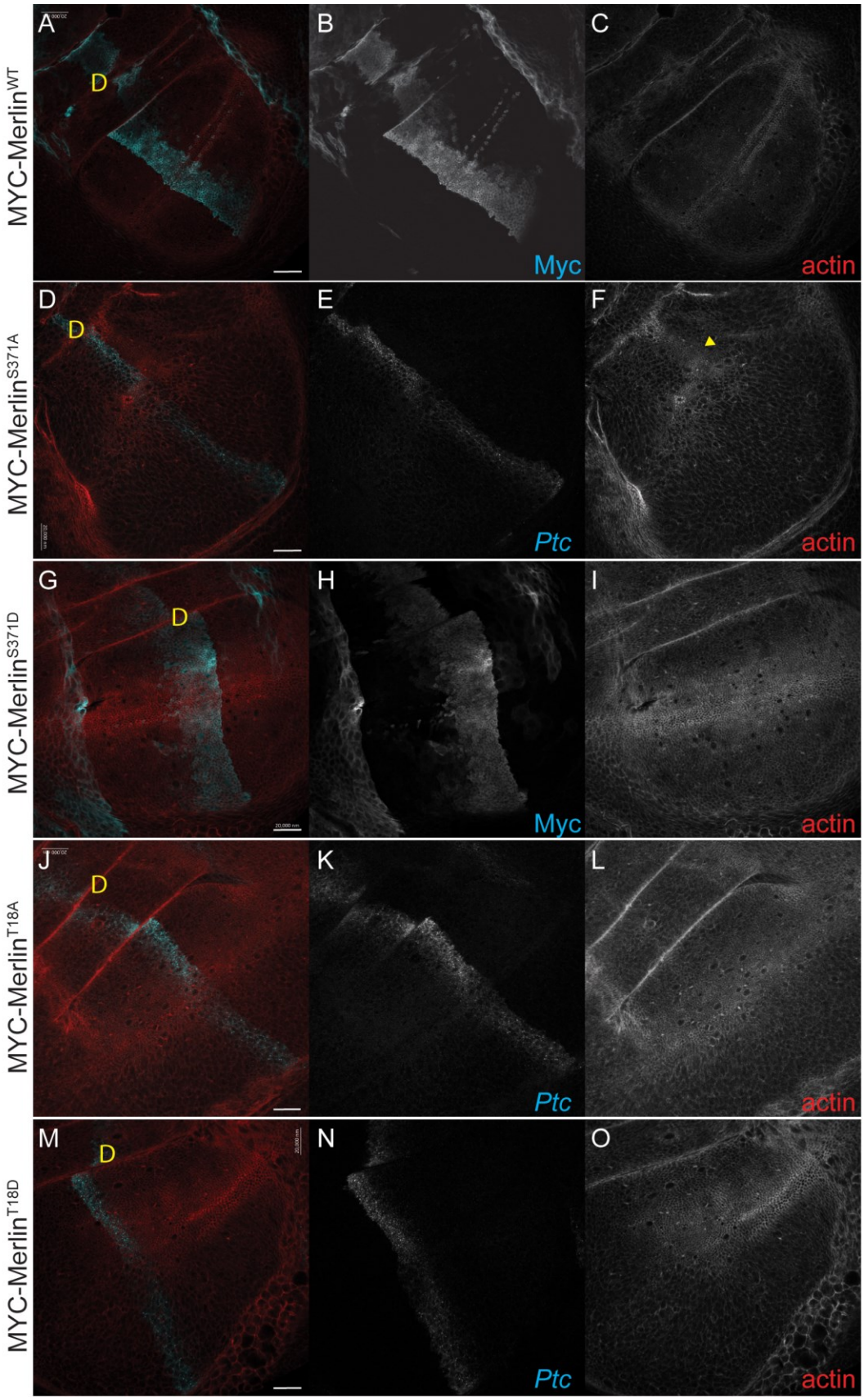
MYC-Merlin^WT
A
D
B
Myc
C
actin
MYC-Merlin^S371A
D
D
E
Ptc
F
actin
MYC-Merlin^S371D
G
D
H
Myc
I
actin
MYC-Merlin^T18A
J
D
K
Ptc
L
actin
MYC-Merlin^T18D
M
D
N
Ptc
O
actin

3.1.2.6 *Serine 371 and Threonine 18 mutations affect epithelial integrity in Drosophila follicle cells*

To further examine the effects of mutating serine 371 and threonine 18 on epithelial integrity, the Mosaic Analysis with a Repressible Cell Marker (MARCM) (Lee and Luo 1999) technique was used. A schematic illustrates this technique in Figure 3-10. In this technique, FLP-mediated recombination at the FRT sites leads to a loss of GAL80 repressor in the homozygous mutant daughter cell (green cell), and the expression of a UAS-tagged transgene is allowed under a specific GAL4 driver. The marker segregation allows for the mutant cells to be differentially marked. The advantage of MARCM compared with Somatic Mosaic Analysis is the ability to over-express the serine 371 or threonine 18 phosphorylation mutants while simultaneously removing endogenous Merlin in a Merlin-null, or Mer^4 (LaJeunesse et al. 1998), background. This approach was chosen to reduce any potential masking effects of endogenous wild-type Merlin *in vivo*, and the MARCM technique also allows for the examination of homologous wild-type cells adjacent to the mutant clones. The follicular epithelium that surrounds the Drosophila egg chambers were chosen because they are a very well-characterised model for studying cell polarity, and the process of egg chamber development has been well-studied (Spradling 1993) (Wu et al. 2008).

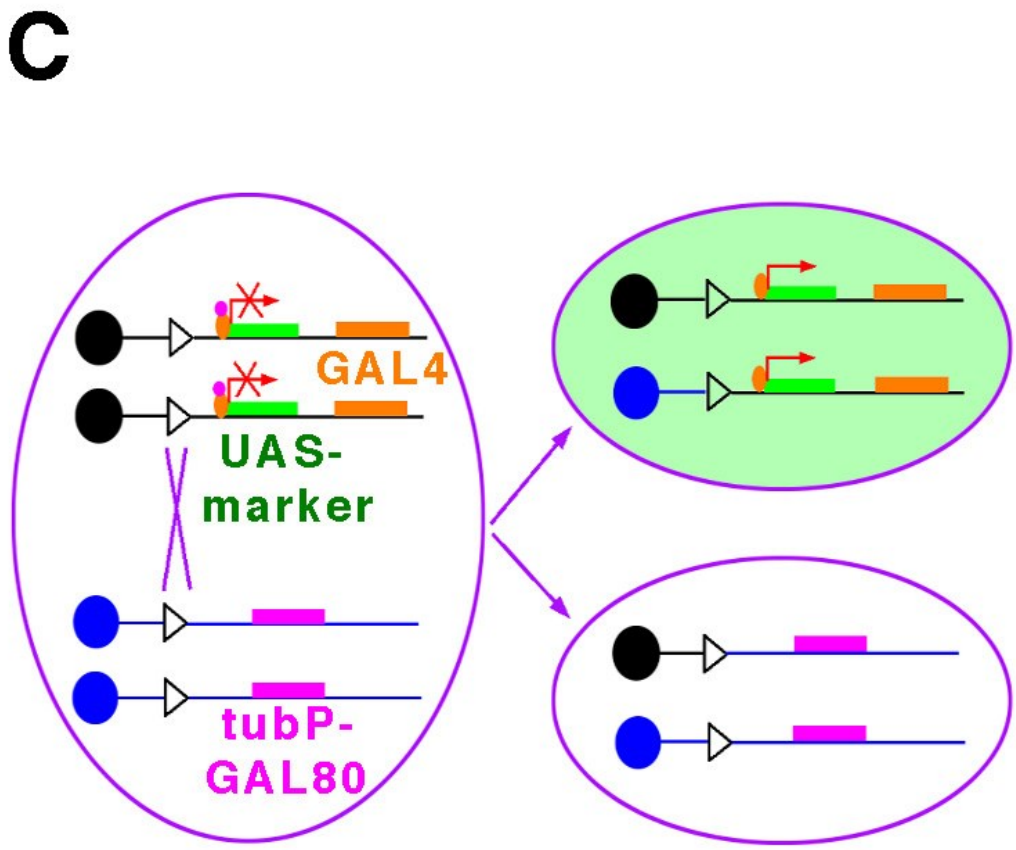

Figure 3-10. Schematic of Mosaic Analysis of a Repressible Cell Marker (MARCM).

The expression of the UAS-tagged transgene under a specific GAL4 driver is repressed by the presence of GAL80 in the parent cell. After FLP-mediated recombination at the FRT sites (white triangles), GAL80 is lost in the homozygous mutant daughter cell (green cell), and the UAS-transgene is expressed along with a GFP marker. The recombination will also give rise to a homozygous wild-type cell (white cell), and a heterozygous daughter cell (not shown). Image used with permission from Lee et al., 1999. Flybrain on-line: [http://www.flybrain.org] Accession Number: AD00021.

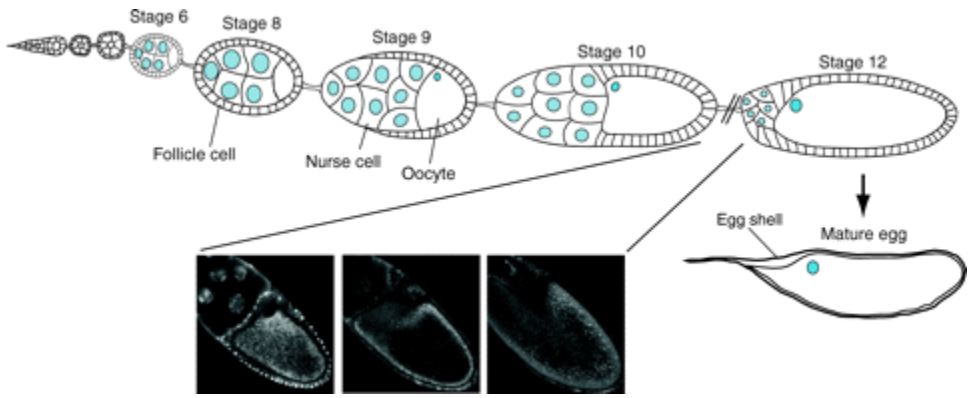

Figure 3-11. Schematic of Drosophila oogenesis.

Drosophila oogenesis occurs within an ovariole in an assembly line-like fashion. A cystoblast is produced from the germarium. The cystoblast divides 4 times and produces a cluster of 16 nuclei. One of the nuclei will differentiate into an oocyte, and the other 15 nuclei become polyploid nurse cells. The somatic follicle cell epithelium surrounds the entire cluster of 16 cells, called the egg chamber. The 14 developmental stages leading to the mature egg (stage 14) are morphologically different. Posterior is the side where the oocyte is located, and apical is facing the oocyte. Image from (Becalska and Gavis 2009), Open Access.

Loss of Merlin expression in follicle cells (Mer^4) did not result in any detectable phenotypes in stages 7 to 9. Single focal plane confocal images taken through an egg chamber with posterior Mer^4 clones show a regular follicle cell epithelium with consistent expression of apical DE-cadherin and the septate junction marker Coracle (Figure 3-12 A-E). Similar observations were seen in the majority of Merlin-null follicle cell clones over-expressing wild-type Merlin (Mer^4;+;$Merlin^{WT}$ Figure 3-13 A-E).

While the majority of Merlin-null clones over-expressing serine 371 or threonine 18 transgenes appeared similar to Merlin-null (Mer^4) or wild-type Merlin ($Merlin^{WT}$) clones, adhesion defects were observed in a small number of egg chambers between developmental stages 7 to 9 in Mer^4 clones over-expressing the phosphorylation mutants. As shown in Figure 3-12 (panels F-J), DE-cadherin was reduced in GFP-positive Mer^4;+;$Merlin^{S371A}$ clones positioned along the main body cells (panel I, yellow rectangle), close to the posterior follicle cells. Coracle staining is unchanged. In Figure 3-12 (panels K-O), a small region of cells in the GFP-positive region, at the anterior side of the egg chamber in the stretched cells, have begun pinching off apically into the egg chamber (Figure 3-12 N, yellow arrowhead). Coracle appears unchanged surrounding the nuclei.

Figure 3-12. Loss of adhesion in Merlin^{S371A} clones.

Singe focal plane confocal images of stage 7 to stage 9 egg chambers with GFP-positive Merlin-null (Mer^{4}) clones simultaneously over-expressing Merlin^{S371A}.

(A-E) Mer^{4} clones at the posterior end of a stage 7-8 egg chamber. DE-cadherin appears reduced at bottom left corner because of the angle of the egg chamber. Both DE-cadherin and coracle are uniform throughout the epithelial layer. Scale bar represents 10 μm.

(F-J) Mer^{4};+;Merlin^{S371A} clones in the main body cells at the posterior region of a stage 7-8 egg chamber. DE-cadherin is reduced in the GFP-positive clone region (I, yellow rectangle). Coracle is unchanged throughout the epithelium. Scale bar represents 5 μm.

(K-O) Mer^{4};+;Merlin^{S371A} clones in the anterior region of a stage 7-8 egg chamber. A region of stretched cells appear to be pinching off apically toward the nurse cells into the egg chamber (N, yellow arrowhead). Coracle staining remains uniform around the cells. Scale bar represents 5 μm.

(P) Schematic of stage 6 to stage 9 egg chambers. Posterior is on the side of the oocyte. Apical faces the oocyte. Image from (Becalska and Gavis 2009).

Mer4 alone
Mer4;+;MerlinS371A
A
B
C
D
E
F
G
H
I
J
K
L
M
N
O
DAPI
GFP+ clones
DCAD
Coracle
Myc
P
Stage 6
Stage 8
Stage 9
Follicle cell
Nurse cell
Oocyte

Mutation of serine 371 to aspartic acid also leads to loss of adhesion in stage 7 to 9 egg chambers. In Figure 3-13 (panels F-J), there appears to be more than one layer of posterior follicle cells in the GFP-positive Mer^{4};+;$Merlin^{S371D}$ region (yellow arrowheads). Apical DE-cadherin is reduced in the GFP-positive Mer^{4};+;$Merlin^{S371D}$ clones, and these cells have lost contact with the follicle cell epithelium to form a double-layer as shown by the two layers of DE-cadherin staining. Coracle staining is also brighter on the apical side of the outer layer (Figure 3-13 J). Figure 3-13 (panels K-O) shows another egg chamber in which a cluster of GFP-positive Mer^{4};+;$Merlin^{S371D}$ cells have detached basally from the epithelial layer, appearing as a cluster of GFP-positive cells sitting on the surface of the follicle cell layer (most visible in Figure 3-13 L). DE-cadherin and Coracle are disrupted in the clones (Figure 3-13 N-O). Figure 3-13 (panels P-T) show a single plane confocal image of the surface of a stage 9 egg chamber with GFP-positive Mer^{4};+;$Merlin^{S371D}$ clones that have lost adhesive properties and have moved basally from the follicle cell epithelium, indicated by the difference in focus of the nuclei (Figure 3-13 Q). DE-cadherin is mislocalised in the clone regions (Figure 3-13 T, yellow arrowheads). Together with the effects observed with Mer^{4};+;$Merlin^{S371A}$ clones, this suggests that the serine 371 site is involved in regulating Merlin's role in adhesion.

Figure 3-13. Loss of adhesion in Merlin^{S371D} clones.

Singe focal plane confocal images of stage 7 to stage 9 egg chambers with GFP-positive Merlin-null (Mer^{4}) clones simultaneously over-expressing wild-type Merlin or Merlin^{S371D}.

(A-E) Mer^{4};+;Merlin^{WT} clones at the anterior end of a stage 7-8 egg chamber. Both DE-cadherin and coracle are consistent throughout the epithelial layer. Scale bar represents 5 μm.

(F-J) Mer^{4};+;Merlin^{S371D} clones in the posterior follicle cells of a stage 7-8 egg chamber. DE-cadherin is reduced in the GFP-positive clone region, and there is more than one layer of cells (I, yellow arrowhead). Coracle staining is brighter on the apical side of the outer epithelial layer (J, yellow arrowhead). Scale bar represents 10 μm.

(K-O) Mer^{4};+;Merlin^{S371D} clones in the posterior end of a stage 8-9 egg chamber. A GFP-positive clone region has detached from the epithelial layer and has moved basally to the surface of the egg chamber (yellow arrowheads). DE-cadherin and coracle are mislocalised in this region (N-O). Scale bar represents 10 μm.

(P-T) *En face* image of two Mer^{4};+;Merlin^{S371D} clone regions on the surface of a stage 9 egg chamber. The position of the nuclei show that the GFP-positive clones are at not at the same focal plane as the rest of the follicle cell epithelium (Q). DE-cadherin is mislocalised in the clone regions (T, yellow arrowheads). Scale bar represents 10 μm.

A
B
DAPI
C
GFP+ clones
D
DCAD
E
Coracle
F
G
DAPI
H
GFP+ clones
I
DCAD
J
Coracle
K
L
DAPI
M
GFP+ clones
N
DCAD
O
Coracle
P
Q
DAPI
R
GFP+ clones
S
Myc
T
DCAD
Mer4;+;MerlinWT
Mer4;+;MerlinS371D

A more severe loss of adhesion was observed in adjacent epithelial layers. Figure 3-14 shows several sections through the follicle cell epithelium of the posterior and anterior end of two adjacent stage 5 to 6 egg chambers. There is a significant disruption of adhesion around the GFP-positive Mer^{4};+;$Merlin^{S371A}$ clone regions. Sections at the top and bottom of the z-stack (Figure 3-14 A-E, A‴-E‴) show that that epithelial layers are orderly and apical F-actin and αPKC localisation is relatively consistent along the apical side at the top of the z-stack. Sections through the center of the epithelial layers (Figure 3-14 A′-E′, A″-E″) show that GFP-positive clone regions surround non-GFP regions of the epithelium that have lost their orderly arrangement and are detaching from the epithelial layer into the interior of the egg chambers. F-actin is severely mislocalised and upregulated (Figure 3-14 D′-D″, yellow arrowhead), and αPKC is lost from these cells (Figure 3-14 E′-E″, yellow arrowhead), suggesting defects in adhesion.

Figure 3-14. Adjacent Mer^4;+;$Merlin^{S371A}$ egg chambers delaminating from each other.

Singe focal plane confocal images of adjacent stage 5-6 egg chambers with GFP-positive Merlin-null (Mer^4) clones simultaneously over-expressing $Merlin^{S371A}$.

Z-sections through the two membranes show them moving away from each other. F-actin is upregulated and mislocalised. aPKC is reduced in the regions that have lost adhesion. Scale bar represents 5 μm.

(A-E) Single-slice image taken 2 μm below the top of the z-stack. A region of GFP-positive clones expressing Mer^4;+;$Merlin^{S371A}$ can be seen in the follicle cell epithelium of both egg chambers (C-C‴). Actin and aPKC expression is consistent throughout the epithelial layers (D-E).

(A′-E′) Single-slice image taken 8.7 μm below the top of the z-stack. The GFP-positive clone regions of the adjacent epithelium layers have begun to move apically away from each other. Actin is highly upregulated and mislocalised (D′, yellow arrowhead), and aPKC is mislocalised or lost in the apical sides of both egg chambers (E′, yellow arrowhead).

(A″-E″) Single-slice image taken 11.6 μm below the top of the z-stack. The two epithelium layers have moved away from each other, resulting in a hole between the two egg chambers. Actin is highly upregulated and mislocalised (D″), and aPKC is mislocalised or lost (E″).

(A‴-E‴) Single-slice image taken 15.7 μm below the top of the z-stack. The two epithelium layers are adjacent to each other again on the other side of the 'hole'. Actin is still upregulated and mislocalised (D‴). aPKC is relatively more consistent throughout the epithelium layers, but still shows some mislocalisation (E‴).

$Mer^{4};+;Merlin^{S371A}$

Effects suggesting loss of adhesion were also observed in early developmental stages when Merlin^{T18D} was over-expressed in a Merlin-null background. Figure 3-15 (panels K-O) shows the anterior region of a stage 8-9 egg chamber with Mer^{4};+;Merlin^{T18D} clones showing brighter Sip1 and Moesin staining on the apical side of the GFP-positive Mer^{4};+;Merlin^{T18D} clones (yellow arrowheads). The morphology of the epithelium in this region also appears uneven. This effect was not observed with the over-expression of wild-type Merlin clones (Figure 3-15 F-J) or in Merlin-null clones (Figure 3-15 A-E). DE-cadherin and coracle is also mislocalised baso-laterally in a small Mer^{4};+;Merlin^{T18D} clone in Figure 3-15 (panels P-T), suggesting an effect on adhesion when threonine 18 is mutated to aspartic acid.

Further evidence supporting the role of the threonine 18 site in regulating Merlin function in maintaining epithelial integrity, Figure 3-16 shows an example of a stage 7 Mer^{4};+;Merlin^{T18D} egg chamber showing a severe loss of adhesion. Single-slice cross-sections through the egg chamber shows a normal epithelial layer (Figure 3-16 A-E) that has lost adhesion in the GFP-positive clone region and has moved apically toward the nurse cells (Figure 3-16 A'-E', yellow arrowhead), resulting in two follicle cell epithelial layers that form a 'donut' shape (Figure 3-16 A"-E", yellow arrowhead). Apical actin and aPKC is completely lost in both layers, suggesting a loss of polarity and adhesion.

Loss of adhesion was also observed in adjacent epithelial layers. Figure 3-17 shows the follicle cell epithelium at the anterior and posterior ends of two adjacent stage 5 to 6 Mer^{4};+;$Merlin^{T18D}$ egg chambers, where GFP-positive clones can be seen around GFP-negative cells that have lost adhesion with the rest of the epithelial layer and have moved apically into the egg chamber (Figure 3-17 C-C", D-D", yellow arrowhead). Apical F-actin staining is highly upregulated and mislocalised in the detached regions, indicating loss of polarity (Figure 3-17 D-D", yellow arrowheads).

Figure 3-15. Mislocalisation of Sip1, Moesin, DE-cadherin, and Coracle in stage 7 to stage 9 Merlin^{T18D} clones.

Singe focal plane confocal images of stage 7 to stage 9 egg chambers with GFP-positive Merlin-null (Mer^{4}) clones simultaneously over-expressing wild-type Merlin or Merlin^{T18D}.

(A-E) Sip1 and Moesin localisation is consistent throughout the follicle cell epithelium in the anterior region of a stage 7-8 egg chamber expressing Merlin-null clones. Scale bar represents 5 μm.

(F-J) Sip1 and Moesin localisation is consistent throughout the follicle cell epithelium in the anterior region of a stage 7-8 egg chamber expressing Mer^{4};+;Merlin^{WT} clones. Scale bar represents 5 μm.

(K-O) Sip1 and Moesin are upregulated in Mer^{4};+;Merlin^{T18D} clones at the anterior region of a stage 8-9 egg chamber (N-O, yellow arrowheads). The morphology of the clones also appears irregular. Scale bar represents 5 μm.

(P-T) A small clone region in a stage 8-9 egg chamber shows baso-lateral mislocalisation of DE-cadherin (S, yellow arrowhead) and coracle (T, yellow arrowhead). Scale bar represents 5 μm.

A
B
DAPI
C
GFP+ clones
D
Sip1
E
Moesin
F
G
DAPI
H
GFP+ clones
I
Sip1
J
Moesin
K
L
DAPI
M
GFP+ clones
N
Sip1
O
Moesin
P
Q
DAPI
R
GFP+ clones
S
DCAD
T
Coracle
Mer4 alone
Mer4;+;MerlinWT
Mer4;+;MerlinT18D

Figure 3-16. Delamination of follicle cells from the follicle cell epithelium layer in a stage 7 Mer^{4};+;$Merlin^{T18D}$ egg chamber.

Singe focal plane confocal images of a stage 7 egg chamber with GFP-positive Merlin-null (Mer^{4}) clones simultaneously over-expressing $Merlin^{T18D}$.

Z-sections taken through the follicle cell layer at the anterior region. Scale bar represents 5 μm.

(A-E) Single-slice image at the top of the z-stack through the center of the egg chamber (relative focus position at 0 μm). The follicle cell epithelium is in a single layer. A small GFP-positive clone region is visible at the bottom of (C). Actin and aPKC staining is consistent throughout the cells.

(A′-E′) Single-slice image taken 6.4 μm below the top of the z-stack. The follicle cell epithelium can be seen moving apically into the egg chamber toward the nurse cell nucleus visible in (B′). Apical actin and aPKC is lost in the cells that have moved apically (D′-E′, yellow arrowheads).

(A″-E″) Single-slice image taken 18.6 μm below the top of the z-stack. The follicle cells are present in two distinct layers with a hole in the centre (B″, yellow arrowhead), with the GFP-positive clones in the interior layer (C″). Apical actin and aPKC is completely lost in both layers (D″-E″).

Mer4;+;MerlinT18D
A
0 µm
A'
-6.4 µm
A''
-18.6 µm
B
B'
B''
DAPI
C
C'
C''
GFP+ clones
D
D'
D''
actin
E
E'
E''
aPKC

Figure 3-17. Loss of adhesion in adjacent Mer^{4};+;$Merlin^{T18D}$ stage 5-6 egg chambers.

Singe focal plane confocal images of adjacent stage 5-6 egg chambers with GFP-positive Merlin-null (Mer^{4}) clones simultaneously over-expressing $Merlin^{T18D}$.

Z-sections through the follicle cell layers show the two membranes moving away from each other. Scale bar represents 5 μm.

(A-D) Single-slice image taken 1.5 μm below the top of the z-stack. A region of GFP-positive clones expressing Mer^{4};+;$Merlin^{T18D}$ can be seen in the follicle cell epithelium of both egg chambers (C-C″). Actin is upregulated where the epithelial layers are moving away from each other, and is beginning to look mislocalised at the apical side of the older egg chamber at the bottom of the image (D).

(A′-D′) Single-slice image taken 9.3 μm below the top of the z-stack. The GFP-positive clone regions of the adjacent epithelial layers have delaminated and moved apically away from each other (C′, yellow arrowhead). Actin is highly upregulated (D′, yellow arrowhead).

(A″-D″) Single-slice image taken 16.9 μm below the top of the z-stack. The epithelial layers on the other side of the delamination have retained a comparatively wild-type morphology. Actin localisation is consistent through the epithelial layer (D″, yellow arrowhead).

Mer4;+;MerlinT18D
A
-1.5 µm
A'
-9.3 µm
A''
-16.9 µm
B
B'
B''
C
C'
C''
D
D'
D''
DAPI
GFP+ clones
actin

The observations in early-stage Drosophila egg chambers show that mutation of serine 371 to either alanine or aspartic acid, and mutation of threonine 18 to aspartic acid affects adhesion and the maintenance of epithelial integrity. No results were obtained from mutating threonine 18 to alanine, likely due to the small number of clones that are generated using the MARCM method. Lethality is not likely as Mer^{4};+;$Merlin^{T18A}$ clones were obtained at stage 14.

Stage 14 eggs were also examined for effects of the serine 371 and threonine 18 mutations in later developmental stages. Clones were identified as GFP-positive regions on the surface of the egg shell, and were often observed as clusters of cells that are located on top of the egg shell layer. Figure 3-18 and Figure 3-19 shows screen captures of 3D displays of z-stacks taken of the surface of stage 14 eggs. In Figure 3-18, the over-expression of $Merlin^{S371A}$ in Merlin-null clones can be identified by the MYC staining (panels E-L). The Mer^{4};+;$Merlin^{S371A}$ clones have clustered on the surface of the stage 14 egg shell layer. The nuclei appear highly irregular, and DE-cadherin is also highly mislocalised in the clones when compared to the regular lattice pattern on the egg shell surface. Mer^{4};+;$Merlin^{S371D}$ clones were also observed to interrupt the DE-cadherin lattice arrangement to a lesser extent whether they were observed in a small surface cluster (Figure 3-18 M-P) or as a large flatter region on the egg shell surface (Figure 3-18 Q-S). The over-expression of wild-type Merlin in the Merlin-null clones (Figure 3-18 A-D)

also results in some mislocalisation of DE-cadherin and coracle, but the lattice pattern of the DE-cadherin on the egg shell layer is retained.

Figure 3-18. 3D screen captures *en face* of Mer^{4};+;$Merlin^{S371}$ clones in stage 14 eggs.

Clones are clustered together on the surface of the egg shell layer. DE-cadherin patterning is disrupted and mislocalised in the clones. BitPlane Imaris was used to visualize the confocal images in 3D.

(A-D) Mer^{4};+;$Merlin^{WT}$ clones on the surface of a stage 14 egg. DE-cadherin and coracle staining is irregular in the clone region, but a maintenance of the lattice pattern can still be observed. The appearance of the nuclei in the clones is comparable to the nuclei in the non-GFP regions. Scale bar represents 10 μm.

(E-L) Mer^{4};+;$Merlin^{S371A}$ clones on the surface of stage 14 eggs. DE-cadherin is highly mislocalised in the clone region. The nuclei in the clone region is clustered and in an irregular pattern compared to the non-GFP regions. Scale bar represents 20 μm.

(M-P) Mer^{4};+;$Merlin^{S371D}$ clones on the surface of a stage 14 egg. DE-cadherin is mislocalised in the clone region, but the lattice pattern is maintained The nuclei in the clone region appear to be in the same layer as the egg shell layer, but appear clustered and in an irregular pattern compared to the non-GFP regions. Scale bar represents 10 μm.

(Q-S) Mer^{4};+;$Merlin^{S371D}$ clones on a flat region of a stage 14 egg shell surface. DE-cadherin is disorganised in the clone region compared to the non-GFP regions, but the nuclei are not clustered together in the clone region. Scale bar represents 10 μm.

(T) Schematic of a stage 14 mature egg. (A-S) depict 3D displays of confocal images taken *en face* of the surface of the egg shell. Image from (Becalska and Gavis 2009).

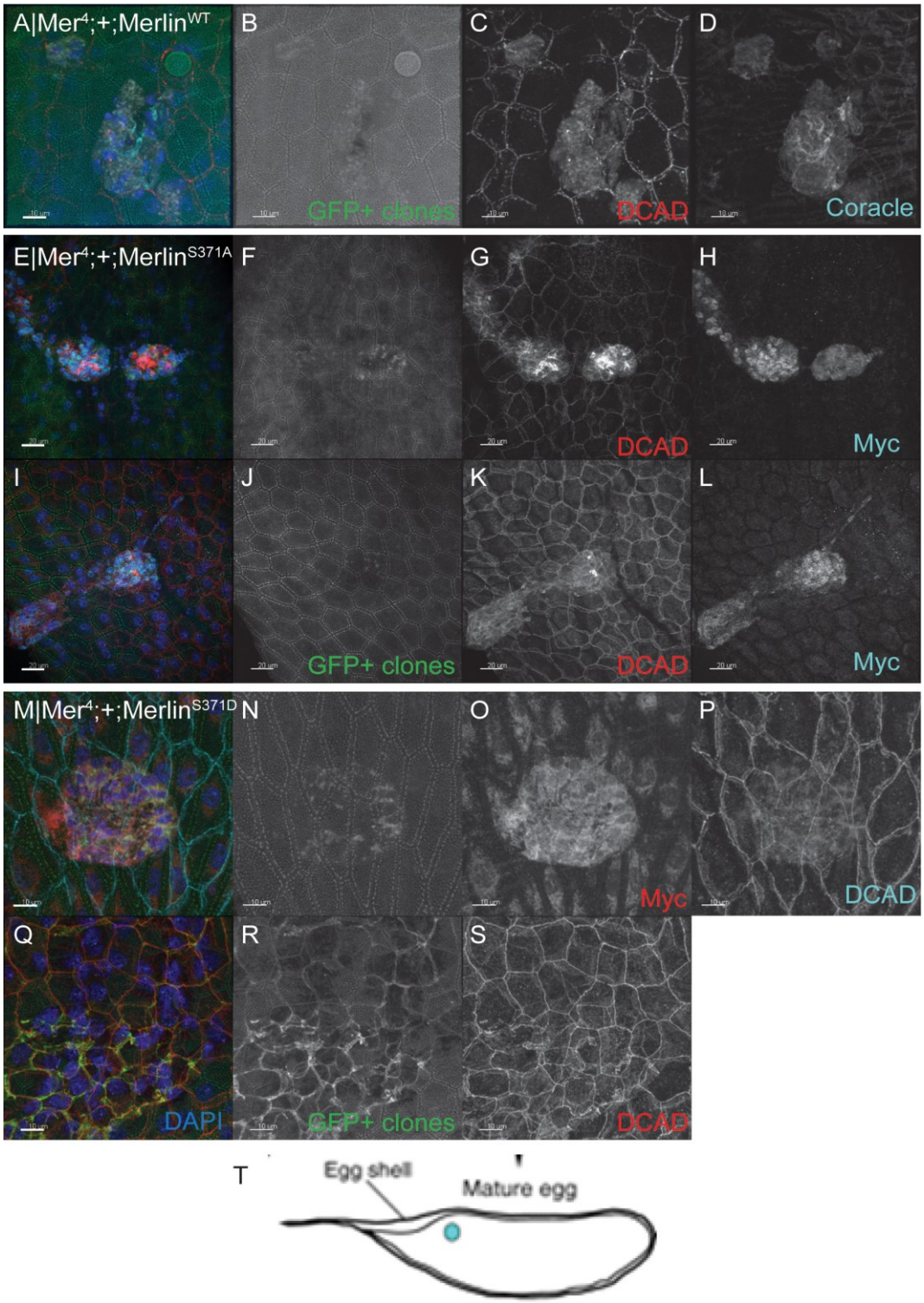
A|Mer4;+;MerlinWT
B
GFP+ clones
C
DCAD
D
Coracle
E|Mer4;+;MerlinS371A
F
G
DCAD
H
Myc
I
J
GFP+ clones
K
DCAD
L
Myc
M|Mer4;+;MerlinS371D
N
O
Myc
P
DCAD
Q
DAPI
R
GFP+ clones
S
DCAD
T
Egg shell
Mature egg

Similar phenotypes were seen in Mer^{4};+;$Merlin^{T18}$ clones in stage 14 eggs. Figure 3-19 (panels E-L) shows GFP-positive Mer^{4};+;$Merlin^{T18A}$ clones on the surface of stage 14 eggs. DE-cadherin (Figure 3-19 G), coracle (Figure 3-19 H), and actin (Figure 3-19 K) appear mislocalised, but a maintenance of the lattice pattern of the egg shell surface can still be observed. aPKC is slightly upregulated in the clone region (Figure 3-19 L). The effect of expressing Mer^{4};+;$Merlin^{T18D}$ has a more severe effect on adhesion (Figure 3-19 M-S), as the nuclei of the GFP-positive regions appear much more clustered and disorganised compared to the GFP-negative regions and in wild-type and $Merlin^{T18A}$. DE-cadherin (Figure 3-19 O, S) and coracle (Figure 3-19 P) is highly upregulated and disorganised, and the lattice pattern is almost completely lost.

Taken together, all of the effects of the serine 371 and threonine 18 mutations on the morphology of the follicle cell epithelium in the Drosophila egg chambers and on the localisation of various adhesion markers suggest that both of these residues are involved in the regulation of Merlin's role in the maintenance of epithelial integrity.

Figure 3-19. 3D screen captures *en face* of Mer^{4};+;$Merlin^{T18}$ clones in stage 14 eggs.

Clones have clustered together on the surface of the egg shell layer. BitPlane Imaris was used to visualize the confocal images in 3D.

(A-D) Mer^{4};+;$Merlin^{WT}$ clones on the surface of a stage 14 egg. DE-cadherin staining is irregular in the clone region, but a maintenance of the lattice pattern can still be observed. The appearance of the nuclei in the clones is comparable to the nuclei in the non-GFP regions. Scale bar represents 10 μm.

(E-L) Mer^{4};+;$Merlin^{T18A}$ clones on the surface of stage 14 eggs. DE-cadherin (G), coracle (H), aPKC (L) is mislocalised in the clone region, and the actin lattice pattern also appears disrupted (K). The nuclei in the clone region are clustered and in an irregular pattern as compared to the non-GFP regions. Scale bar represents 5 μm.

(M-S) Mer^{4};+;$Merlin^{T18D}$ clones on the surface of stage 14 eggs. DE-cadherin (O, S) and coracle (P) is severely disorganised in the clone region compared to the non-GFP regions. Scale bar represents 10 μm.

(T) Schematic of a stage 14 mature egg. (A-S) depict 3D displays of confocal images taken *en face* of the surface of the egg shell. Image from (Becalska and Gavis 2009).

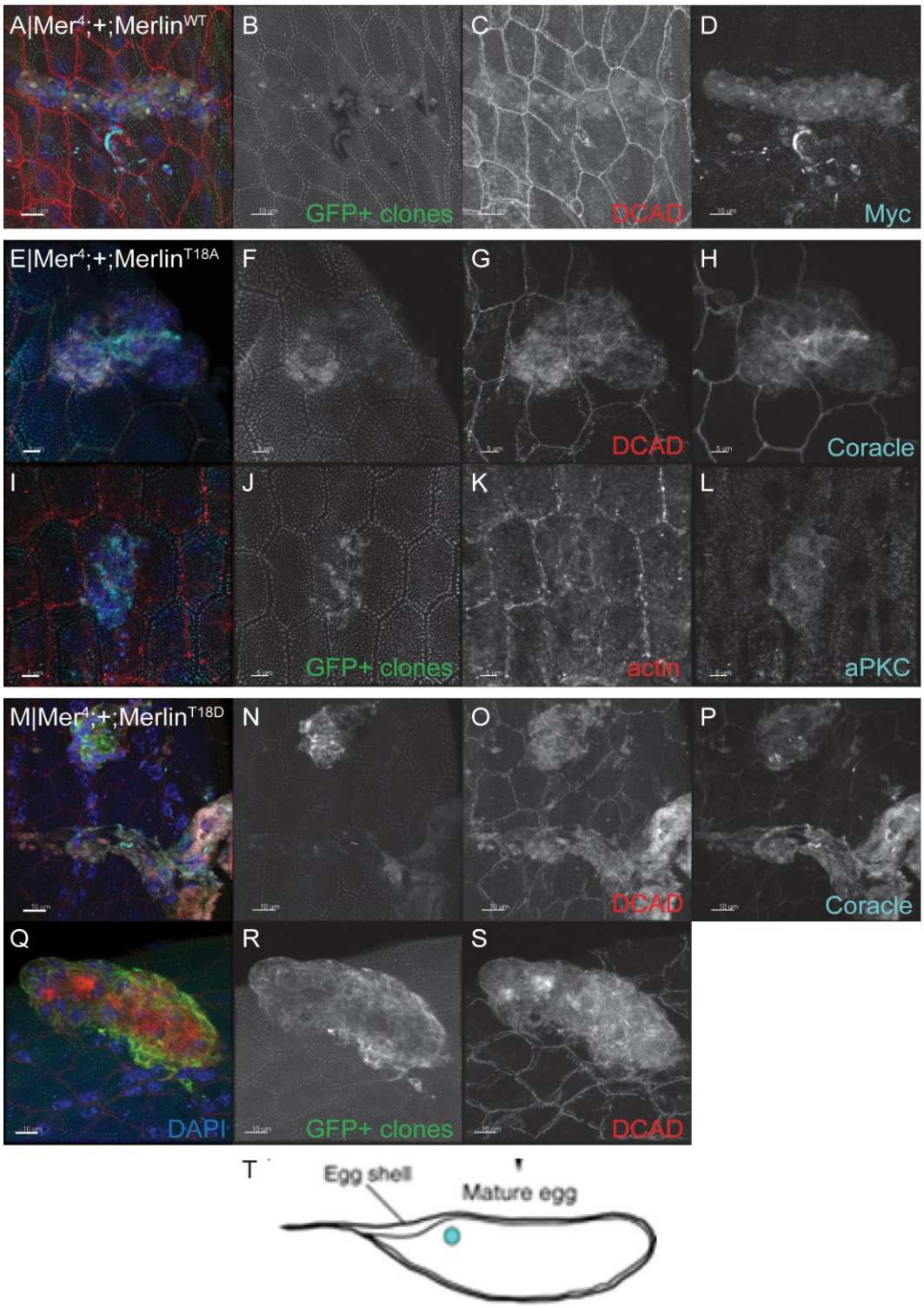
A|Mer4;+;MerlinWT
B
GFP+ clones
C
DCAD
D
Myc
E|Mer4;+;MerlinT18A
F
G
DCAD
H
Coracle
I
J
GFP+ clones
K
actin
L
aPKC
M|Mer4;+;MerlinT18D
N
O
DCAD
P
Coracle
Q
DAPI
R
GFP+ clones
S
DCAD
T
Egg shell
Mature egg

3.1.3 Phosphorylated Threonine 18 is ubiquitinated and targeted for degradation

Previous studies in human merlin have identified serine 10 as a key residue in regulating merlin degradation through phosphorylation by the kinase Akt, which directs merlin for proteasome-mediated degradation (Laulajainen et al. 2011). As threonine 18 is also located at the N-terminal region of Drosophila Merlin, we hypothesised that this residue may be involved in regulating Merlin degradation through phosphorylation.

Preliminary experiments over-expressing Merlin^{T18A} and Merlin^{T18D} in S2 cells using a ubiquitous actin-GAL4 driver suggest that mutation of threonine 18 to a phosphomimetic aspartic acid results in increased ubiquitin of the Merlin protein when the proteasome is inhibited with MG132 (Figure 3-20). Mutation of threonine 18 to a non-phosphorylatable alanine is comparable to wild-type. This suggests that the phosphorylation of threonine 18 is involved in proteasome-mediated degradation of Merlin.

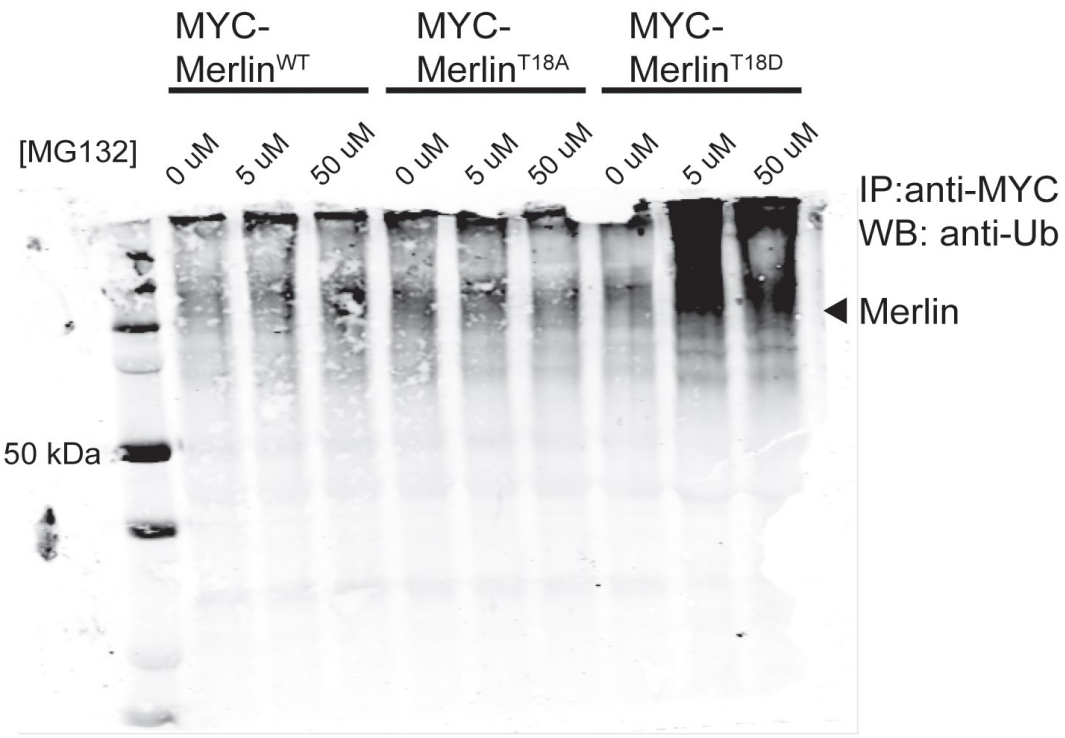

Figure 3-20. Increased ubiquitination of Merlin^{T18D}.

Higher levels of ubiquitin is detected in S2 cells over-expressing Merlin^{T18D} when the proteosome is inhibited (with the proteasome inhibitor MG132 at 5 μM and 50 μM concentrations) when compared to wild-type Merlin and Merlin^{T18A}. Experiment performed by David Primrose.

Table 4. Summary of observations in adult Drosophila wings and third instar larval wing discs.

	$Merlin^{WT}$	$Merlin^{S371A}$	$Merlin^{S371D}$	$Merlin^{T18A}$	$Merlin^{T18D}$
patched region area	N/A	Significantly larger compared to $Merlin^{WT}$		No significant differences compared to $Merlin^{WT}$	Significantly smaller compared to $Merlin^{WT}$
MYC localisation	Membranous	Membranous and cytoplasmic	Membranous and cytoplasmic; more cytoplasmic than $Merlin^{S371A}$	Membranous and cytoplasmic	Membranous and cytoplasmic; more cytoplasmic than $Merlin^{T18A}$
DE-cadherin localisation	Over-expression effects; slightly brighter DE-cadherin staining below apical surface in expression region	Brighter DE-cadherin staining right below apical surface of wing disc, especially at the intersection of the dorsal-ventral and anterior-posterior boundaries. Brighter than what is observed with over-expression of $Merlin^{WT}$.			
Sip1 localisation	No changes				
F-actin localisation	No changes	Subtle increase in F-actin staining along edge of expression region in dorsal compartment	No changes		

Table 5. Summary of MARCM clonal analysis observations.

	Mer^{4}	$Merlin^{WT}$	$Merlin^{S371A}$	$Merlin^{S371D}$	$Merlin^{T18A}$	$Merlin^{T18D}$
Stage 6-9 egg chambers, Follicle cell epithelium	No changes	No changes	Reduced DE-cadherin, Loss of adhesion, Disrupted apical actin and aPKC	Disrupted DE-cadherin and Coracle, Loss of adhesion	No clones observed	Increased basolateral DE-cadherin and Coracle, Loss of adhesion, Disrupted apical actin and aPKC Upregulated Moesin and Sip1
Proportions			6/15 N=5	5/26 N=5		4/12 N=4
Stage 14 eggs, Egg shell	8 clones imaged	Some mis-localisation of DCAD; Lattice pattern maintained 4 clones imaged	Clustering of nuclei on egg shell surface, Mis-localised DE-cadherin 9 clones imaged	Clustering of nuclei on egg shell surface, Mis-localised DE-cadherin; Lattice pattern maintained 14 clones imaged	Clustering of nuclei on egg shell surface Mis-localised DE-cadherin, Coracle, Slightly disrupted actin and aPKC 7 clones imaged	Severe clustering of nuclei on egg shell surface, Severely mislocalised DE-cadherin 12 clones imaged

Chapter 4

Discussion

4 Chapter 4: Discussion

4.1 Role of Serine 371 in regulating Merlin cellular localisation and tumour suppressor function

Over-expression of the phosphomimetic Merlin mutant Merlin^{S371D} resulted in a change in Merlin localisation pattern in S2 cells over time when compared to wild-type. The trafficking of Merlin from the plasma membrane into intracellular punctae is delayed (Figure 3-4). This effect was similar to, but weaker than, what was previously found using an inactive Merlin phosphomimetic mutant at threonine 616 (Merlin^{T616D}), where Merlin^{T616D} was found at high proportions at the plasma membrane even at 6 hours after heat-shock (Hughes and Fehon 2006). This suggests that phosphorylation at serine 371 inactivates Merlin. There was no change in the localisation pattern of Merlin^{S371A} compared to wild-type Merlin. The changes in localisation patterns could be due to a defect in endocytosis, as Merlin can associate with endocytic structures in S2 cells (McCartney and Fehon 1996). This defect could also be affecting Merlin inhibition of EGFR, affecting the kinetics of EGFR internalisation and signaling, consequently affecting cell cycle progression, as it has been shown that the kinetics of EGFR endocytosis changes during M phase (Liu et al. 2011). However, the modified pulse-chase assay in S2 cells is not a direct test for Merlin function in cell proliferation or cell adhesion, as the cell line is semi-adherent (Schneider 1972). Therefore, adult wings and

larval wing discs were used as an *in vivo* system to further examine Merlin function.

Adult Drosophila wings were used to examine the effects of the serine 371 mutations on cell proliferation (Figure 3-6 B). Mutation of serine 371 to non-phosphorylatable alanine ($Merlin^{S371A}$), when over-expressed in the *patched* region of the adult wing, caused a significant increase in the *patched* area compared to over-expression of wild-type Merlin. Mutation to a phosphomimetic aspartic acid ($Merlin^{S371D}$) also caused a significant increase in the *patched* area compared to both wild-type Merlin and to $Merlin^{S371A}$. Mutation of serine 371 to alanine was hypothesised to mimic Merlin activation, therefore repressing cell proliferation and reducing tissue size. Thus, it was not expected that both mutations would lead to an increase in tissue size. This result suggests that both mutations are inactivating in terms of Merlin's function in inhibiting cell proliferation. This also suggests that Merlin phosphorylation does not simply confer a binary 'active-inactive' effect on the protein, where the phosphorylation status of a residue completely activates or inactivates Merlin, but instead may involve many levels of regulation leading to different levels of Merlin activity depending on the combination of phosphorylation statuses of one or more residues. The mutation of serine 371 to alanine or aspartic acid thus may be changing the level of activity of the Merlin protein.

Previous studies in mammalian Merlin have shown that wild-type and hypophosphorylated Merlin localises to the cell membrane of RT4 cells, whereas a phosphomimetic Merlin mutant was also observed in the perinuclear region in addition to localisation at the plasma membrane (Kissil et al. 2002, Surace et al. 2004). Merlin phosphorylation has also been linked to localisation (Kissil et al. 2002); an inactivating Merlin mutation at serine 518 to aspartic acid causes Merlin localisation to vesicular structures, whereas wild-type and an activating Merlin mutation at serine 518 to alanine localises to the membrane. In larval wing discs, the non-phosphorylatable Merlin^{S371A} showed a membranous and cytoplasmic localisation pattern (Figure 3-7), and the phosphomimetic Merlin^{S371D} was more cytoplasmic compared both wild-type Merlin and Merlin^{S371A}. The localisation pattern of both Merlin^{S371A} and Merlin^{S371D} in the cytoplasm away from the plasma membrane in larval wing discs, taken together with the increase in the *patched* region area in the adult wings when either mutant is over-expressed as compared to wild-type Merlin, suggest that this phosphorylation site is involved in the deactivation of Merlin in its tumour suppressor function. The mechanism regulating this deactivation may involve Merlin binding with Sip1 and/or Merlin conformation.

4.1.1 Role of Serine 371 in Merlin-Sip1 binding

Previous work by A. Leung (Leung 2011) identified a 100-amino acid region in the coiled-coil domain of the Merlin protein immediately following the Merlin FERM domain. This region was shown to be crucial for binding to Sip1. Serine 371 is located within these 100 amino acids, and both Merlin^{S371A} and Merlin^{S371D} reduced Merlin binding to Sip1. Effects of the alanine and aspartic acid mutations in serine 371 on Merlin conformation was suggested as a possible cause of reduced Merlin-Sip1 binding; thus, the phosphorylation at this site was suggested as a mechanism for regulating Merlin-Sip1 binding. Reduced binding to Sip1 could lead to a reduced tethering of Merlin to the membrane. This is a possible explanation for the localisation pattern of Merlin^{S371A} and Merlin^{S371D} away from the plasma membrane in larval wing discs. Previous work *in vitro* showed that mutation of serine to alanine or aspartic acid reduced but did not abolish Sip1-Merlin binding, providing a possible explanation for why the majority of Merlin^{S371A} and Merlin^{S371D} mutant protein was still localised close to the membrane and was not highly cytoplasmic.

In studies using mammalian merlin, binding affinity to the mammalian Sip1 homolog EBP50 was examined in a non-phosphorylatable Merlin^{S518A} mutant and a phosphomimetic Merlin^{S518D} mutant (Sher et al. 2012). The non-phosphorylatable Merlin^{S518A} bound EBP50 with a higher affinity than Merlin^{S518D},

in agreement with previous findings that the non-phosphorylatable Merlin^{S371A} binds Sip1 with a slightly higher affinity than Merlin^{S371D} (Leung 2011).

The effect of the serine 371 site on the binding affinity with Sip1 could have implications on the regulation of Merlin and Moesin in our switch hypothesis presented in Chapter 1 and Figure 1-3, in which Sip1 is hypothesised to be involved in a complex with Slik and Flapwing to regulate Merlin and Moesin through phosphorylation and dephosphorylation of the two proteins. Sip1 has been previously shown to be required for the proper localisation of Slik and the activation of Moesin through phosphorylation (Hughes and Fehon 2006, Hughes et al. 2010), and it is possible that interaction with Sip1 may also be required for proper Merlin localisation and possibly Merlin activation, leading to a loss of repression of cell proliferation and the increase in wing size that was observed.

Previous work in mammalian cells examining the binding affinity of the mammalian Sip1 homolog EBP50 with one of the mammalian ERMs ezrin and merlin showed that EBP50 changes its preference for ezrin over merlin after the activation of ezrin (Nguyen et al. 2001). Thus, the phosphorylation status of serine 371 may influence Merlin-Sip1 binding affinities, affecting the balance between the activities of Merlin and Moesin in regulating cell proliferation and the maintenance of epithelial integrity.

4.1.2 Role of Serine 371 on Merlin conformation

The effect of the serine 371 mutations on Merlin tumour suppressor function could also be due to an effect on Merlin protein conformation. Merlin conformation has been shown to be related to function: in Drosophila the active form in repressing proliferation is thought to be in a more open conformation (LaJeunesse et al. 1998). Studies using a mammalian system have suggested that the closed form of merlin is active in repressing proliferation (Sherman et al. 1997, Shaw et al. 1998, Gutmann et al. 1999, Morrison et al. 2001).

Recent studies in mammalian merlin have proposed a hierarchical model of merlin conformation where merlin does not solely exist in a binary open or closed conformation (Hennigan et al. 2010, Sher et al. 2012), but instead undergoes a series of subtle conformation changes. These changes lead to a rheostat model to regulate merlin function.

Sher et al. (Sher et al. 2012) presented a hierarchical model where phosphorylated merlin at serine 518 induces the intracellular association to inactivate the molecule not by being fully closed, but by being more tightly closed than wild-type merlin, and non-phosphorylated merlin at serine 518 is more open and is the active form in repressing cell proliferation. Hennigan et al. (Hennigan et al. 2010) also found that the central α-helical domain of merlin, where serine 371 is

found, is the main region mediating the closed conformation. My observations of the effect of serine 371 on the area of the *patched* region show that Merlin^{S371A} is not as effective in growth suppression as wild-type Merlin, and Merlin^{S371D} is even less effective. It is possible that Merlin^{S371D} may be more inactive in repressing cell proliferation due to it being more tightly closed than Merlin^{S371A} and wild-type Merlin (illustrated in Figure 4-1). In addition, the change in conformation may be affecting Merlin interaction with Sip1 at this region, as discussed in Section 4.1.1. In the study by Sher et al. (Sher et al. 2012), binding affinity to the mammalian Sip1 homolog EBP50 was used as a test for the conformation state of a the Merlin^{S518A} and Merlin^{S518D} mutants. They found that Merlin^{S518A} bound EBP50 with a higher affinity than Merlin^{S518D}, agreeing with a model where Merlin^{S518A} is more open than wild-type, which in turn is more open than Merlin^{S518D}. Based on the conformation hierarchy model, it is possible that Merlin^{S371A} may be more open, but due to a change in the phosphorylation status at this residue the mutant protein does not bind Sip1 with the same efficiency as wild-type Merlin, resulting in reduced effectiveness at suppressing cell growth. Merlin^{S371D} may be more tightly closed compared to wild-type Merlin, and binds Sip1 with further reduced efficiency, resulting in a protein form that is even less effective at suppressing cell growth compared to Merlin^{S371A}. My observations differ with the Sher study in the effects of Merlin^{S371A} on suppressing cell

proliferation. In their experiments, the non-phosphorylatable form (Merlin^{S518A}) represses growth at a level similar to wild-type, but my findings show that Merlin^{S371A} has an effect that is similar to, but milder, than Merlin^{S371D}. This may be due to the position of serine 371 in the coiled-coiled region, and thus may be having a different effect on Merlin conformation than the C-terminal serine 518. There is also the possibility of a relationship between different phosphorylatable residues. Previous work has shown that phosphorylation of serine 518 in mammalian merlin is abrogated when threonine 230 and serine 315 is mutated to non-phosphorylatable alanine (Laulajainen et al. 2011), suggesting the possibility that phosphorylation sites on Merlin may have a level of interdependence, and the phosphorylation of specific residues may be regulated by the phosphorylation status of other residues, adding another layer of regulation for Merlin function.

Figure 4-1. Illustration of hypothesised conformation changes in response to mutation at serine 371.

Merlin^{S371D} may be more inactive in repressing cell proliferation due to being more tightly closed than Merlin^{S371A} and wild-type Merlin. Blue clover-shaped domain represents the N-terminal Merlin FERM domain. Orange domain represents the coiled-coil and C-terminal domains.

4.2 Role of Threonine 18 in the regulation of Merlin protein stability and levels

4.2.1 Localisation of Merlin^{T18} mutants in S2 cells and larval wing discs

Non-phosphorylatable Merlin^{T18A} was localised normally when over-expressed in S2 cells when compared to over-expression of wild-type Merlin. Over-expression of the phosphomimetic Merlin^{T18D} showed a strong membranous localisation (Figure 3-5). This is similar to what was previously observed with Merlin^{T616D} (Hughes and Fehon 2006). In larval wing discs, however, these results were opposite to what was expected based on the S2 cell localisation patterns. Merlin^{T18A} is mostly membranous with some cytoplasmic localisation, whereas Merlin^{T18D} is highly cytoplasmic (Figure 3-7). This expression pattern is similar to what was previously found in a similar experiment using Merlin^{T616A} and Merlin^{T616D} (Yang et al. 2012). Based on previous findings linking Merlin localisation to function (Kissil et al. 2002, Hughes and Fehon 2006), the cytoplasmic localisation of Merlin^{T18D} suggests that phosphorylation of threonine 18 deactivates Merlin. The difference in localisation between S2 cells and larval wing discs could be due to interactions with proteins in larval discs that are not present in S2 cells, such as Sip1, which is present in very low endogenous levels in S2 cells but is highly expressed in third instar larval wing discs (modENCODE data from FlyBase http://flybase.org/reports/FBgn0010620.html). This could also

be due to the difference between semi-adherent S2 cells and the intact larval wing disc.

To examine the effects of phosphorylation at the threonine 18 site on cell proliferation, effects of overexpression of Merlin^{T18A} and Merlin^{T18D} in the *patched* expression region were examined. Over-expression of Merlin^{T18A} resulted in a *patched* region area that was not significantly different from over-expression of wild-type Merlin, whereas over-expression of Merlin^{T18D} resulted in a significantly reduced area of the *patched* region compared to over-expression of wild-type Merlin, but was comparable to the area of the standard w^{1118} out-cross (Figure 3-6). This result suggests that the threonine 18 phosphorylation site is not involved in Merlin function in inhibition of cell proliferation, and is instead involved in other aspects of Merlin regulation. One possibility is the involvement of this residue in ubiquitination and degradation of Merlin. Previous work has shown that phosphorylation of mammalian Merlin at serine 10 by Akt directs Merlin for proteasome-mediated degradation (Laulajainen et al. 2011). Preliminary experiments examining this possibility showed that when Merlin^{T18D} is over-expressed and immunoprecipitated from S2 cells, increased levels of ubiquitin can be detected when the proteasome is inhibited, compared to over-expression of wild-type Merlin and Merlin^{T18A} (Figure 3-20). Further experiments will have to be performed to confirm these findings. Ubiquitination of Merlin^{T18D}

could lead to rapid degradation of the over-expressed Merlin^{T18D} protein in the proteosome, thus removing all of the over-expression effects, resulting in a *patched* wing area comparable to the w^{1118} outcross.

4.3 Effects of serine 371 and threonine 18 on Merlin's role in maintenance of epithelial integrity

In addition to its role in regulating cell proliferation, Merlin has a role in establishing stable adherens junctions and in contact-dependent inhibition of proliferation in mammalian cells (Morrison et al. 2001, Johnson et al. 2002, Lallemand et al. 2003, McClatchey and Giovannini 2005, Okada et al. 2005, McLaughlin et al. 2007). Merlin is involved with the maturation of the adherens junction complex through interactions with α-catenin, supporting that idea that Merlin has a dual function in regulating cell polarity and cell proliferation (Gladden et al. 2010).

To examine the effects of serine 371 and threonine 18 phosphorylation on epithelial integrity, Merlin^{S371} and Merlin^{T18} mutants were over-expressed at the anterior-posterior boundary of the Drosophila wing imaginal discs using a *patched*-GAL4 driver. The localisation patterns of actin, DE-cadherin, and Sip1 were examined. Over-expression of both non-phosphorylatable mutations and phosphomimetic mutations lead to a subtle but consistent increase of DE-cadherin below the apical surface of the wing disc along the *patched* stripe, which

is brighter than what was observed with the expression of wild-type Merlin (Figure 3-8). Sip1 localisation did not appear to be affected by the over-expression of the phosphorylation mutants. Over-expression of Merlin^{S371A} resulted in a subtle increase of actin expression along the edge of the *patched* stripe, and over-expression of the other mutants did not appear to have an effect on actin localisation (Figure 3-9). The effects of the mutants in the wing discs were all very subtle, and the effects of the different mutants were not easily discernible from each other, possibly due to the presence of endogenous Merlin that may have masked any effects of the mutants. Drosophila wing imaginal discs have also been shown to have the ability to self-repair and undergo compensatory proliferation through the activity of the apical cell death caspase Dronc (Huh et al. 2004), which may also have made the effects of the Merlin mutants less readily detectable.

To overcome these two limitations, the MARCM technique was used to examine the effects of the serine 371 and threonine 18 mutations in maintenance of epithelial integrity in the follicle cell epithelium of developing egg chambers. This system allows for a simultaneous removal of endogenous Merlin using the Merlin-null Mer^{4} allele and over-expression of the phosphorylation mutants in the same clone. The clones were generated through homologous recombination,

and thus also conferred the advantage of having wild-type cells adjacent to mutant cells for comparison within the same tissue.

Merlin-null (Mer^4) egg chambers did not show any detectable phenotypes on cell morphology or cell adhesion at stages 7 to 9, which agrees with what has been previously observed in Merlin-null clones in early egg chamber developmental stages (S. Hughes, personal communication). The effects of the loss of Merlin become detectable in developmental stage 14, and this could be due to the changes in cellular processes, including follicle cell migration in stage 9 to surround the oocyte, that occur between stage 9 and 14 (Bastock and St Johnston 2008).

The majority of egg chambers with clones over-expressing $Merlin^{S371A}$ and $Merlin^{S371D}$ did not show detectable proliferation or adhesion defects in the follicle cell epithelium in the stage 7 to stage 9 developmental stages. In a small number of egg chambers for both serine 371 mutations, DE-cadherin was reduced in large clone regions, especially at the anterior and posterior ends of the egg chambers (observations summarised in Table 5). This observation is striking as phenotypes have not been previously detected in early stages of egg chamber development in Mer^4 clones (S. Hughes, personal communication). A loss of cell adhesion was also observed in some egg chambers, resulting in multiple

epithelium layers and clusters of cells that have delaminated from the epithelium in stage 7 to stage 9 egg chambers. GFP-positive clusters of cells were also observed on the surface of stage 14 eggs. DE-cadherin, F-actin, and aPKC were mislocalised in the clone regions. This suggests a loss of adhesion, and a role for serine 371 in regulating Merlin function in cell adhesion. Both Merlin^{S371A} and Merlin^{S371D} clones exhibited these properties, and there were no detectable differences between the two mutations. This was expected based on previous observations of these two mutations in the adult wing, the larval wing discs, and binding to Sip1, which suggest that both hypophosphorylation and phosphorylation at the serine 371 residue are inactivating. Thus the effects of both mutants on Merlin function in epithelial integrity would also be expected to be similar.

The majority of clones over-expressing Merlin^{T18D} also did not show any detectable phenotypes in stages 7 to 9 egg chambers. In a small number of egg chambers (4/12 observed egg chambers), however, there were examples of a loss of epithelial integrity and adhesive properties with the epithelial layer. These effects are more severe in developmental stage 14, resulting in clusters of nuclei on the surface of stage 14 egg shells. The observation that Mer^{4} clones over-expressing the phosphorylation mutants show multiple layers of cells or cells that appear to have detached from the follicle cell epithelium suggests that serine

371 and threonine 18 may have a role in regulating Merlin's tumour suppressor mechanism in the context of contact-dependent inhibition of proliferation. Merlin can suppresses the activity of the Rac-PAK signaling pathway (Shaw et al. 2001, Kissil et al. 2002, Okada et al. 2005), and Shaw et al (Shaw et al. 1998). found that Merlin phosphorylation is influenced by different growth conditions (confluency or serum-deprivation), suggesting that the adhesion defects seen in the follicle cell clones may be due to defects in Merlin's activity in this context.

The expression of Sip1 and Moesin also appear to be affected by Merlin^{T18D} expression. Experiments to test for ubiquitination of Merlin^{T18D} suggested that threonine 18 is involved in promoting the ubiquitination and subsequent degradation of Merlin (Figure 3-20). It is possible that the degradation of Merlin^{T18D} is affecting the balance of Merlin and Moesin activity in the follicle cells, leading to the effects in adhesion and the maintenance of epithelial integrity. Merlin has been shown to co-localise with E-cadherin at the adherens junctions, and the loss of Merlin leads to the reduction of aPKC-Par3 complexes, suggesting a role for Merlin in junction maturation (Gladden et al. 2010).

Previous work examining the effect of Flapwing phosphatase, which dephosphorylates both Merlin and Moesin in Drosophila, showed that the reduction of Flapwing leads to increased levels of phosphorylated (and thus

inactive) Merlin as well as increased levels of phosphorylated (active) Moesin. The simultaneous activation of Moesin and inactivation of Merlin resulted in very severe phenotypes in epithelial tissues indicating loss of polarity and adhesion (Yang et al. 2012). Excess active Moesin in the *patched* region paradoxically leads to abnormalities in adhesion in that region, suggesting that a balance between these two proteins is crucial for the proper development of the epithelium. Increased phosphorylation of Moesin due to loss of the PP1 phosphatase Sds22 was previously observed to cause disruption of epithelial polarity in follicle cells (Grusche et al. 2009). Yang et al. (Yang et al. 2012) also showed that either phosphomimetic or non-phosphorylatable mutations of Merlin and Moesin will recapitulate loss of Flapwing phenotypes. This further suggests that high levels of either active or inactive forms of Merlin or Moesin lead to epithelial effects, and that precise regulation of the two proteins is crucial for proper development. The reduced Merlin activity of Merlin^{S371A} and Merlin^{S371D}, as well as the loss of Merlin^{T18D} could lead to an imbalance and excess active Moesin in the follicle cells, which could lead to the adhesion effects that were observed. This is supported with the preliminary results in Figure 3-15 showing increased apical Sip1 and Moesin in the Mer^{4};+;Merlin^{T18D} clones, suggesting a coordinate upregulation of Moesin and Sip1 in response to the expression of Merlin^{T18D}. Further work to determine whether active Moesin levels

are increased when Merlin^{T18D} is expressed can provide further insight into this hypothesis.

4.4 Future Directions

4.4.1 Further characterising the serine 371 phosphorylation site

Using the NetPhosK 1.0 server (http://www.cbs.dtu.dk/services/NetPhosK/) to predict possible kinases that can phosphorylate serine 371, CKII was predicted with a score of 0.51. A score above 0.5 indicates that a particular site is a target of a particular kinase (Miller and Blom 2009), suggesting that serine 371 may be a target of CKII. Future biochemical experiments can be done to confirm whether CKII is the kinase responsible for phosphorylating this site, such as kinase assays, or by using genetic methods *in vivo*, such as examining the effect of removing CKII on proliferation and epithelial integrity in various Drosophila tissues.

As serine 371 could be affecting Merlin function through conformational changes and/or interactions with Sip1, interactions of Merlin^{S371A} and Merlin^{S371D} with Sip1 can be further tested *in vivo* using immunoprecipitation assays. The relationship of the serine 371 site with the established threonine 616 site can also be examined to see whether serine 371 has a role in regulating the phosphorylation of threonine 616 (and thus the activation and deactivation of Merlin).

4.4.2 Further characterising the threonine 18 site

Preliminary observations suggest that the threonine 18 site may be involved in the ubiquitin-mediated degradation of the Merlin protein. In mammalian cells, the serine/threonine kinase Akt was shown to be the kinase involved in this pathway (Laulajainen et al. 2011). It would be interesting to examine whether this kinase is also involved in the phosphorylation of threonine 18 through methods such as kinase assays, or *in vivo* by examining the effect of removing Akt on the phosphorylation of threonine 18 in various Drosophila tissues. Also, the role of this site in Merlin degradation can also be examined by examining any changes in the levels of Merlin in response the phosphorylation status of this site, and whether any changes in Merlin levels affects the activity of Moesin and Sip1 in the context of our switch hypothesis.

4.4.3 Determining whether the serine 371 and threonine 18 phosphorylation sites are linked

In mammalian merlin, the phosphorylation of serine 518 can be abrogated by mutating threonine 230 and serine 315 to non-phosphorylatable alanines (Laulajainen et al. 2011), suggesting that the multiple phosphorylation sites in merlin can affect each other. It would be interesting to see whether a serine 371/threonine 18 double mutant will show synergistic phenotypes on cell proliferation and epithelial integrity when compared to mutations of the serine

371 and threonine 18 sites alone. Phospho-specific antibodies can also be used to examine whether mutating either one of the two sites will affect level of phosphorylation of Merlin at other sites, and could give more insight into the many layers of regulation of Merlin.

4.4.4 Further approaches to examine effects on epithelial integrity

One limitation to the MARCM approach using a heat shock-induced FLP recombination system is the random generation of clones. This results in the inability to control for the location, size, and timing of the clones in the egg chambers, resulting in a very small percentage of egg chambers that had successfully undergone homologous recombination. Possible methods to overcome this could be to use specific follicle cell drivers such as *traffic jam-GAL4*, or an anterior follicle cell driver such as *C306-GAL4*. Duffy et al. have also developed a system using *e22c*-GAL4 and UAS-FLP to specifically create high numbers of MARCM clones in the follicle cells (Duffy et al. 1998). Generation of follicle cell clones at specific developmental stages and in specific locations within the egg chamber will allow us to examine the effects of the Merlin mutants during specific cellular processes (cell division, cell migration), and to further elucidate Merlin's mechanisms during these processes. Further work to examine if the observed cell clusters arise as a result of cellular extrusion would also provide insight into the mechanisms leading to metastasis, as the cell

clusters, especially in the stage 14 eggs, are located on the basal side of the epithelium, similar to what is observed in abnormal cell extrusion due to oncogenic signaling (Slattum and Rosenblatt 2014).

4.5 Conclusions

My research characterised two novel potential phosphorylation sites, serine 371 and threonine 18, in Drosophila Merlin. I found that substitutions of these two residues to non-phosphorylatable alanine or a phosphomimetic aspartic acid affect localisation of Merlin in S2 cells and in wing disc tissue, the function of Merlin in the repression of cell proliferation, and the role of Merlin in maintenance of epithelial integrity.

Studying phosphorylation control of Merlin's alternative role in the maintenance of epithelial integrity has implications for understanding the development of NF2. In a study examining the activities of disease-causing NF2 mutations, Stokowski et al. (Stokowski and Cox 2000) found that 80% of the examined mutants altered cell adhesion, and the authors proposed that changes in cell adhesion may be an initial step in the development of NF2. The authors of this study also found that four of the missense mutations lead to decreased Merlin-EBP50 interaction, and that some mutants behaved similarly to gain-of-function alleles, further supporting our Sip1/Moesin/Merlin switch hypothesis in which the balance controlling cell proliferation and epithelial integrity plays a key role in Merlin's tumour suppressor function in the context of NF2. Loss of polarity also has further implications in cancer, as loss of polarity leads to epithelial-to-

mesenchymal transition, or EMT, which is a potential mechanism in cancer metastasis (Huber et al. 2005).

Understanding phosphorylation regulation of Merlin stability may also provide insight into severe NF2. Nonsense and frameshift mutations have been correlated to increased disease severity in patients (Baser et al. 2005), and nonsense mutations lead to unstable Merlin protein (Gutmann et al. 1998). Insights on the regulation of Merlin stability may lead to potential approaches for treatment of severe NF2 related to Merlin instability.

My work identified two potential novel phosphorylation sites in Drosophila Merlin that affect Merlin function as a tumour suppressor and a regulator of epithelial integrity. The findings can eventually be translated into a mammalian system to understand the mechanisms regulating Merlin in the context of NF2, as well as insight into mechanisms of other processes in cancer, potentially leading to future approaches to treatments for these diseases.

5 References

Alfthan, K., L. Heiska, M. Gronholm, G. H. Renkema and O. Carpen (2004). "Cyclic AMP-dependent protein kinase phosphorylates merlin at serine 518 independently of p21-activated kinase and promotes merlin-ezrin heterodimerization." The Journal of biological chemistry **279**(18): 18559-18566.

Bagrodia, S. and R. A. Cerione (1999). "Pak to the future." Trends Cell Biol **9**(9): 350-355.

Baser, M. E., L. Kuramoto, H. Joe, J. M. Friedman, A. J. Wallace, R. T. Ramsden and D. G. Evans (2003). "Genotype-phenotype correlations for cataracts in neurofibromatosis 2." J Med Genet **40**(10): 758-760.

Baser, M. E., L. Kuramoto, R. Woods, H. Joe, J. M. Friedman, A. J. Wallace, R. T. Ramsden, S. Olschwang, E. Bijlsma, M. Kalamarides, L. Papi, R. Kato, J. Carroll, C. Lazaro, F. Joncourt, D. M. Parry, G. A. Rouleau and D. G. Evans (2005). "The location of constitutional neurofibromatosis 2 (NF2) splice site mutations is associated with the severity of NF2." J Med Genet **42**(7): 540-546.

Bastock, R. and D. St Johnston (2008). "Drosophila oogenesis." Current Biology **18**(23): R1082-R1087.

Becalska, A. N. and E. R. Gavis (2009). "Lighting up mRNA localization in Drosophila oogenesis." Development **136**(15): 2493-2503.

Blom, N., S. Gammeltoft and S. Brunak (1999). "Sequence and structure-based prediction of eukaryotic protein phosphorylation sites." J Mol Biol **294**(5): 1351-1362.

Brand, A. H. and N. Perrimon (1993). "Targeted gene expression as a means of altering cell fates and generating dominant phenotypes." Development **118**(2): 401-415.

Bretscher, A. (1983). "Purification of an 80,000-dalton protein that is a component of the isolated microvillus cytoskeleton, and its localization in nonmuscle cells." J Cell Biol **97**(2): 425-432.

Bretscher, A. (1989). "Rapid phosphorylation and reorganization of ezrin and spectrin accompany morphological changes induced in A-431 cells by epidermal growth factor." J Cell Biol **108**(3): 921-930.

Bretscher, A., K. Edwards and R. G. Fehon (2002). "ERM proteins and merlin: integrators at the cell cortex." Nat Rev Mol Cell Biol **3**(8): 586-599.

Curto, M., B. K. Cole, D. Lallemand, C. H. Liu and A. I. McClatchey (2007). "Contact-dependent inhibition of EGFR signaling by Nf2/Merlin." The Journal of cell biology **177**(5): 893-903.

Doyle, D. A., A. Lee, J. Lewis, E. Kim, M. Sheng and R. MacKinnon (1996). "Crystal structures of a complexed and peptide-free membrane protein-binding domain: molecular basis of peptide recognition by PDZ." Cell **85**(7): 1067-1076.

Duffy, J. B., D. A. Harrison and N. Perrimon (1998). "Identifying loci required for follicular patterning using directed mosaics." Development **125**(12): 2263-2271.

Eker, R. and J. Mossige (1961). "A Dominant Gene for Renal Adenomas in Rat." Nature **189**(476): 858-&.

Evans, D. G., S. M. Huson, D. Donnai, W. Neary, V. Blair, V. Newton and R. Harris (1992). "A clinical study of type 2 neurofibromatosis." Q J Med **84**(304): 603-618.

Evans, D. G., A. Moran, A. King, S. Saeed, N. Gurusinghe and R. Ramsden (2005). "Incidence of vestibular schwannoma and neurofibromatosis 2 in the North West of England over a 10-year period: higher incidence than previously thought." Otol Neurotol **26**(1): 93-97.

Evans, D. G., M. Sainio and M. E. Baser (2000). "Neurofibromatosis type 2." J Med Genet **37**(12): 897-904.

Fernandez-Valle, C., Y. Tang, J. Ricard, A. Rodenas-Ruano, A. Taylor, E. Hackler, J. Biggerstaff and J. Iacovelli (2002). "Paxillin binds schwannomin and regulates its density-dependent localization and effect on cell morphology." Nat Genet **31**(4): 354-362.

Gary, R. and A. Bretscher (1995). "Ezrin self-association involves binding of an N-terminal domain to a normally masked C-terminal domain that includes the F-actin binding site." Mol Biol Cell **6**(8): 1061-1075.

Gavilan, H. S., R. M. Kulikauskas, D. H. Gutmann and R. G. Fehon (2014). "In vivo functional analysis of the human NF2 tumor suppressor gene in Drosophila." PloS one **9**: e90853.

Giovannini, M., E. Robanus-Maandag, M. Niwa-Kawakita, M. van der Valk, J. M. Woodruff, L. Goutebroze, P. Merel, A. Berns and G. Thomas (1999). "Schwann cell hyperplasia and tumors in transgenic mice expressing a naturally occurring mutant NF2 protein." Genes Dev **13**(8): 978-986.

Gladden, A. B., A. M. Hebert, E. E. Schneeberger and A. I. McClatchey (2010). "The NF2 tumor suppressor, Merlin, regulates epidermal development through the establishment of a junctional polarity complex." Dev Cell **19**(5): 727-739.

Gonzalez-Agosti, C., L. Xu, D. Pinney, R. Beauchamp, W. Hobbs, J. Gusella and V. Ramesh (1996). "The merlin tumor suppressor localizes preferentially in membrane ruffles." Oncogene **13**(6): 1239-1247.

Gronholm, M., M. Sainio, F. Zhao, L. Heiska, A. Vaheri and O. Carpen (1999). "Homotypic and heterotypic interaction of the neurofibromatosis 2 tumor suppressor protein merlin and the ERM protein ezrin." J Cell Sci **112 (Pt 6)**: 895-904.

Grusche, F. A., C. Hidalgo, G. Fletcher, H. H. Sung, E. Sahai and B. J. Thompson (2009). "Sds22, a PP1 phosphatase regulatory subunit, regulates epithelial cell polarity and shape [Sds22 in epithelial morphology]." BMC Dev Biol **9**: 14.

Gutmann, D. H., R. T. Geist, H. Xu, J. S. Kim and S. Saporito-Irwin (1998). "Defects in neurofibromatosis 2 protein function can arise at multiple levels." Hum Mol Genet **7**(3): 335-345.

Gutmann, D. H., M. J. Giordano, A. S. Fishback and A. Guha (1997). "Loss of merlin expression in sporadic meningiomas, ependymomas and schwannomas." Neurology **49**(1): 267-270.

Gutmann, D. H., C. A. Haipek and K. Hoang Lu (1999). "Neurofibromatosis 2 tumor suppressor protein, merlin, forms two functionally important intramolecular associations." J Neurosci Res **58**(5): 706-716.

Gutmann, D. H., L. Sherman, L. Seftor, C. Haipek, K. Hoang Lu and M. Hendrix (1999). "Increased expression of the NF2 tumor suppressor gene product, merlin, impairs cell motility, adhesionand spreading." Hum Mol Genet **8**(2): 267-275.

Heiska, L., K. Alfthan, M. Gronholm, P. Vilja, A. Vaheri and O. Carpen (1998). "Association of ezrin with intercellular adhesion molecule-1 and -2 (ICAM-1 and ICAM-2). Regulation by phosphatidylinositol 4, 5-bisphosphate." J Biol Chem **273**(34): 21893-21900.

Hennigan, R. F., L. A. Foster, M. F. Chaiken, T. Mani, M. M. Gomes, A. B. Herr and W. Ip (2010). "Fluorescence resonance energy transfer analysis of merlin conformational changes." Mol Cell Biol **30**(1): 54-67.

Hino, O., H. Mitani, H. Katsuyama and Y. Kubo (1994). "A novel cancer predisposition syndrome in the Eker rat model." Cancer Lett **83**(1-2): 117-121.

Huang, L., E. Ichimaru, K. Pestonjamasp, X. Cui, H. Nakamura, G. Y. Lo, F. I. Lin, E. J. Luna and H. Furthmayr (1998). "Merlin differs from moesin in binding to F-actin and in its intra- and intermolecular interactions." Biochemical and biophysical research communications **248**(3): 548-553.

Huber, M. A., N. Kraut and H. Beug (2005). "Molecular requirements for epithelial–mesenchymal transition during tumor progression." Current Opinion in Cell Biology **17**(5): 548-558.

Hughes, S. C. and R. G. Fehon (2006). "Phosphorylation and activity of the tumor suppressor Merlin and the ERM protein Moesin are coordinately regulated by the Slik kinase." The Journal of cell biology **175**(2): 305-313.

Hughes, S. C., E. Formstecher and R. G. Fehon (2010). "Sip1, the Drosophila orthologue of EBP50/NHERF1, functions with the sterile 20 family kinase Slik to regulate Moesin activity." J Cell Sci **123**(Pt 7): 1099-1107.

Huh, J. R., M. Guo and B. A. Hay (2004). "Compensatory proliferation induced by cell death in the Drosophila wing disc requires activity of the apical cell death caspase Dronc in a nonapoptotic role." Curr Biol **14**(14): 1262-1266.

Jaffer, Z. M. and J. Chernoff (2002). "p21-activated kinases: three more join the Pak." Int J Biochem Cell Biol **34**(7): 713-717.

James, M. F., S. Han, C. Polizzano, S. R. Plotkin, B. D. Manning, A. O. Stemmer-Rachamimov, J. F. Gusella and V. Ramesh (2009). "NF2/merlin is a novel negative regulator of mTOR complex 1, and activation of mTORC1 is associated with meningioma and schwannoma growth." Mol Cell Biol **29**(15): 4250-4261.

James, M. F., N. Manchanda, C. Gonzalez-Agosti, J. H. Hartwig and V. Ramesh (2001). "The neurofibromatosis 2 protein product merlin selectively binds F-actin but not G-actin, and stabilizes the filaments through a lateral association." Biochem J **356**(Pt 2): 377-386.

Johnson, K. C., J. L. Kissil, J. L. Fry and T. Jacks (2002). "Cellular transformation by a FERM domain mutant of the Nf2 tumor suppressor gene." Oncogene **21**(39): 5990-5997.

Kalamarides, M., M. Niwa-Kawakita, H. Leblois, V. Abramowski, M. Perricaudet, A. Janin, G. Thomas, D. H. Gutmann and M. Giovannini (2002). "Nf2 gene inactivation in arachnoidal cells is rate-limiting for meningioma development in the mouse." Genes Dev **16**(9): 1060-1065.

Kastan, M. B., O. Onyekwere, D. Sidransky, B. Vogelstein and R. W. Craig (1991). "Participation of p53 protein in the cellular response to DNA damage." Cancer Res **51**(23 Pt 1): 6304-6311.

Kissil, J. L., K. C. Johnson, M. S. Eckman and T. Jacks (2002). "Merlin phosphorylation by p21-activated kinase 2 and effects of phosphorylation on merlin localization." The Journal of biological chemistry **277**(12): 10394-10399.

Kissil, J. L., E. W. Wilker, K. C. Johnson, M. S. Eckman, M. B. Yaffe and T. Jacks (2003). "Merlin, the product of the Nf2 tumor suppressor gene, is an inhibitor of the p21-activated kinase, Pak1." Mol Cell **12**(4): 841-849.

Knudson, A. G. (1971). "Mutation and cancer: statistical study of retinoblastoma." Proceedings of the National Academy of Sciences of the United States of America **68**: 820-823.

Kobayashi, T., Y. Hirayama, E. Kobayashi, Y. Kubo and O. Hino (1995). "A germline insertion in the tuberous sclerosis (Tsc2) gene gives rise to the Eker rat model of dominantly inherited cancer." Nat Genet **9**(1): 70-74.

LaJeunesse, D. R., B. M. McCartney and R. G. Fehon (1998). "Structural analysis of Drosophila merlin reveals functional domains important for growth control and subcellular localization." The Journal of cell biology **141**(7): 1589-1599.

Lallemand, D., M. Curto, I. Saotome, M. Giovannini and A. I. McClatchey (2003). "NF2 deficiency promotes tumorigenesis and metastasis by destabilizing adherens junctions." Genes Dev **17**(9): 1090-1100.

Lallemand, D., J. Manent, A. Couvelard, A. Watilliaux, M. Siena, F. Chareyre, A. Lampin, M. Niwa-Kawakita, M. Kalamarides and M. Giovannini (2009). "Merlin regulates transmembrane receptor accumulation and signaling at the plasma membrane in primary mouse Schwann cells and in human schwannomas." Oncogene **28**(6): 854-865.

Lallemand, D., A. L. Saint-Amaux and M. Giovannini (2009). "Tumor-suppression functions of merlin are independent of its role as an organizer of the actin cytoskeleton in Schwann cells." J Cell Sci **122**(Pt 22): 4141-4149.

Lankes, W., A. Griesmacher, J. Grunwald, R. Schwartz-Albiez and R. Keller (1988). "A heparin-binding protein involved in inhibition of smooth-muscle cell proliferation." Biochem J **251**(3): 831-842.

Lankes, W. T. and H. Furthmayr (1991). "Moesin: a member of the protein 4.1-talin-ezrin family of proteins." Proc Natl Acad Sci U S A **88**(19): 8297-8301.

Laulajainen, M., T. Muranen, O. Carpen and M. Gronholm (2008). "Protein kinase A-mediated phosphorylation of the NF2 tumor suppressor protein merlin at serine 10 affects the actin cytoskeleton." Oncogene **27**(23): 3233-3243.

Laulajainen, M., T. Muranen, T. A. Nyman, O. Carpen and M. Gronholm (2011). "Multistep phosphorylation by oncogenic kinases enhances the degradation of the NF2 tumor suppressor merlin." Neoplasia **13**(7): 643-652.

Lee, T., A. Lee, L. Luo. (1999). Development of the Drosophila Mushroom Bodies: Sequential Generation of Three Distinct Types of Neurons from a Neuroblast. Flybrain on-line [www.flybrain.org] Accession Number: AD00021.

Lee, T. and L. Luo (1999). "Mosaic analysis with a repressible cell marker for studies of gene function in neuronal morphogenesis." Neuron **22**(3): 451-461.

Leung, A. C. C. (2011). Structure and function analysis of the Merlin Sip1 complex. MR90293 M.S., University of Alberta (Canada).

Levene, H. (1960). In Contributions to Probability and Statistics: Essays in Honor of Harold Hotelling, I, Stanford University Press.

Liu, L., H. Shi, X. Chen and Z. Wang (2011). "Regulation of EGF-Stimulated EGF Receptor Endocytosis During M Phase." Traffic **12**(2): 201-217.

Lopez-Lago, M. A., T. Okada, M. M. Murillo, N. Socci and F. G. Giancotti (2009). "Loss of the tumor suppressor gene NF2, encoding merlin, constitutively activates integrin-dependent mTORC1 signaling." Mol Cell Biol **29**(15): 4235-4249.

Lutchman, M. and G. A. Rouleau (1995). "The neurofibromatosis type 2 gene product, schwannomin, suppresses growth of NIH 3T3 cells." Cancer Res **55**(11): 2270-2274.

MacCollin, M., N. Braverman, D. Viskochil, M. Ruttledge, K. Davis, R. Ojemann, J. Gusella and D. M. Parry (1996). "A point mutation associated with a severe phenotype of neurofibromatosis 2." Ann Neurol **40**(3): 440-445.

Maeda, M., T. Matsui, M. Imamura and S. Tsukita (1999). "Expression level, subcellular distribution and rho-GDI binding affinity of merlin in comparison with Ezrin/Radixin/Moesin proteins." Oncogene **18**(34): 4788-4797.

Manchanda, N., A. Lyubimova, H. Y. Ho, M. F. James, J. F. Gusella, N. Ramesh, S. B. Snapper and V. Ramesh (2005). "The NF2 tumor suppressor Merlin and the ERM proteins interact with N-WASP and regulate its actin polymerization function." The Journal of biological chemistry **280**(13): 12517-12522.

Manetti, M. E., S. Geden, M. Bott, N. Sparrow, S. Lambert and C. Fernandez-Valle (2012). "Stability of the tumor suppressor merlin depends on its ability to bind paxillin LD3 and associate with beta1 integrin and actin at the plasma membrane." Biol Open **1**(10): 949-957.

Maruyama, R. and D. J. Andrew (2012). "Drosophila as a model for epithelial tube formation." Dev Dyn **241**(1): 119-135.

McCartney, B. M. and R. G. Fehon (1996). "Distinct cellular and subcellular patterns of expression imply distinct functions for the Drosophila homologues of moesin and the neurofibromatosis 2 tumor suppressor, merlin." The Journal of cell biology **133**(4): 843-852.

McCartney, B. M., R. M. Kulikauskas, D. R. LaJeunesse and R. G. Fehon (2000). "The neurofibromatosis-2 homologue, Merlin, and the tumor suppressor expanded function together in Drosophila to regulate cell proliferation and differentiation." Development **127**(6): 1315-1324.

McClatchey, A. I. and M. Giovannini (2005). "Membrane organization and tumorigenesis--the NF2 tumor suppressor, Merlin." Genes Dev **19**(19): 2265-2277.

McClatchey, A. I., I. Saotome, K. Mercer, D. Crowley, J. F. Gusella, R. T. Bronson and T. Jacks (1998). "Mice heterozygous for a mutation at the Nf2 tumor suppressor locus develop a range of highly metastatic tumors." Genes Dev **12**(8): 1121-1133.

McClatchey, A. I., I. Saotome, V. Ramesh, J. F. Gusella and T. Jacks (1997). "The Nf2 tumor suppressor gene product is essential for extraembryonic development immediately prior to gastrulation." Genes Dev **11**(10): 1253-1265.

McLaughlin, M. E., G. M. Kruger, K. L. Slocum, D. Crowley, N. A. Michaud, J. Huang, M. Magendantz and T. Jacks (2007). "The Nf2 tumor suppressor regulates cell-cell adhesion during tissue fusion." Proceedings of the National Academy of Sciences of the United States of America **104**(9): 3261-3266.

Meng, J. J., D. J. Lowrie, H. Sun, E. Dorsey, P. D. Pelton, A. M. Bashour, J. Groden, N. Ratner and W. Ip (2000). "Interaction between two isoforms of the NF2 tumor suppressor protein, merlin, and between merlin and ezrin, suggests modulation of ERM proteins by merlin." J Neurosci Res **62**(4): 491-502.

Miller, M. and N. Blom (2009). Kinase-Specific Prediction of Protein Phosphorylation Sites. Phospho-Proteomics. M. Graauw, Humana Press. **527:** 299-310.

Morrison, H., L. S. Sherman, J. Legg, F. Banine, C. Isacke, C. A. Haipek, D. H. Gutmann, H. Ponta and P. Herrlich (2001). "The NF2 tumor suppressor gene product, merlin, mediates contact inhibition of growth through interactions with CD44." Genes Dev **15**(8): 968-980.

Muqit, M. M. K. and M. B. Feany (2002). "Modelling neurodegenerative diseases in Drosophila: a fruitful approach?" Nat Rev Neurosci **3**(3): 237-243.

Murthy, A., C. Gonzalez-Agosti, E. Cordero, D. Pinney, C. Candia, F. Solomon, J. Gusella and V. Ramesh (1998). "NHE-RF, a regulatory cofactor for Na(+)-H+ exchange, is a common interactor for merlin and ERM (MERM) proteins." The Journal of biological chemistry **273**(3): 1273-1276.

Nguyen, R., D. Reczek and A. Bretscher (2001). "Hierarchy of merlin and ezrin N- and C-terminal domain interactions in homo- and heterotypic associations and their relationship to binding of scaffolding proteins EBP50 and E3KARP." The Journal of biological chemistry **276**(10): 7621-7629.

Okada, M., Y. Wang, S. W. Jang, X. Tang, L. M. Neri and K. Ye (2009). "Akt phosphorylation of merlin enhances its binding to phosphatidylinositols and inhibits the tumor-suppressive activities of merlin." Cancer research **69**(9): 4043-4051.

Okada, T., M. Lopez-Lago and F. G. Giancotti (2005). "Merlin/NF-2 mediates contact inhibition of growth by suppressing recruitment of Rac to the plasma membrane." The Journal of cell biology **171**(2): 361-371.

Pelton, P. D., L. S. Sherman, T. A. Rizvi, M. A. Marchionni, P. Wood, R. A. Friedman and N. Ratner (1998). "Ruffling membrane, stress fiber, cell spreading and proliferation abnormalities in human Schwannoma cells." Oncogene **17**(17): 2195-2209.

Phelps, C. B. and A. H. Brand (1998). "Ectopic Gene Expression inDrosophilaUsing GAL4 System." Methods **14**(4): 367-379.

Pietromonaco, S. F., P. C. Simons, A. Altman and L. Elias (1998). "Protein kinase C-theta phosphorylation of moesin in the actin-binding sequence." J Biol Chem **273**(13): 7594-7603.

Pirraglia, C., J. Walters and M. M. Myat (2010). "Pak1 control of E-cadherin endocytosis regulates salivary gland lumen size and shape." Development **137**(24): 4177-4189.

Reczek, D., M. Berryman and A. Bretscher (1997). "Identification of EBP50: A PDZ-containing phosphoprotein that associates with members of the ezrin-radixin-moesin family." The Journal of cell biology **139**(1): 169-179.

Reczek, D. and A. Bretscher (1998). "The carboxyl-terminal region of EBP50 binds to a site in the amino-terminal domain of ezrin that is masked in the dormant molecule." The Journal of biological chemistry **273**(29): 18452-18458.

Rochdi, M. D. and J. L. Parent (2003). "Galphaq-coupled receptor internalization specifically induced by Galphaq signaling. Regulation by EBP50." J Biol Chem **278**(20): 17827-17837.

Rong, R., E. I. Surace, C. A. Haipek, D. H. Gutmann and K. Ye (2004). "Serine 518 phosphorylation modulates merlin intramolecular association and binding to critical effectors important for NF2 growth suppression." Oncogene **23**(52): 8447-8454.

Rouleau, G. A., P. Merel, M. Lutchman, M. Sanson, J. Zucman, C. Marineau, K. Hoang-Xuan, S. Demczuk, C. Desmaze, B. Plougastel and et al. (1993). "Alteration in a new gene encoding a putative membrane-organizing protein causes neuro-fibromatosis type 2." Nature **363**(6429): 515-521.

Ruttledge, M. H., J. Sarrazin, S. Rangaratnam, C. M. Phelan, E. Twist, P. Merel, O. Delattre, G. Thomas, M. Nordenskjold, V. P. Collins and et al. (1994). "Evidence for the complete inactivation of the NF2 gene in the majority of sporadic meningiomas." Nat Genet **6**(2): 180-184.

Sato, N., S. Yonemura, T. Obinata, S. Tsukita and S. Tsukita (1991). "Radixin, a barbed end-capping actin-modulating protein, is concentrated at the cleavage furrow during cytokinesis." J Cell Biol **113**(2): 321-330.

Schneider, I. (1972). "Cell lines derived from late embryonic stages of Drosophila melanogaster." J Embryol Exp Morphol **27**(2): 353-365.

Scoles, D. R., D. P. Huynh, P. A. Morcos, E. R. Coulsell, N. G. Robinson, F. Tamanoi and S. M. Pulst (1998). "Neurofibromatosis 2 tumour suppressor schwannomin interacts with betaII-spectrin." Nat Genet **18**(4): 354-359.

Shaw, R. J., A. I. McClatchey and T. Jacks (1998). "Localization and functional domains of the neurofibromatosis type II tumor suppressor, merlin." Cell Growth Differ **9**(4): 287-296.

Shaw, R. J., A. I. McClatchey and T. Jacks (1998). "Regulation of the neurofibromatosis type 2 tumor suppressor protein, merlin, by adhesion and growth arrest stimuli." The Journal of biological chemistry **273**(13): 7757-7764.

Shaw, R. J., J. G. Paez, M. Curto, A. Yaktine, W. M. Pruitt, I. Saotome, J. P. O'Bryan, V. Gupta, N. Ratner, C. J. Der, T. Jacks and A. I. McClatchey (2001). "The Nf2 tumor suppressor, merlin, functions in Rac-dependent signaling." Dev Cell **1**(1): 63-72.

Sher, I., C. O. Hanemann, P. A. Karplus and A. Bretscher (2012). "The tumor suppressor merlin controls growth in its open state, and phosphorylation converts it to a less-active more-closed state." Dev Cell **22**(4): 703-705.

Sherman, L., H. M. Xu, R. T. Geist, S. Saporito-Irwin, N. Howells, H. Ponta, P. Herrlich and D. H. Gutmann (1997). "Interdomain binding mediates tumor growth suppression by the NF2 gene product." Oncogene **15**(20): 2505-2509.

Simons, P. C., S. F. Pietromonaco, D. Reczek, A. Bretscher and L. Elias (1998). "C-terminal threonine phosphorylation activates ERM proteins to link the cell's cortical lipid bilayer to the cytoskeleton." Biochem Biophys Res Commun **253**(3): 561-565.

Slattum, G. M. and J. Rosenblatt (2014). "Tumour cell invasion: an emerging role for basal epithelial cell extrusion." Nat Rev Cancer **14**(7): 495-501.

Speck, O., S. C. Hughes, N. K. Noren, R. M. Kulikauskas and R. G. Fehon (2003). "Moesin functions antagonistically to the Rho pathway to maintain epithelial integrity." Nature **421**(6918): 83-87.

Spradling, A. C. (1993). "Germline cysts: communes that work." Cell **72**(5): 649-651.

Stemmer-Rachamimov, A. O., T. Wiederhold, G. P. Nielsen, M. James, D. Pinney-Michalowski, J. E. Roy, W. A. Cohen, V. Ramesh and D. N. Louis (2001). "NHE-RF, a merlin-interacting protein, is primarily expressed in luminal epithelia, proliferative endometrium, and estrogen receptor-positive breast carcinomas." The American journal of pathology **158**(1): 57-62.

Stemmer-Rachamimov, A. O., L. Xu, C. Gonzalez-Agosti, J. A. Burwick, D. Pinney, R. Beauchamp, L. B. Jacoby, J. F. Gusella, V. Ramesh and D. N. Louis (1997). "Universal absence of merlin, but not other ERM family members, in schwannomas." The American journal of pathology **151**(6): 1649-1654.

Stokowski, R. P. and D. R. Cox (2000). "Functional analysis of the neurofibromatosis type 2 protein by means of disease-causing point mutations." Am J Hum Genet **66**(3): 873-891.

Surace, E. I., C. A. Haipek and D. H. Gutmann (2004). "Effect of merlin phosphorylation on neurofibromatosis 2 (NF2) gene function." Oncogene **23**(2): 580-587.

Tang, X., S. W. Jang, X. Wang, Z. Liu, S. M. Bahr, S. Y. Sun, D. Brat, D. H. Gutmann and K. Ye (2007). "Akt phosphorylation regulates the tumour-suppressor merlin through ubiquitination and degradation." Nat Cell Biol **9**(10): 1199-1207.

Thiery, J. P. (2002). "Epithelial-mesenchymal transitions in tumour progression." Nature reviews. Cancer **2**(6): 442-454.

Tikoo, A., M. Varga, V. Ramesh, J. Gusella and H. Maruta (1994). "An anti-Ras function of neurofibromatosis type 2 gene product (NF2/Merlin)." The Journal of biological chemistry **269**(38): 23387-23390.

Trofatter, J. A., M. M. MacCollin, J. L. Rutter, J. R. Murrell, M. P. Duyao, D. M. Parry, R. Eldridge, N. Kley, A. G. Menon, K. Pulaski and et al. (1993). "A novel moesin-, ezrin-, radixin-like gene is a candidate for the neurofibromatosis 2 tumor suppressor." Cell **72**(5): 791-800.

Tsukita, S., Y. Hieda and S. Tsukita (1989). "A new 82-kD barbed end-capping protein (radixin) localized in the cell-to-cell adherens junction: purification and characterization." J Cell Biol **108**(6): 2369-2382.

Tsukita, S., K. Oishi, N. Sato, J. Sagara, A. Kawai and S. Tsukita (1994). "ERM family members as molecular linkers between the cell surface glycoprotein CD44 and actin-based cytoskeletons." J Cell Biol **126**(2): 391-401.

Tsukita, S. and S. Tsukita (1989). "Isolation of cell-to-cell adherens junctions from rat liver." J Cell Biol **108**(1): 31-41.

Turunen, O., T. Wahlstrom and A. Vaheri (1994). "Ezrin has a COOH-terminal actin-binding site that is conserved in the ezrin protein family." The Journal of cell biology **126**(6): 1445-1453.

Weinberg, R. A. (1995). "The retinoblastoma protein and cell cycle control." Cell **81**(3): 323-330.

Wu, X., P. S. Tanwar and L. A. Raftery (2008). "Drosophila follicle cells: morphogenesis in an eggshell." Semin Cell Dev Biol **19**(3): 271-282.

Xiao, G. H., A. Beeser, J. Chernoff and J. R. Testa (2002). "p21-activated kinase links Rac/Cdc42 signaling to merlin." The Journal of biological chemistry **277**(2): 883-886.

Xu, N., G. Bagumian, M. Galiano and M. M. Myat (2011). "Rho GTPase controls Drosophila salivary gland lumen size through regulation of the actin cytoskeleton and Moesin." Development **138**(24): 5415-5427.

Xue, Y., J. Ren, X. Gao, C. Jin, L. Wen and X. Yao (2008). "GPS 2.0: Prediction of kinase-specific phosphorylation sites in hierarchy." Molecular & Cellular Proteomics.

Yang, Y., D. A. Primrose, A. C. Leung, R. B. Fitzsimmons, M. C. McDermand, A. Missellbrook, J. Haskins, A. S. Smylie and S. C. Hughes (2012). "The PP1 phosphatase flapwing regulates the activity of Merlin and Moesin in Drosophila." Developmental biology **361**(2): 412-426.

Yeung, R. S., G. H. Xiao, F. Jin, W. C. Lee, J. R. Testa and A. G. Knudson (1994). "Predisposition to Renal-Carcinoma in the Eker Rat Is Determined by Germ-Line Mutation of the Tuberous-Sclerosis-2 (Tsc2) Gene." Proceedings of the National Academy of Sciences of the United States of America **91**(24): 11413-11416.

Yogesha, S. D., A. J. Sharff, M. Giovannini, G. Bricogne and T. Izard (2011). "Unfurling of the band 4.1, ezrin, radixin, moesin (FERM) domain of the merlin tumor suppressor." Protein Sci **20**(12): 2113-2120.

Yonemura, S., M. Hirao, Y. Doi, N. Takahashi, T. Kondo, S. Tsukita and S. Tsukita (1998). "Ezrin/radixin/moesin (ERM) proteins bind to a positively charged amino acid cluster in the juxta-membrane cytoplasmic domain of CD44, CD43, and ICAM-2." J Cell Biol **140**(4): 885-895.

Yun, C. H., S. Oh, M. Zizak, D. Steplock, S. Tsao, C. M. Tse, E. J. Weinman and M. Donowitz (1997). "cAMP-mediated inhibition of the epithelial brush border Na+/H+ exchanger, NHE3, requires an associated regulatory protein." Proc Natl Acad Sci U S A **94**(7): 3010-3015.

Zhang, N., H. Bai, K. K. David, J. Dong, Y. Zheng, J. Cai, M. Giovannini, P. Liu, R. A. Anders and D. Pan (2010). "The Merlin/NF2 tumor suppressor functions through the YAP oncoprotein to regulate tissue homeostasis in mammals." Dev Cell **19**(1): 27-38.

Appendix

APPENDIX

Sip1 tissue immunoprecipitation

To examine the possibility of the Merlin/Moesin/Sip1/Slik/Flapwing switch hypothesis presented in Figure 1-3, HA-tagged Sip1 was immunoprecipitated from whole third instar larvae (which are undergoing high levels of cell proliferation) and from whole pupae (which are not proliferating 48 hours after pupal formation but are undergoing changes in cell morphology). The relative amounts of Merlin and Moesin are expected to change according to whether the tissue is undergoing proliferation or undergoing changes in morphology. Active Moesin is hypothesised to be present in greater relative amounts at cell division stages, whereas active Merlin is expected to be present in greater relative amounts at differentiation stages.

Immunoprecipitation of endogenous Sip1 proved difficult, and the conditions to immunoprecipitate HA-tagged Sip1 from larvae and pupae have not been optimised. Immunoprecipitation conditions will have to be optimised to solubilise Merlin from the plasma membrane without disrupting the interaction with Sip1. The conditions will also have to allow for the successful binding of the antibody to Sip1.

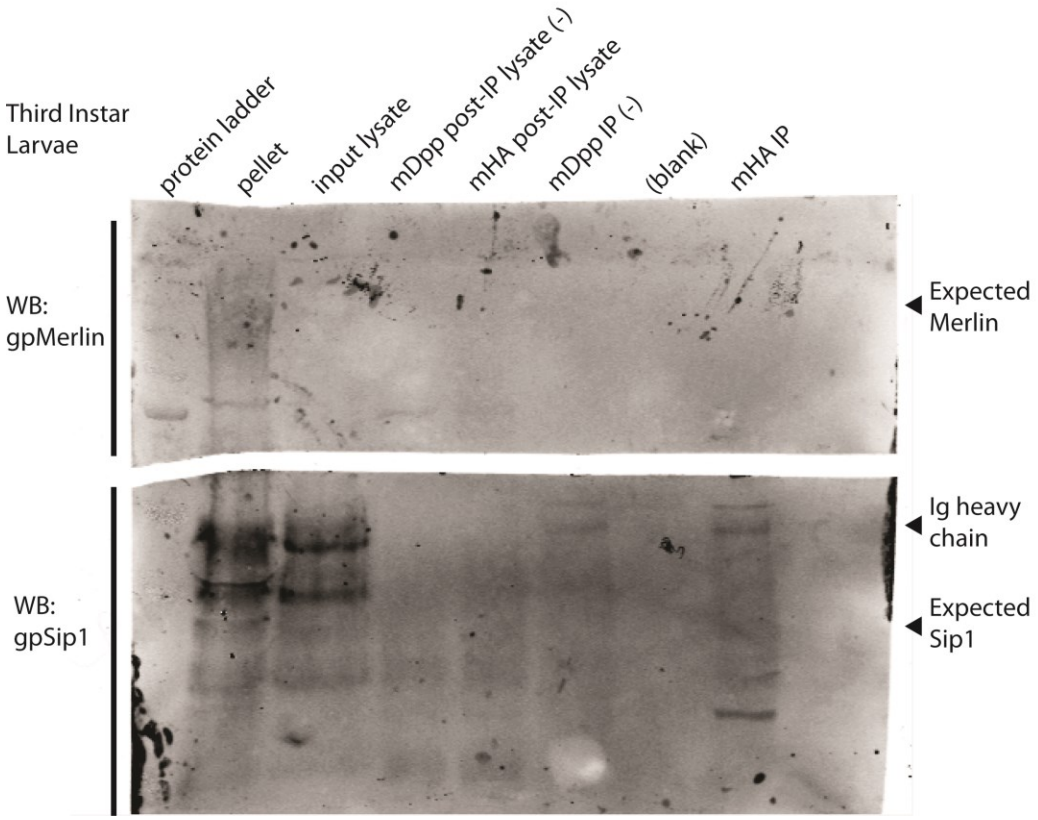

Figure A1. HA-Sip1 immunoprecipitated from third instar larvae. Sip1 can be detected in the pellet and input lysate, but the IP was not successful.

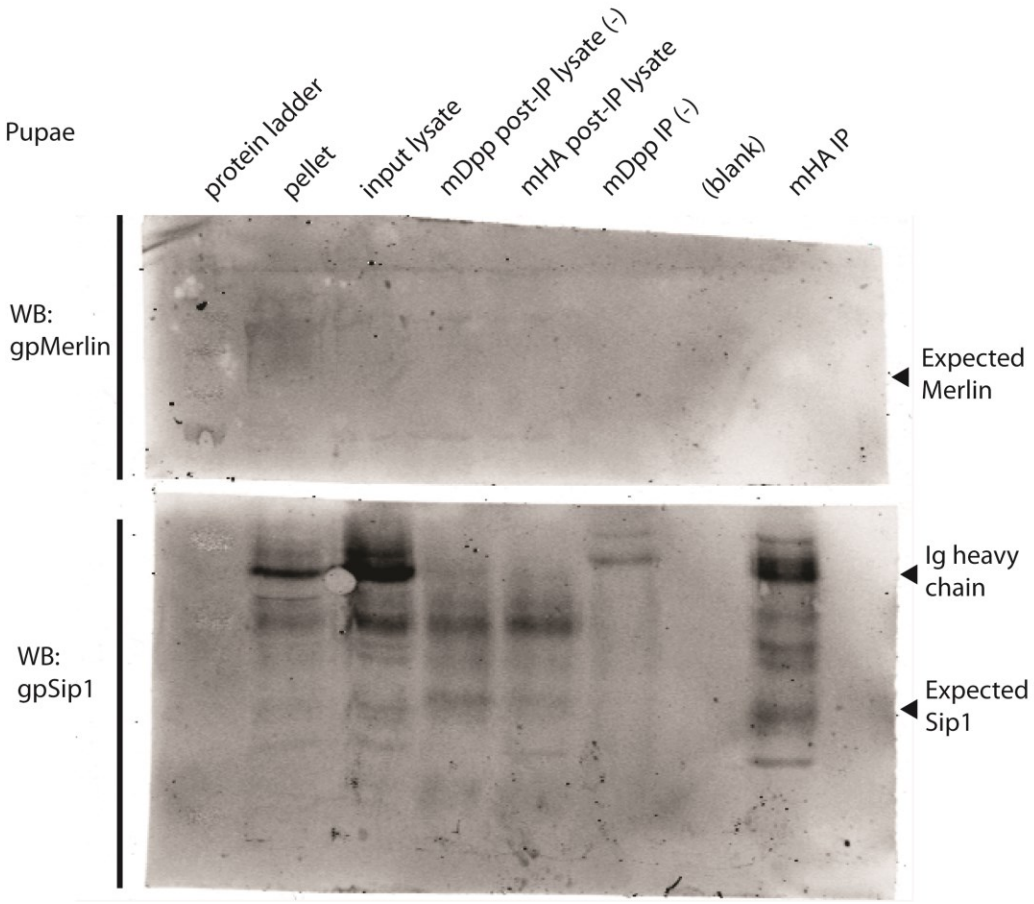

Figure A2. HA-Sip1 immunoprecipitated from pupae. Sip1 can be detected in the pellet and input lysate, but the IP was not successful.

Drosophila salivary glands are not a suitable model in which to study the effects of the serine 371 and threonine 18 mutants

Mechanisms to maintain epithelial integrity and apical-basal polarity are important to study as the epithelial-mesenchymal transition (EMT) is recognised as a critical event in cancer metastasis (Thiery 2002). The Drosophila salivary gland consists of a pair of elongated epithelial tubes, comprising of a single epithelial cell layer surrounding a lumen (Pirraglia et al. 2010). To test the salivary gland as a model to study the effects of the Merlin phosphorylation mutants, transgenic flies carrying serine 371 and threonine 18 mutants were crossed to a fly line expressing *forkhead*-GAL4 (fkh^{III}-GAL4) to over-express the mutant Merlin protein in the Drosophila salivary gland. Previous work in the lab has shown effects of Merlin mutants on cell adhesion and lumen morphology in third instar larval salivary glands (Maruyama, unpublished), and Merlin has also been implicated as an inhibitor of p21-activated kinase (Pak1) (Shaw et al. 2001), as well as in Pak1 regulation of salivary gland size and shape (Pirraglia et al. 2010). Pak1 has been shown to be involved in cytoskeleton reorganization and transcriptional activation (Bagrodia and Cerione 1999, Jaffer and Chernoff 2002). Moesin has also been implicated in the Rho1 GTPase mediated regulation of salivary gland lumen size (Xu et al. 2011), and has been shown to maintain epithelial integrity by antagonising the Rho GTPase (Speck et al. 2003). As neither

cell death or cell proliferation occurs after Drosophila salivary glands are formed, they are a useful system in which to examine the effects of Merlin in the context of maintaining epithelial integrity, such as cell shape and cell adhesion (Maruyama and Andrew 2012).

The salivary glands were determined to be an unsuitable system in which to study the effects of the serine 371 and threonine 18 mutations. The tissue is highly sensitive, and the physical treatment of the tissue affected the morphology of the lumen and lead to difficulties in interpreting the results. Examples of the observed lumen phenotypes are presented in Figure A3.

Figure A3. Examples of observed salivary gland lumen phenotypes.

Merlin phosphorylation mutants were over-expressed in late L2 larvae using the *forkhead*-GAL4 driver (fkh^{III}-GAL4). Salivary glands were dissected from late L2 larvae, fixed in 4% paraformaldehyde for 20 minutes, and stained with phalloidin for F-actin. Constitutively active $Merlin^{T616D}$ was used as a positive control (O,P). When $Merlin^{T616D}$ is over-expressed in the salivary gland and stained with phalloidin, the lumen surface was expanded when compared to control glands (A-B,C-D).

When $Merlin^{S371A}$ is over-expressed (E,F), the morphology of the lumen is comparable to control glands. When $Merlin^{S371D}$ is over-expressed, the lumen surface is even but the lumen size is visibly expanded (G,H).

When $Merlin^{T18A}$ is over-expressed in the salivary gland, phalloidin staining showed a range of lumen morphology from smooth and lobular (I) to ridged (C) to wild-type (not shown). The shape of the lumen surface when $Merlin^{T18D}$ is over-expressed (K,L) is comparable to that of wild-type (C,D), but there appears to be increased phalloidin staining in the basolateral membranes.

Images were taken with a 40X (N.A 1.3 oil) immersion lens.

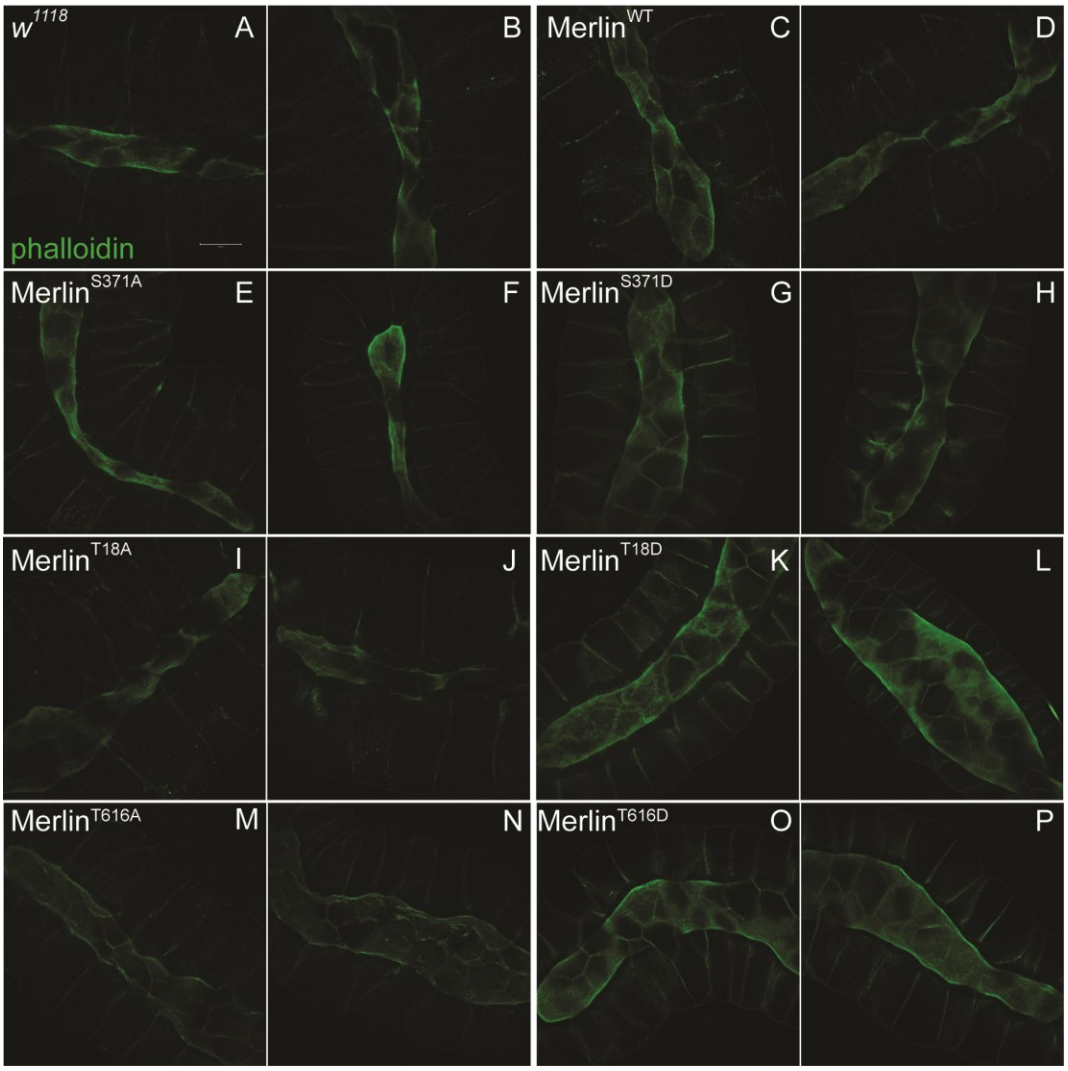
w1118
A
B
MerlinWT
C
D
phalloidin
MerlinS371A
E
F
MerlinS371D
G
H
MerlinT18A
I
J
MerlinT18D
K
L
MerlinT616A
M
N
MerlinT616D
O
P